ISSN 0975 2595

PRAJÑĀ

Volume 26, December 2018

Journal of Pure and Applied Sciences

A Peer Reviewed Journal

SARDAR PATEL UNIVERSITY
VALLABH VIDYANAGAR
Gujarat - 388 120, INDIA
www.spuvvn.edu

PRAJÑĀ - Journal of Pure and Applied Sciences
(Abbreviation: *PRAJÑĀ - J. Pure & Appl. Sci.*)

PRAJÑĀ - Journal of Pure and Applied Sciences

A Peer Reviewed Journal

Volume 26, December 2018

ISSN 0975 – 2595

An Official Publication of

Sardar Patel University

Vallabh Vidyanagar, Gujarat - 388 120, India

www.spuvvn.edu E-mail: spu.prajna@gmail.com

http://spuvvn.edu/academics/publications/index.php?sphrase_id=486549

Sardar Patel University Press, Vallabh Vidyanagar, Gujarat - 388 120, INDIA

Sardar Patel University
is grateful to

Prof. Vithalbhai A. Patel

**Humboldt State University, Arcata, Califonia, USA,
whose generous donation to organize academic activities
in the name of Shri Ishwarbhai Ambalal Patel (Shertha) helped
to meet a part of the publication cost of PRAJÑĀ Journal.**

****

The Editorial Board of PRAJÑĀ is grateful to all those experts who rendered their valuable services as referees for reviewing the papers received for this volume of the Journal.

****

**The computational assistance received from
Miss. Darshana Kanthecha,
Research Students of Chemistry Department
for making of this volume of
PRAJÑĀ Journal is also gratefully acknowledged.**

****

Since 1991 Sardar Patel University has been regularly publishing the ***PRAJÑĀ* - Journal of Pure and Applied Sciences** with an aim of providing a platform to Academicians, Researchers and Scientists for the rapid dissemination of original scientific work carried out in the University and Research Laboratories. All articles published in *PRAJÑĀ* are deemed to reflect the individual views of the authors and not the official points of view of the Sardar Patel University.

A Peer Reviewed Journal
Indexed in Indian Science Abstracts
Published by the Registrar, Sardar Patel University, Vallabh Vidyanagar, Gujarat - 388 120
Printed at Sardar Patel University Press, Vallabh Vidyanagar, Gujarat-388 120

PRAJÑĀ - Journal of Pure and Applied Sciences
Volume 26 December 2018

CONTENTS

Sardar Patel University Press, Vallabh Vidyanagar, Gujarat - 388 120, INDIA

PHARMACEUTICAL SCIENCE

HOMESCIENCE

MATHEMATICS

Guidelines for Contributors

PRAJÑĀ - Journal of Pure and Applied SciencesVol. 26 : 1 – 7 (2018)
ISSN 0975 - 2595

ISOLATION AND IDENTIFICATION OF PATHOGENIC FUNGI FROM BANANA FIELDS

ZALAK PATEL AND SIVA SATYA MOHAN JAMPALA*
Post Graduate Department of Biosciences, Sardar Patel University,
Vallabh Vidyanagar, Anand, Gujarat, India.

ABSTRACT

Banana is one of the oldest fruit crop belonging to the genus Musa which supports livelihood of millions of people. Global banana production is severely affected by the fungal pathogens among which Panama disease is the major problem to banana industry. This study was carried out to survey Fusarium wilt in banana fields near Bakrol village. During 2014-15, two Fusarium sp. were isolated from two different fields and identified by molecular technique. The pathogenicity test on detached banana leaves and pots were carried out. Fusarium sp. isolated from fruits showed symptomatic yellow leaf spots and necrosis within ten days after spore inoculation while no symptoms were observed with pseudostem isolate and distilled water inoculated leaves. The information about the occurrence of disease may be useful for developing resistant banana cultivars and adopting the appropriate agronomic practices to control the disease.

Keywords: Banana, Fusarium oxysporum f.sp. cubense, Panama disease, Tropical race 4, Plant pathogenic fungi.

INTRODUCTION

Bananas (*Musa* spp.) are giant perennial herbs belonging to the order Zingiberales of the monocotyledon group and originated in Southeast Asia and the Western Pacific. The cultivated bananas have evolved from the hybridization of wild species of *M. acuminata* and *M. balbisiana* [1]. Banana provides more balanced food than any other fruits or vegetable for millions of people across the globe. Bananas serve as an ideal and low cost staple food source for developing countries [2]. India is the largest producer of banana in the world contributing 37.2% of total world production [3]. Banana occupies only 11.1% of total cultivated area under fruits while contributing 32.6% of total fruit production in India. Gujarat is the second largest producer of banana following Tamilnadu [4].

Global banana production is adversely affected by the re-emergence of a Fusarium wilt [5]. Fusarium wilt (also known as "Panama disease") is a devastating disease caused by fungi *Fusarium oxysporum* f. sp. *cubense* (Foc) [6]. It is a soil borne pathogen which infects the root system and goes on to colonize the plant through the vascular system, subsequently occludes the xylem vessels. The hyphae of the fungus can even reach the leaves leading to wilting and death of banana plant. However, one of the worst effects of Panama disease is the production of chlamydospores or resting spores which survive in the soil for decades and cannot be controlled by fungicides. As soon as a susceptible banana plant grows nearby, these spores germinate, infect the plant, and kill it. However, only two races namely Foc race 1 and race 4 have been shown to endanger banana production worldwide [7]. The tropical race 4 strain of Fusarium wilt is regarded as one of the most serious threats to banana production since disease resistant varieties, for replacing Cavendish which are currently the source of 99% of banana exports, are not yet widely available [8].

Therefore, this study was carried out for detection and identification of Fusarium wilt in diseased banana plants in the fields near Bakrol village (22°33'50"N, 72°54'40"E), Anand, Gujarat, India.

METHODOLOGY

Sample collection and isolation of pathogens

The survey was carried out for fungal diseases in the banana fields near Bakrol, Gujarat in the year 2014-15. The samples of infected pseudostem and fruit bunch of Grand naine from different fields were collected and brought to the lab in the air tight polybags. The vascular tissue showing symptomatic reddish brown lesions from pseudostem was cut in to small pieces, surface sterilized and

inoculated on PDA media. Similarly, pieces of infected fruit peel showing surface grown mycelia were collected and placed over PDA medium [9]. After incubation for 3-5 days at 27±2°C temperature, the pinkish white cottony colonies of *Fusarium* sp. were isolated and subcultured. Pure cultures of the isolates were stored at 4°C in refrigerator for further study.

Cultural studies

The actively growing cultures of both isolates were evaluated for morphological characteristics. Actively growing mycelia were suspended in sterile distilled water and agitated to release spores. Conidial morphology was observed by lactophenol cotton blue staining under (x40 and x100) light microscope and spore size was measured using calibrated micrometer.

Identification by molecular technique

The consensus sequence of D2 region of LSU gene was generated by amplification of 28S rDNA fragment using the primers (DF-ACCCGCTGAACTTAAGC and DR-GGTCCGTGTTTCAAGACGG) similar to LROR and NL4. Based on maximum identity score first fifteen sequences were aligned using Clustal W. The phylogenetic tree was constructed using MEGA5 [10]. Sequence of both fungi has been submitted to NCBI GeneBank.

Pathogenicity test using detached leaf assay

To confirm pathogenicity, detached banana leaf assay was carried out. Spore suspensions were prepared by suspending mycelial mat into sterile distilled water followed by agitation. Spore counting was carried out by placing a drop of spore suspension on Neubauer chamber and spore concentration was adjusted to working concentration of 10^4 spores/ml.

The fresh and healthy leaves of three to four months old banana plants were surface sterilized with 70% alcohol for 1 minute in aseptic condition and washed with sterile distilled water for several times. Leaves rubbed with sterile blades to remove waxy layer from the surface were inoculated with spore suspension (10^4 spores/ml) of each fungus separately in sterile petriplates containing wet Whatman filter paper. These plates were incubated under dark-light condition at room temperature. The plates were daily observed for characteristic disease symptoms on detached banana leaves as observed on original plants in the fields. The experiment was conducted in triplicate.

RESULTS AND DISCUSSION

In the study, *Fusarium* sp. from two different fields of Bakrol village were isolated during the year 2014-15. In September 2014, the heavily infected banana pseudostem with yellowing and wilting of leaves which caused death of whole plant within two months after planting (Figure 1 A) was collected from field 1. *Fusarium* infected bunch with yellow necrosis of banana fingers was observed on healthy looking plant and collected in June 2015 from field 2 (Figure 1 B).

On the basis of colony characteristics and microscopic study, the isolates from both samples were found to be *Fusarium* sp. The pinkish white cottony colonies showing reddish pigmentation underside were isolated as shown in figure 2 A and C. The growth of *Fusarium* sp. FoF isolated from fruits was more and appeared fluffy as compared to that of *Fusarium* sp. FoS isolated from pseudostem.

The spore showed the characteristic sickle shaped, 3-4 septate macroconidia and oval shaped microconidia under the light microscope (figure 2 B and D) when stained using lactophenol cotton blue. The size of macroconidia from both isolates varied from 18-30 × 3-3.8 µm. Fusarium sp. causing banana fruit rot was isolated from local market of Anand with cottony, pinkish white mycelial growth on PDA medium [11]. Significant variations were observed in cultural characteristics, production of microconidia, macroconidia and chlamydospores and also colony pigmentation from white to pinkish in the *Fusarium* isolates from various pseudostem bits of infected banana plants [9]. The different isolates of *Fusarium oxysporum* f. sp. *ciceri* causing wilting of chickpea isolated from various region of West Bengal also showed differences in the growth of colony, color of pigment produced and size of macro- and micro-conidia [12]. A diverse population of *F. oxysporum* isolated from different tomato fields of Uttar Pradesh showed the morphological and cultural

differences as well as large variability appeared in conidial morphology [13]. *Fusarium* sp. isolated from fruits were showed fluffier mycelial growth.

The sequences of 852 bp and 621 bp of D2 region of 28S rDNA (LSU) gene were generated from forward and reverse sequences obtained by amplification of 28S rDNA fragment from both the fungi isolated from field 1 and 2 respectively. The phylogenetic tree constructed showed the maximum identity (100%) of these fungi with *Fusarium* sp. KF215 (Accession number: KM096153.1) and *Fusarium* sp. NRRL45996 (Accession number: GQ505760.1) respectively for the isolates *Fusarium* sp. FoS and FoF (figure 3-A and B). The nucleotide sequences of both isolates were submitted to the NCBI GenBank and the accession numbers allotted are KY548401 and KY548402 for the *Fusarium* isolated from pseudostem FoS (field 1) and fruits FoF (field 2) respectively. Foc race identification is cumbersome therefore other methods unveiling genetic diversity can be used. Species specific primer sets FOF1 and FOR1 have been used to detect *F. oxysporum* strains in tomato [13]. Dita et al. [14] developed a PCR based diagnostic tool specifically to detect Foc Tropical race 4 which is presently the best option for the rapid and reliable detection of TR4. Using this PCR based molecular tool, Ordonez et al., [15] has reported the TR4 causing Panama disease in Cavendish bananas in Pakistan and Lebanon in 2016. In India, the dominant VCG 0124/5 complex was isolated from ABB bananas i.e. Monthan and the Pisang Awak cultivar Karpooravalli, AB bananas i.e. Ney Poovan and the Silk cultivars Rasthali, Malbhog and Mortaman (AAB). The cultivars from which most VCGs were collected in India were Karpooravalli and Ney Poovan and not a single isolate from Cavendish bananas [16]. TR4 has been reported to infect Cavendish variety in Jordan, Lebanon, Oman, Pakistan [17] and recently in Australia [18]. The *Fusarium* isolates in this study do not match the characteristics of Tropical Race 4.

In detached banana leaf assay as shown in Figure 4, minor 1-2 cm size blackish lesion was observed within ten days after spore inoculation of *Fusarium* sp. FoF (KY548402) in wounded leaves, showing similar symptoms as observed on infected fruits. While no symptoms were observed with *Fusarium* sp. FoS (KY548401) strain isolated from pseudostem and distilled water inoculated leaves. The same fungus was consistently reisolated from the symptomatic leaf tissue. Thus, detached leaf assay revealed that *Fusarium* sp. isolated from fruits are more virulent than that isolated from pseudostem. The detached leaf assay in petri dishes which is the easiest and most reliable laboratory test was used to evaluate virulence and pathogenicity of numerous strains of *Pseudomonas syringae* pv. *syringae* on Pear [19]. The effectiveness of the detached leaf assay was found to be similar with whole seedling assay and applied for assessing wheat genotypes against leaf rust [20]. Detached leaf assay, a rapid and inexpensive method, demonstrated a relationship between pathogenic *Pythium* inoculum concentration in soil and the expression of root rot symptoms in *Chrysanthemum* [21]. Wounded and unwounded *in vitro* detached leaf assay demonstrated that *Fusarium langsethiae* is a pathogen of wheat and oats and may have developed some host preference towards oats [22]. In this study the *Fusarium* isolates FoF (KY548402) appeared to be more virulent than *Fusarium* sp. FoS (KY548401) isolate.

CONCLUSION

Detection of Fusarium wilt in various region is the threatening signal for Cavendish production which is a major component of local agriculture economies in India and the world. The losses will increase without a heightened awareness of the threat that TR4 poses and the execution of actions to prevent its spread. A systematic understanding of Foc epidemiology and pathology is immediately required so as to develop effective methods to destroy infected plants and (biological) soil treatments.

REFERENCES

[1] Chai, J., Feng, R., Shi, H., Ren, M., Zhang, Y., Wang, J. (2015) Bioinformatic Identification and Expression Analysis of Banana MicroRNAs and Their Targets. *PLoS ONE,* **10**: 1–15. doi:10.1371/journal.pone.0123083.

[2] Surendar, K. K., Devi, D. D., Ravi, I., Krishnakumar, S., Kumar, S. R., Velayudham, K. (2013) Water Stress in

Banana- A Review. *Bulletin of Environment, Pharmacology and Life Sciences,* **2**: 1–18.

[3] Shekhawat, U. K. S., Ghag, S. B., Ganapathi, T. R. (2014) Transgenic Approaches for Development of Disease Resistance in Banana. *BARC Newsl*, **337**: 18–23.

[4] Mitra, S. (2014) Tropical and subtropical fruits in India. *Journal of Tropical Crop Science,* **Vol 1**: 1-2

[5] Pérez-vicente, L., Dita, M. A., D la Parte, E. M. (2014) Technical Manual Prevention and diagnostic of Fusarium Wilt (Panama disease) of banana caused by *Fusarium oxysporum* f. sp. *cubense* Tropical Race 4 (TR4). *Food and Agriculture Organization of The United Nations,* **4:** 1–74.

[6] Njoroge, M. A. (2012) Strategies for improved disease resistance in micro-propagated bananas. Ph.D. Thesis, Queensland University of Technology, Brisbane, Australia.

[7] Sun, Y., Yi, X., Peng, M., Zeng, H., Wang, D., Li, B., Tong, Z., Chang, L., Jin, X., Wang, X. (2014) Proteomics of *Fusarium oxysporum* Race 1 and Race 4 reveals enzymes involved in carbohydrate metabolism and ion transport that might play important roles in banana *Fusarium* wilt. *PLoS ONE,* 9(12). e113818. doi:10.1371/journal.pone.0113818.

[8] Brunschot, S. V. (2006) *Fusarium* Wilt of Banana Laboratory Diagnostics Manual. *Plant Health Australia*.

[9] Das, A., Venkataramana, M., Chandranayaka, S., Murali, H. S., Batra, H. V. (2012) Molecular characterization of *Fusarium oxysporum* f. sp. *cubense* isolates from banana. *Pest Management in Horticultural Ecosystems,* **18**: 171–178.

[10] Tamura, K., Peterson, D., Peterson, N., Stecher, G., Nei, M., Kumar, S. (2011) MEGA5: Molecular evolutionary genetics analysis using maximum likelihood, evolutionary distance, and maximum parsimony methods., *Molecular Biology and Evolution,* **28**: 2731–2739.

[11] Singh, K. B. (2011) Studies on Fusarium Fruit Rot (Fusarium moniliforme Sheldon) of Banana (Musa paradisiaca L.) and its management, A dissertation thesis submitted to Anand Agricultural University, Anand for the award of the degree of M.Sc. in Agriculture (Plant Pathology).

[12] Patra, S., Biswas, M. K. (2017) Studies on cultural, morphological and pathogenic variability among the isolates of *Fusarium oxysporum* f. sp. *ciceri* causing wilt of chickpea. *International Journal of Plant, Animal and Environmental Sciences*. **7**: 11–17. doi:10.21276/Ijpaes.

[13] Joshi, M., Srivastava, R., Sharma, K., Prakash, A. (2013) Isolation and characterization of *Fusarium oxysporum*, a wilt causing fungus, for its pathogenic and non-pathogenic nature in tomato (*Solanum lycopersicum*). *Journal of Applied and Natural Science,* **5**: 108–117.

[14] Dita, M. A., Waalwijk, C., Buddenhagen, I. W., Souza, J. T., Kema, G. H. J. (2010) A molecular diagnostic for tropical race 4 of the banana Fusarium wilt pathogen. *Plant Pathology,***59**:348–357. doi:10.1111/j.13653059.2009.02221.x.

[15] Ordonez, N., Garcia-Bastidas, F., Laghari, H. B., Akkary, M. Y., Hartfouche, E. N., Al Awar, B. N., Kema, G. H. J. (2017) First report of *Fusarium oxysporum* f.sp. *cubense* Tropical Race 4 causing Panama disease in Cavendish bananas in Pakistan and Lebanon. *Plant Disease,* **100**:209. doi:https://doi.org/10.1094/PDIS-12-14-1356-PDN.

[16] Mostert, D., Molina, A. B., Daniells, J., Fourie, G., Hermanto, C., Chao, C. P., Fabregar, E., Sinohin, V. G., Masdek, N., Thangavelu, R., Li, C., Yi, G., Mostert, L., Viljoen, A. (2017) The distribution and host range of the banana *Fusarium* wilt fungus, *Fusarium oxysporum* f . sp . *cubense*, in Asia. *PLoS ONE,* **12**: 1–24.

[17] Ploetz, R. C. (2015) *Fusarium* Wilt of Banana. *Phytopathology*, 105: 1512–1521. doi:10.1094/PHYTO-04-15-0101-RVW.

[18] Mcconchie, R., Mckillop, C. (2017) Panama disease tropical race 4 confirmed on Mackays Queensland banana farm, Australia's largest grower. Retrived 27-7-2017 from ABC-Rural ABC-NEWS. Website: http://www.abc.net.au/news/rural/2017-07-26/panama-tropical-race-4-confirmed-on-tully-queensland-banana-farm/8745706.

[19] Yessad, S., Manceau, C., Luisetti, J. (1992) A detached leaf assay to evaluate virulence and pathogenicity of strains of *Pseudomonas syringae* pv. *syringae* on Pear. *Plant Disease*. **76:** 370–373.

[20] Boydom, A., Dawit, W., W/Ab, G. (2013) Evaluation of detached leaf assay for

assessing leaf rust (*Puccinia triticina* Eriks .) resistance in Wheat. *Journal of Plant Pathology and Microbiology*. **4**:176. doi:10.4172/2157-7471.1000176.

[21] Pettitt, T. R., Wainwright, M. F., Wakeham, A. J., White, J. G. (2011) A simple detached leaf assay provides rapid and inexpensive determination of pathogenicity of *Pythium* isolates to "all year round" (AYR) chrysanthemum roots. *Plant Pathology*. **60**: 946–956. doi:10.1111/j.1365-3059.2011.02451.x.

[22] Imathiu, S. M., Ray, R. V., Back, M., Hare,M. C., Edwards, S. G. (2009) *Fusarium langsethiae* pathogenicity and aggressiveness towards oats and wheat in wounded and unwounded *in vitro* detached leaf assays. *Europian Journal of Plant Pathology*. **124:** 117–126. doi:10.1007/s10658-008-9398-7.

Figure 1: Diseased banana plants (A) banana pseudostem showing typical symptoms of wilt and necrosis. (B) Banana bunch showing yellowing and necrosis of fruits.

Figure 2: (A, C) Isolated pinkish white cottony colonies of *Fusarium* sp. and (B, D) photomicrograph showing sickle shaped spores of *Fusarium* sp.

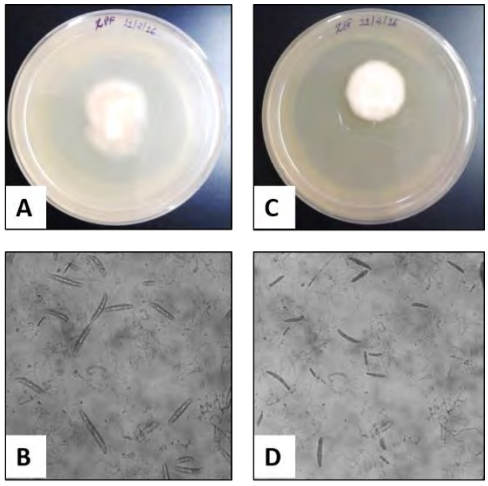

Figure 3: Phylogenetic analysis of isolates KY548401 and KY548402 showing maximum similarity of BLAST analysis.

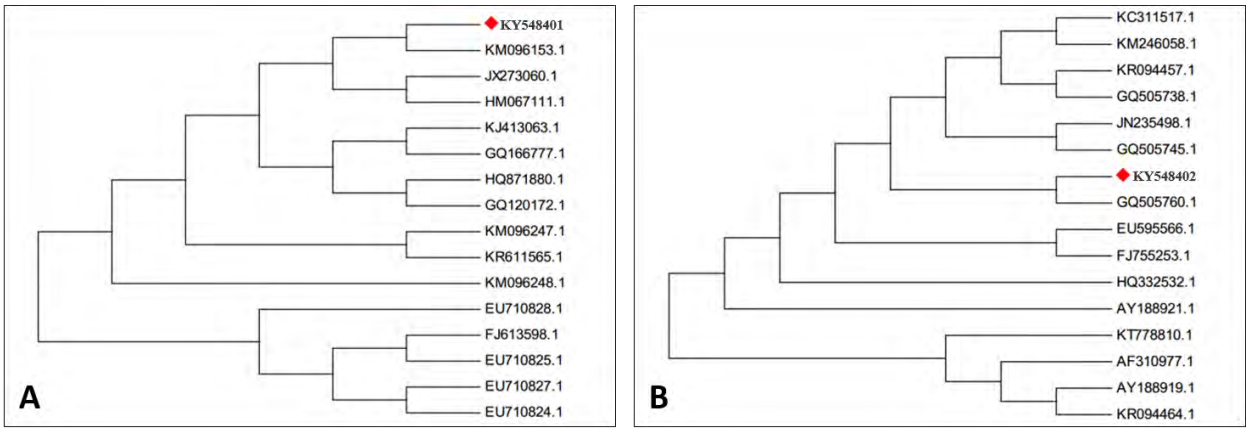

Figure 4: Pathogenicity testing on detached banana leaf pieces indicating symptomatic necrosis upon spore inoculation of isolated *Fusarium* sp.

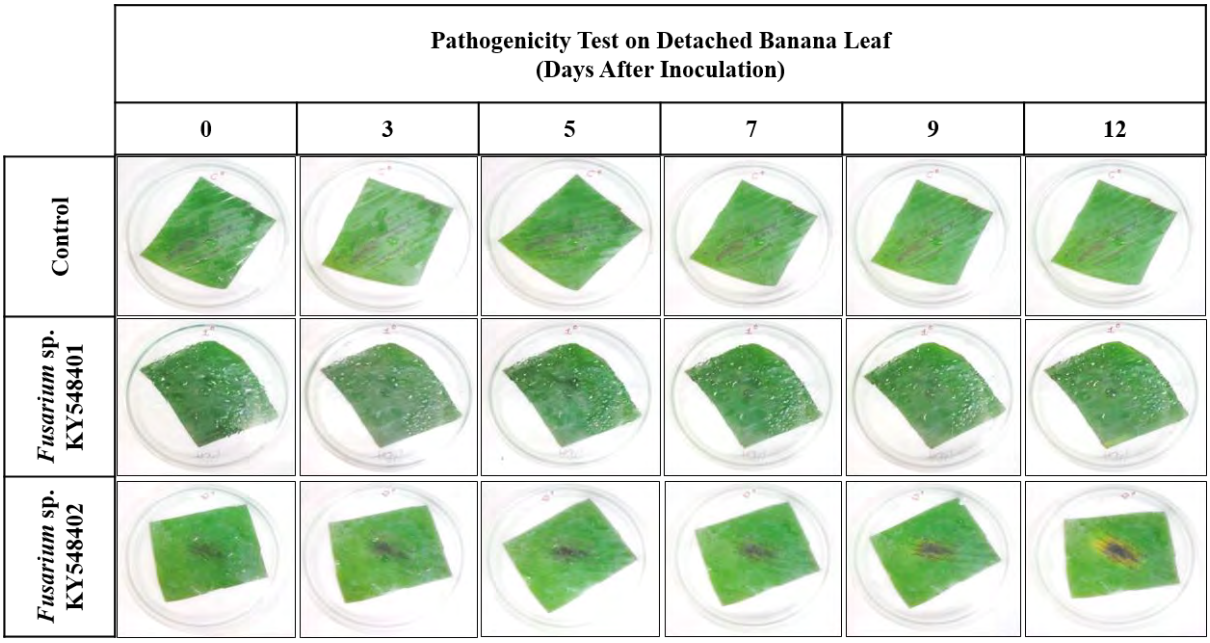

PRAJÑĀ - Journal of Pure and Applied Sciences Vol. 26 : 8 – 23 (2018)
ISSN 0975 - 2595

COMPOSITE COATING MEDIATED IMPROVEMENT OF NUTRITIONAL QUALITY AND SAFETY OF FRESH-CUT PINEAPPLE (*ANANAS COMOSUS* L. MERRIL)

SONU SHARMA AND T. V. RAMANA RAO*

P. G. Department of Biosciences, Sardar Patel University, Vallabh Vidyanagar – 388 120, Gujarat, India

Email address: tadapanenirao@yahoo.com, brjshsharma56@gmail.com

ABSTRACT

In the present work, the efficacy of three different composite coatings in maintaining quality and storability of fresh-cut pineapple at 5°C was evaluated. The coatings consisted of sodium alginate (1.29%), carrageenan (0.5%) and xanthan gum (0.25%) as polysaccharides, enriched with olive oil (0.1%) as a lipid component and cinnamic acid (0.1%) as an antibrowning agent. During 16 days of storage, the coated fresh-cut pineapples displayed better retention in all their physicochemical characteristics like firmness, color, weight loss, ascorbic acid, total phenolic content (TPC), carotenoids, and antioxidant activity during 16 days of their storage as compared to that of uncoated samples. The coated fresh-cut pineapples displayed lower specific activity of browning-related enzymes as compared to that of untreated samples. Sensory analysis indicated that alginate coated fresh-cut pineapples have better textural and visual properties than that of uncoated samples throughout the storage period. Thus, the developed composite coating formulation can be considered as useful in fresh produce industry to enhance the shelf-life of healthy and convenient fresh-cut fruit.

Key words: Edible coating, Fresh-cut, Pineapple, Quality, Shelf-life, Safety.

INTRODUCTION

The regular consumption of fruit and vegetables has significant impact in maintaining good health as evidenced by several epidemiological studies [1]. Among many tropical and subtropical fruits, pineapple is one of the important fruit crops due to presence of several health promoting compounds such as carotenoids, vitamin C, vitamin B1 and B6, manganese and dietary fibers. However, pineapple requires preparation like removal of thorny inedible peel, crown and cutting before being consumed and therefore fresh-cut produce industries have shown interest to launch its minimally processed product. It has considerable demand in the fresh-cut market due to its exotic flavor, attractive appearance and convenient nature. But as compared to whole fruit, the faster metabolic activity of fresh-cut produce renders rapid deterioration of its overall quality due to browning, weight loss and microbial contamination which ultimately shortens their storage life.

Edible coating may prevent moisture and solute migration, respiration and oxidative reaction rates and thereby extend the shelf-life of fresh-cut fruits and vegetables [2]. It is still challenging to develop edible coating formulations with desirable characteristics for application on fresh-cut fruits or vegetables because coatings may be dissolved and absorbed by the wet surfaces instead of drying to form a smooth and unique layer [3]. So far there is no such edible coating material which possesses all the functional properties required to slow down rapid ripening or deteriorative processes have been identified.

The development of composite coatings combining hydrocolloids (protein and polysaccharides) and lipids has emerged as one of the advanced approaches for fresh and minimally processed fruit preservation [4]. Composite coatings can be applied as a monolayer in a single step or multilayer in more than one step. In a monolayer composite edible coating, the lipid is dispersed in the hydrophilic phase (protein or polysaccharides solution) so as to obtain an emulsified coating formulation [5].

Polysaccharides such as sodium alginate, carrageenan, chitosan, pectin, gellan gum, hydroxypropylmethylcellulose (HPMC) and xanthan gum possess an excellent film forming ability against gas and solute migration

between food products and the environment [6]. In addition, these can act as the polymeric matrices for the incorporation of bioactive compounds (antimicrobial and antioxidant agents), nutraceuticals, minerals and probiotics [7]. However, most of the polysaccharides are hydrophilic in nature, limiting their moisture barrier property. In order to improve the water retention ability of edible coating formulation, the incorporation of lipid component, especially plant derived may help reduce water loss from the fresh-cut fruits due to their hydrophobic nature. Olive oil is a vegetable oil derived from fruit of olive tree (*Olea europaea* L.). It is a kind of glycerolipid with three fatty acids, mainly oleic acid and palmitic acid, attached to a glycerol backbone. It is also rich in antioxidants like vitamin E and polyphenols. Cinnamic acid, an aromatic carboxylic acid, has been reported as an effective polyphenol oxidase (PPO) inhibitor [8, 9] and approved as Generally Recognized as Safe (GRAS) substances for its use as food additive (FDA, 2013).

In the past decade, several research efforts have been attempted to design the composite coating for extending the storability of fresh and fresh-cut fruit. For instant, Dave et al. [11] observed that composite coating of soy protein, HPMC and olive oil have improved functionality as semipermeable barrier for both moisture and gaseous exchange and thereby extended shelf-life of 'Babughosha' pear fruit. Rao et al. [12] reported the effectiveness of alginate-olive oil based composite coating enriched with antioxidant in enhancing the storage life and nutritional quality of *Ziziphus mauritiana* var. Gola fruit. Similarly, Baraiya et al. [13] also demonstrated the enhanced postharvest shelf-life of carambola fruit along with improved surface appearance by using alginate-olive oil composite coating. Likewise, the incorporation of olive oil into gum arabic formulation reduces the weight loss percentage in coated citrus fruit as compared to uncoated fruit [14]. Olivas et al. [15] reported that application of methylcellulose-stearic acid based edible coating reduced the weight loss of fresh-cut pear fruit. The application of pectin-sunflower oil edible coatings helped maintain firmness and moisture content of fresh-cut melon [16]. Hence, the application of composite edible coating on fresh and fresh-cut fruit has potentiality to overcome the drawbacks associated with only lipid or protein/polysaccharide based edible coatings [17].

In line with these reports, the present study was conducted to evaluate three different composite edible coatings [sodium alginate (1.29%), carrageenan (0.5%) and xanthan gum (0.25%) as polysaccharides, blended with olive oil (0.1%) as a lipid component and cinnamic acid (0.1%) as an antibrowning agent] for quality improvement of fresh-cut pineapple fruit**.**

MATERIALS AND METHODS

Fruit material

Pineapple (*Ananas comosus* L. Merril cv. Smooth Cayenne) fruits were purchased from a wholesale fresh produce distributor in fruit market of Anand, Gujarat. The fruits at maturity stage 4 (40 – 80% of eyes yellow) were selected based on the uniformity in shape, size, peel color and free from any damage.

Preparation of composite coatings formulation

Sodium alginate-based edible coating formulation was prepared according to the method described by Azarakhsh et al. [18]. Sodium alginate powder (1.29 %, w/v) was dissolved in distilled water while heating it on a stirring hot plate at 70°C until it became homogenous solution and glycerol (1.18%, v/v) was added as a plasticizer. Carrageenan solution was prepared by dissolving 0.5 g carrageenan powder in 100 mL of sterilized distilled water and glycerol was added into it at the concentration of 0.75 g/g carrageenan. Similarly, xanthan gum based edible coating solution was prepared by dissolving 0.25 g of xanthan powder into 100 mL of distilled water on magnetic stirrer at 60ºC, followed by addition of glycerol (1%, v/v). Cinnamic acid (0.1 %, w/v) as antibrowning agent and olive oil

(0.1 %, v/v) as lipid component were added into each coating solution and stirring was continued on magnetic stirrer until formation of clear solution. Calcium chloride (2 %, w/v) solution was used as a cross-linker which allows the gelling of alginate and carrageenan based coatings over the cut surface of pineapple.

Application of composite coatings

After removal of pineapple crown leaves, the fruits were surface sterilized with sodium hypochlorite solution (0.2 mL L^{-1}, pH 6.5) for 10 min and then rinsed with distilled water. The fruits were manually peeled and both end parts were disposed off and the central region was sliced (0.03±0.005 m thickness) and each slice was cut in truncated cone format weigh of each cone was ~10 g. Then, pineapple pieces were dipped for 3 min into each composite coating formulation. The excess solution was drained off for 3 min on tissue paper. The control was set by dipping cut pineapple in distilled water for same duration. Both coated and uncoated samples were packed in food grade clamshell of 2.5×10^{-4} m^3 (0.10 m × 0.05 m × 0.05 m) containing 300 g of cut chunks of pineapple in each box. For every treatment and control, three boxes were prepared and stored at 5 °C±1 °C and 95 % relative humidity (RH) to follow the changes in their quality characteristics at the regular intervals of 4 days during storage period. The details of edible coatings treatments given to the fresh-cut pineapple fruits are given in Table 1.

EVALUATION OF QUALITY PARAMETERS

Color

The color changes of fresh-cut pineapple fruits during storage were measured in terms of color coordinates, lightness (L^*) and blue to yellowness (b^*) values. The digital images of fresh-cut pineapple fruits were captured using digital camera (FinePix S2950, FUJIFILM, Japan) and analyzed in Adobe Photoshop CS 8.0 software (Adobe Systems, Inc., San Jose, CA, USA) by pointing the cursor at different areas of images [19].

Firmness

The firmness of fruit samples was recorded with fruit pressure tester (FT-327, FACCHINI srl, Alfonsine, Italy) applying force with an 11 mm flat-bottomed probe and penetrated up to 5 mm into the flesh. The force required to penetrate the probe into fruit tissue is expressed in terms of Newton (N).

Weight loss percentage (WLP)

The change in weight loss was analyzed as per the method described by Bico et al. [20]. Fruit samples from each replicate were placed into previously tarred Petri dish and were dried at 70°C for 48 h. After drying, the Petri dish was put in a desiccator to cool to room temperature. The weight was recorded before and after drying by using an analytical balance (Shimadzu BW 380 H, Tokyo, Japan). Weight loss was calculated according to the formula:

$$\text{Weight loss (\%)} = 100 - [100 \times \text{DM (\%)}_{\text{Day 0}} / \text{DM (\%)}_{\text{Day N}}]$$

DM $(\%)_{\text{Day 0}}$ and DM $(\%)_{\text{Day N}}$ stand for dry matter on day 0 and dry matter on day N, respectively.

Bioactive compounds and antioxidant activity

Estimation of ascorbic acid was performed as per the method of Roe and Oesterling [21]. The amount of ascorbic acid was estimated as per the standard curve prepared using L-ascorbic acid and expressed as milligram per 100 gram fresh weight (mg . 100 g^{-1}fresh weight). Total carotenoids were measured using the method described by Tomes [22] and was expressed as microgram per gram fresh weight (µg .g^{-1}). Total phenolic content was determined by following Folin-Ciocalteu's method described by Lim et al. [22]. The different concentrations of gallic acid were used to prepare standard curve and expressed in milligrams gallic acid equivalent per gram fresh weight (mg g^{-1}). The DPPH free

radical scavenging activity was carried out as per the method described by Brand-Williams et al. [24]. The obtained results were expressed as percentage of inhibition of the DPPH radical.

Browning-related enzymes

Extraction and assay of Polyphenol oxidase (PPO) and Peroxidase (POX) activity

Two grams fruit pulp was homogenized in 25 mL of sodium phosphate buffer (0.1 mol L^{-1} , pH 6.5). The homogenate was centrifuged for 30 min at 20,627 × g for PPO and 29,703 × g for POX at 4 °C. The supernatant was collected and used as crude enzyme extracts. Assay for PPO activity was carried out by incubating 0.1 mL enzyme extract with 2.5 mL of catechol (0.5 mol L^{-1} in sodium phosphate buffer 0.1 mol L^{-1}, pH 6.5) and change in absorbance at 420 nm was recorded at the interval of 30 s up to 3 min from the time the enzyme extract was added. The specific activity of PPO was expressed in Units min^{-1} mg^{-1} protein. One unit of PPO activity was defined as a change of 0.001 in absorbance per minute [25].

POX activity was assayed as per the procedure described by Mazumdar and Majumder [26]. The substrate ortho-dianisidine and hydrogen peroxide was reacted with enzyme extract at 30 °C, followed by addition of sulphuric acid after 5 min of incubation to stop the reaction and optical density (OD) was measured at 430 nm. The specific activity of POX was expressed in Unit min^{-1} mg^{-1} protein. One unit of POX was defined as a change of 1.0 in absorbance per min.

Extraction and assay of Phenylalanine ammonia lyase (PAL) activity

PAL activity was assayed according to the method described by Malik and Singh [27]. One gram fruit tissue was extracted in sodium borate buffer (0.1 mol L^{-1} , pH 8.8) and the homogenate was centrifuged at 14000 × g for 20 min at 4°C. The supernatant was collected and used as crude enzyme extract. The reaction mixture consisted of 0.2 mL L-phenylalanine (0.1 mol L^{-1}) with 3.2 mL of sodium borate buffer (0.1 mol L^{-1}, pH 8.8), and 0.2 mL enzyme extract at 37 °C for 2 h. The product released was measured at 290 nm. The PAL activity was expressed in Unit min^{-1} mg^{-1} protein, where one unit is defined as micromole of cinnamic acid released per hour (μM h^{-1}).

Sensory evaluation

Sensory evaluation of fresh-cut pineapple fruit was performed according to the method described by Oms-Oliu et al. [16] to determine the overall acceptability by assessing color, taste, odor and texture during 16 days of storage. Samples of fresh-cut pineapple fruits were randomly presented to the fourteen non-trained panelists consisting of students and researchers and they rated the quality attributes on the basis of a nine-point hedonic scale: 9 = excellent; 7 = good; 5 – fair; 3 - poor and 1 - unusable. A score of 6 was considered the limit of market acceptability.

Microbial analysis

Samples were examined for microbial contamination by enumeration of total aerobic bacteria and yeasts and moulds colonies. Serial dilutions of samples were prepared by washing vigorously 10 g tissue with 90 mL of 1 g L^{-1} sterile buffered peptone water in sterilized round bottom tubes at room temperature and inoculated over plate count agar (PCA) at 35 °C for 48 h and potato dextrose agar (PDA) supplemented with 0.05 g L^{-1} chloramphenicol at 21 °C for 5 - 7 days, respectively by the spread plate method [28]. After incubation, the number of colonies were counted and expressed as log colony forming units per gram fresh weight (log CFU g^{-1} FW).

Statistical analysis

A completely randomized design was used with three replications. Statistical analysis was performed using GraphPad Prism software version 3 (GraphPad Software, Inc, San Diego, USA). Data of all analysis were expressed as mean ± standard deviation. Analysis of

Variance (ANOVA) followed by Tukey's multiple comparison post-hoc test for multiple comparisons was used to assess the statistical differences among means ($p< 0.05$).

RESULTS AND DISCUSSION

Changes in Color

The effect of composite edible coatings on the changes in color attributes in terms of L^* and b^* values of fresh-cut pineapple fruit is presented in Table 2. The results revealed that uncoated samples had greater decline in L^* and b^* values and reached to their minimum values i.e., 42.38 and 16.75 units, respectively during 16 days of storage period. Gil et al. [29] also observed the changes in the b^* coordinate of approx. 10 units in pineapple pieces stored at 5ºC after 9 days of storage. In the study, the color change in fresh-cut pineapple occurred due to decrement of b^* values through their storage period. CG and XG coated samples have higher L^* values i.e., 51.5 and 50 units than that of AG coated samples with 46.44 units, but their lower b^* values i.e., 20.38 and 19.13 units, respectively at the end of storage are responsible for their degraded color quality as compared to the AG coated samples with 26.56 units. This indicated that AG retained better color quality than XG and CG coated samples which have negative effect on color attributes during storage period of 16 days. Similarly, Benítez et al. [30] reported that alginate coatings of MD2 pineapple wedges helped retain better L^* value as compared to chitosan and antioxidants treated samples after 15 days of storage.

Changes in Firmness

Texture is critical quality attribute that determines market acceptability of fruits and vegetables by consumer. The direct contact with the atmospheric oxygen accelerate loss of firmness in fresh-cut fruits since oxidative damage cause a reduction in membrane integrity, cellular leakage and flooding of intercellular spaces [31]. With the increase of storage period, there was a progressive decline in firmness of coated and uncoated fresh-cut pineapple fruits (Table 2). The uncoated samples had significant loss in firmness ~60% during 8 days; whereas the application of edible coating emulsions showed only 25% - 30% decline in firmness compared to their initial values. During 16 days of storage period, the control samples showed ~71% firmness loss reaching to its least value, while the loss in firmness was reduced by 10% - 15% in coated fresh-cut pineapple, but no significant difference was observed for the change in firmness of fresh-cut pineapple among the applied treatments. Calcium ions play a critical role in keeping the alginate chains together through ionic interactions after the formation of hydrogen bonds between the chains, which produce a gel with a three-dimensional network structure. The results obtained in the present investigation are in line with that obtained by Mantilla et al. [32] who found that the fresh-cut pineapple coated with 1% and 2% alginate had better firmness than that of uncoated fruit samples during 15 days of storage at 4º C.

Changes in Weight loss percentage (WLP)

There was a significant increment ($p<0.05$) in WLP for both coated and uncoated samples during storage (Table 2). Interestingly, the observed WLP among treated samples ranged from 5% - 7%, while it was 16% for uncoated samples during 4 days of storage. By the end of storage period, AG coated samples exhibited least WLP (~16%), followed by CG coated samples (~24%), while it was almost similar for XG and uncoated samples (37%). This indicates that the performance and physicochemical properties of the coating formulations of different polysaccharides varies according to their molecular characteristics such as molecular weight, degree of blanching, conformation, electrical charges and hydrophobicity [33]. It can be inferred that the decrease in weight loss of alginate coated fresh-cut pineapple fruits might be related to its better ability for semipermeable layer formation over the cut surface than that of carrageenan and xanthan gum based edible coatings. Furthermore, the calcium chloride

treatment followed by edible coating application might have resulted in cross linking of alginate rendering it insoluble and thus enhanced water barrier property, as reported by Olivas et al. [34] in minimally processed 'Gala' apples.

Changes in Ascorbic acid (AA)

Klein [35] documented that ascorbic acid oxidation increases to a much greater extent on cutting during extended storage, which could be due to enzymes such as ascorbic acid oxidase. Gil et al. [29] also documented a considerable degradation in ascorbic acid in fresh-cut pineapple chunks with respect to whole unprocessed pineapple stored for 6 days at 5 °C. The coated samples displayed slight reduction i.e., ~8%, ~4% and ~1% for AG, CG and XG, respectively in vitamin C content up to 8 days of storage period and thereafter the higher concentrations i.e., 84.02±5.42, 92.01±1.05 and 96.19±2.08 mg g^{-1} in AG, CG and XG, respectively as compared to its initial value (67.36±1.59 mg g^{-1}) at the end of storage (Table 3). The accumulation of vitamin C consistently increased in uncoated samples with extend of storage time, and reached to its peak value i.e., 105.21±4.77 mg g^{-1} at the end of storage. The higher concentrations of vitamin C in coated and uncoated fresh-cut pineapple fruits could be due to increased water loss with the advance of storage period rather than the biosynthesis of vitamin C [36].

Changes in Carotenoids

In the present study, minimal processing of pineapple lead to reduction of more than 70% of carotenoids during storage period of 12 days. The amount of carotenoids noted initially was 9.97±0.13 mg g^{-1}, which eventually declined in both coated and uncoated fresh-cut pineapple as the time of storage increased and reached to its least concentration at the end of analysis (Table 3). The decline of carotenoids was also reported by Gil et al. [29]. However, AG coated samples had insignificant change in carotenoids up to 8 days of evaluation time and thereafter exhibited diminishing pattern with ~43% lower amount relative to its initial concentration as compared to ~70% decline in CG, XG coated and uncoated samples at the end of storage. This beneficial effect of alginate coating may be because of its better film-forming ability, thereby created a protective barrier against oxidative reactions over the fruit surface.

Changes in Total phenolics (TP) content

The amount of TP content of coated and uncoated fresh-cut pineapple fruits at 5°C initially was 3.49±0.29 mg g^{-1} which accumulated in all the samples at certain time of storage period depending upon the metabolic activity of that particular sample (Table 3). For eg., uncoated samples had significant ($p<0.05$) increment of ~17% on 4th day of storage, whereas coated samples experienced maximum accumulation of ~21% on 8th, 12th and 16th days of storage in samples treated with XG, CG and AG, respectively. At the end of storage time, uncoated samples displayed highest TP content i.e., 4.62±0.16 mg g^{-1}, whereas the least (3.30±0.07) was depicted in XG coated samples. This faster TP accumulation in control samples as compared to the treated fruits could possibly be attributed to enhanced oxidative stress in uncoated samples as a result of minimal processing. Surjadinata and Cisneros-Zevallos [37] demonstrated that increasing the wound stress intensity in tissues of three carrot cultivars lead to the enhanced accumulation of phenolic compounds. Among applied edible coatings, AG coated samples had slower extent of TP accumulation during 16 days of storage period.

Changes in Antioxidant activity

Oxidative stress due to cutting cause membrane damage and altering the composition and concentration of bioactive compounds mainly phenolics and vitamin C, resulting in changes in the total antioxidant activity of fresh-cut fruits and vegetables [38]. The results of antioxidant activity based on the DPPH assay are presented in Table 3. The initial antioxidant activity reported in fresh-cut pineapple fruits was 58.54±3.80 %. Uncoated

samples had highest antioxidant activity (~93%) on 4th day of storage but exhibited gradual decline in it till the end of storage. XG coated samples displayed the peak antioxidant activity (~78%) on 8th day, but eventually decreased to ~34% at the end of storage. However, there was significant ($p<0.05$) reduction of antioxidant activity on 4th and 8th day of storage in CG and AG coated samples respectively; however, the activity increased on 12th day and again decreased, reaching to least antioxidant activity (23% - 32%) at the end of storage period. The study on the fresh-cut pineapple fruit showed that the antioxidant activity increased during initial days of storage which subsequently declined towards the end of storage. The greater rise of antioxidant activity indicates the higher stressed condition within the tissue, as a result of cutting of fruit. As the storage time increases, the reduction may be attributed to the loss of bioactive antioxidants due to their reactions with free radicals to mitigate the consequence of minimal processing. According to Stewart et al. [39], the decrease in antioxidant capacity with prolonged storage may be due to the O^{2-} promoted oxidation of the constitutive phenolic compounds and vitamin C.

Changes in Browning-related enzymes

Polyphenol oxidase (PPO) activity

Enzymatic browning in fresh-cut fruits and vegetables occur as a result of the oxidation of phenolic compounds, catalyze by PPO and POX enzymes [40]. At 0 day of storage, PPO activity was 173.20±44.82 Units min^{-1} mg^{-1} protein (Fig. 1a). With the advance of storage period, PPO activity enhanced significantly ($p<0.05$) in all the samples. In control samples, PPO reached to its peak level i.e., 696.76±62.48 Units min^{-1} mg^{-1} protein on 4th day of storage and thereafter declined at the end of storage. The coated samples had 10% - 18% lower PPO activity as compared to that of control on 4th day of storage (Fig. 1a); thereafter, AG coated samples showed least fluctuation in PPO activity till the end of storage, while in CG and XG coated samples, it increased up to 12 days of storage. At the end of storage, coated samples displayed lower PPO activity which ranged from 361.34±24.18– 399.49±115.49 Units min^{-1} mg^{-1} protein as compared to 521.65±27.98 Units min^{-1} mg^{-1} protein in control samples. This significant variation regarding PPO activity pattern in coated and uncoated samples may be due to the incorporation of cinnamic acid in composite coating formulation.

Peroxidase (POX) activity

The POX activity also exhibited declining behavior throughout the storage period in AG and CG coated samples while XG coated samples showed reduction up to 8 days and then increased significantly at the end of storage period (Fig. 1b). POX activity measured before processing was 0.26±0.03 Units min^{-1} mg^{-1} protein. Application of AG and CG coated help diminishing the activity ~65% during 16 days of storage period. In case of uncoated samples, though POX activity declined on 12th day but at the end it rose suddenly reaching to its peak level equivalent to its initial activity. This trend could be explained by the fact that incorporation of cinnamic acid as in alginate and carrageenan solution maintained its effective amount over the cut surface of pineapple, thereby prevented induction of oxidative stress condition.

Phenylalanine ammonia lyase (PAL) activity

As a response to wounding, the PAL activation of the phenylpropanoid metabolism could be elicited through induced reactive oxygen species, which in turn initiates the accumulation of phenolic compounds during storage [41]. PAL activity measured at the time of processing was highest i.e., 4.56±0.41 Units min^{-1} mg^{-1} protein, but it decreased subsequently in all the samples reached to its minimum level with highest reduction ranged from ~61% - 75% at 12th day of storage period (Fig. 1c). After significant reduction on 12th day of storage, PAL activity had slightly increased at the end of storage in AG, CG and control

samples, while XG coated samples did not exhibit further induction in PAL activity. In the present study, the accumulation trend of TP is not correlated with the changing behavior of PAL activity during storage period of 16 days.

Sensory evaluation

The sensory evaluation was carried out based on the color, taste, texture, odor and overall acceptability of coated and uncoated samples. The sensory properties were evaluated after 6 and 12 days of storage period. The score for all sensory characteristics were significantly ($p<0.05$) higher in coated samples as compared to those of the control samples (Table 4). Among the coated samples, the application of alginate based edible coating on fresh-cut pineapple retained higher scores for all the sensory traits on 6th day of storage. After 12 days of storage period, the score values for color, texture and odor declined and reached close to the limit of market acceptability. Both XG and control samples were observed with significant decline in their sensory traits and these reached to the limit of market acceptability on 6th day, earlier than that of AG and CG coated samples.

Microbial contamination

The effect of polysaccharide based composite coatings on total plate counts and yeast and mould counts of fresh-cut pineapple fruits were evaluated after 6 and 12 days of storage (Table 5). It was revealed that total plate count increased on 6th and 12th day of storage in all the samples but remained in the range from 3.02±0.03 – 4.21±0.01 log CFU/g. However, yeasts and mold growth were found below the detection level throughout the storage period of 16 days in all the coated and uncoated samples. This beneficial effect might be result of incorporation of cinnamic acid as bioactive compound with antibrowning and antimicrobial activity.

CONCLUSION

The results obtained from this investigation indicated that the application of composite coatings enriched with cinnamic acid on fresh-cut pineapple fruits maintained color, firmness, retained ascorbic acid content, reduced the weight loss, delayed the increase in PPO and POX of coated samples as compared to those of the uncoated samples. In addition, the results of the present study also demonstrated that the proliferation of mesophilic bacteria and yeasts and molds was significantly lesser in coated samples in comparison with that of uncoated samples. Thus, it can be concluded that alginate-based composite coating could be used for the quality improvement and shelf-life extension of fresh-cut pineapple fruits up to 16 days of storage at 5°C.

ACKNOWLEDGEMENT

The authors are thankful to the Head, P.G. Department of Biosciences, Sardar Patel University, Gujarat, India for providing necessary facilities for carrying out this work.

REFERENCES

[1] Huxley, R. R., Lean, M., Crozier, A., John, J. H. and Neil, H. A.W. (2004): Effect of dietary advice to increase fruit and vegetable consumption on plasma flavonol concentrations: Results from a randomised controlled intervention trial. *Journal of Epidemiology Community Health,* **58,** 288-289.

[2] Park, H.J. (1999): Development of advanced edible coatings for fruits. *Trends in Food Science and Technology,* **10:** 254 – 260.

[3] Lin, S.Y. and Zhao, Y. (2007) Innovations in development and application of edible coatings for fresh and minimally processed fruits and vegetables. *Comprehensive Reviews in Food Science and Food Safety,* **6:** 60-75.

[4] Vargas, M., Pastor, C., Chiralt, A., McClements, D.J. and González-Martıínez, C. (2008) Recent advances in edible coatings for fresh and minimally processed fruits. *Critical Reviews in*

Food Science and Nutrition, **48:** 496-511.

[5] Shellhammer, T.H. and Krochta, J.M. (1997): Whey protein emulsion film performance as affected by lipid type amount. *Journal of Food Science,* **62:** 390 – 394.

[6] Dhall, R.K. (2013): Advances in edible coatings for fresh fruits and vegetables: a review. *Critical Reviews in Food Science and Nutrition,* **53:** 435–450.

[7] Quirós-Sauceda, A.E., Ayala-Zavala, J.F., Olivas, G.I. and González-Aguilar, G.A. (2014): Edible coatings as encapsulating matrices for bioactive compounds: a review. *Journal of Food Science and Technology,* **51:** 1674–1685.

[8] Shi, Y., Chen, Q. X, Wang, Q., Song, K. K. and Qiu, L. (2005): Inhibitory effects of cinnamic acid and its derivatives on the diphenolase activity of mushroom (*Agaricus bisporus*) tyrosinase. *Food Chemistry,* **92:** 707-712.

[9] Sharma, S. and Rao, T.V. R. (2015): Xanthan gum based edible coating enriched with cinnamic acid prevents browning and extends the shelf-life of fresh-cut pears. *LWT - Food Science and Technology,* **62:** 791-800.

[10] FDA (Food and Drug Administration) (2013): Title 21 Food and Drugs Section 172, Code of Federal Regulations. http://www.accessdata.fda.gov/scripts/cdrh/cfdocs/cfcfr/cfrsearch.cfm?fr=172.515.

[11] Dave, R.K., Rao, T.V.R. and Nandane, A.S. (2017): Improvement of post-harvest quality of pear fruit with optimized composite edible coating formulations. *Journal of Food Science and Technology,* **54**: 3917-3927.

[12] Rao, T.V.R., Baraiya, N.S., Vyas, P.B. and Patel, D.M. (2015): Composite coating of alginate-olive oil enriched with antioxidants enhances postharvest quality and shelf life of Ber fruit (*Ziziphus mauritiana* Lamk. Var. Gola). *Journal of Food Science and Technology,* **53:** 748–756.

[13] Baraiya, N. S., Rao, T. V. R. and Thakkar, V. R. (2014): Enhancement of storability and quality maintenance of carambola (*Averrhoa carambola* L.) fruit by using composite edible coating. *Fruit,* **69***:* 195–205.

[14] Eskandari, A., Heidari, M., Daneshvar, M, H. and Taheri, S. (2014): Studying effects of edible coatings of Arabic Gum and olive oil on the storage life and maintain quality of postharvest Sweet Lemon (*Citrus lemontta*). *International Journal of Agriculture and Crop Science,* **7:** 207-213.

[15] Olivas, G.I., Rodriguez, J.J. and Barbosa-Canovas, G.V. (2003): Edible coatings composed of methylcellulose, stearic acid, and additives to preserve quality of pear wedges. *Journal of Food Processing and Preservation,* **27:** 299-320.

[16] Oms-Oliu, G., Soliva-Fortuny, R. and Martín-Belloso, O. (2008): Using polysaccharide-based edible coatings to enhance quality and antioxidant properties of fresh-cut melon. *LWT - Food Science and Technology*, **41**: 1862-1870.

[17] Greener, I. and Fennema, O. (1994): Edible films and coatings: Characteristics, formation, definitions, and testing methods, In Edible coatings and films to improve food quality (Eds. Krochta, J. M., Baldwin, E. A. and Nisperos-Carriedo M. O.), Technomic Publishing Company, Inc., Lancaster, pp. 1–24.

[18] Azarakhsh, N., Osman, A., Ghazali, H. M., Tan, C. P. and Mohd Adzahan, N. (2012): Optimization of alginate and gellan-based edible coating formulations for fresh-cut pineapples. *International Food Research Journal,* **19:** 279–285.

[19] Papadakis, S. E., Abdul-Malek, S., Kamdem, R. E. and Yam, K. L. (2000): A versatile and inexpensive technique for

measuring color of foods. *Food Technology,* **54:** 48-51.

[20] Bico, S.L.S., Raposo, M.F.J., Morais, R.M.S.C. and Morais, A.M.M.B. (2009): Combined effects of chemical dip and/or carrageenan coating and/or controlled atmosphere on quality of fresh-cut banana. *Food Control,* **20:** 508–514.

[21] Roe, J. H. and Oesterling, M. J. (1944): The determination of dehydroascorbic acid and ascorbic acid in plant tissues by the 2, 4-dinitrophenylhydrazine method. *Journal of Biological Chemistry,* **152:** 511-517.

[22] Tomes, M. L. (1963): Temperature inhibition of carotene synthesis in tomato. *Botanical Gazette,* **124:** 180–185.

[23] Lim, Y. Y., Lim, T. T. and Tee, J. J. (2006): Antioxidant properties of guava fruit: comparison with some local fruits. *Sunway Academic Journal,* **3:** 9-20.

[24] Brand-Williams, W., Cuvelier, M. E. and Berset, C. (1995): Use of a free radical method to evaluate antioxidant activity. *LWT-Food Science and Technology,* **28:** 25-30.

[25] Zhu, Z. J. and Zhan, L. J. (2010): Characterization of polyphenoloxidase from water Caltrop (*Trapa acornis* Nakano) fruits. *Journal of Food Biochemistry,* **34:** 1125-1140.

[26] Mazumdar, B. C. and Majumder, K. (2003): Methods on physico-chemical analysis of fruits. Daya Publishing House, Delhi.

[27] Malik, C. P. and Singh, M. B. (1980): Plant enzymology and histo-enzymology. New Delhi, Kalyani Publishers, India.

[28] ICMSF (International Commission on Microbiological Specifications for Foods) (1978): Microorganisms in Foods. I. Their Significance and Methods of Enumeration, (2nd Ed). University of Toronto Press, Toronto.

[29] Gil, M. I., Aguayo, E. and Kader, A. A. (2006): Quality changes and nutrient retention in fresh-cut versus whole fruit during storage. *Journal of Agricultural and Food Chemistry,* **54:** 4284–4296.

[30] Benítez, S., Soro, L., Achaerandio, I., Sepulcre, F. & Pujolá, M. (2014): Combined effect of a low permeable film and edible coatings or calcium dips on the quality of fresh-cut pineapple. *Journal of Food Process Engineering,* **37**: 91–99.

[31] Soliva-Fortuny, R. C., Biosca-Biosca, M., Grigelmo-Miguel, N. and Martín-Belloso, O. (2002): Browning, polyphenol oxidase activity and headspace gas composition during storage of minimally processed pears using modified atmosphere packaging. *Journal of the Science of Food and Agriculture,* **82:** 1490–1496.

[32] Mantilla, N., Castell-Perez, M. E., Gomes, C. and Moreira, R. G. (2013): Multilayered antimicrobial edible coating and its effect on quality and shelf-life of fresh-cut pineapple (*Ananas comosus*). *LWT–Food Science and Technology***, 51:** 37–43.

[33] Neito, M. B. (2009): Structure and function of polysaccharide gum-based edible films and coatings in edible films and coatings for food applications (Eds. Embuscado M. E. & Huber, K. C.) Springer Dordrecht Heidelberg London, New York.

[34] Olivas, G.I., Mattinson, D.S. and Barbosa-Canovas, G.V. (2007): Alginate coatings for preservation of minimally processed 'Gala' apples. *Postharvest Biology and Technology,* **45:** 89-96.

[35] Klein, B.P. (1987): Nutritional consequences of minimal processing on fruits and vegetables. *Journal of Food Quality,* **10:** 179-193.

[36] Nunes, M.C.N., Brecht, J.K., Morais, A.M.M.B. and Sargent, S.A. (1998): Controlling temperature and water loss to maintain ascorbic acid levels in strawberries during postharvest handling. *Journal of Food Science,* **63:** 1033–1036.

[37] Surjadinata, B. B. and Cisneros-Zevallos, L. (2012): Biosynthesis of phenolic antioxidants in carrot tissue increases with wounding intensity. *Food Chemistry,* **134:** 615–624.

[38] De Ancos, B., Sánchez-Moreno, C., Plaza, L. and Cano, M.P. (2011): Nutritional and health aspects of fresh-cut vegetables, In Advances in Fresh-Cut Fruits and Vegetables Processing (Ed. Martín-Belloso, O. and Soliva-Fortuny R.) CRC Press, London, pp.145-184.

[39] Stewart, D., Oparka, J., Johnstone, C., Iannetta, P.P.M. and Davies, H.V. (1999): Effect of modified packaging (MAP) on soft fruit quality, In Annual report of the Scottish Crop Research Institute, Scottish Crop Research Institute, Scotland, pp. 119–124.

[40] Lamikanra, O. and Watson, M.A. (2001): Effect of ascorbic acid on peroxidase and polyphenoloxidase activities in fresh-cut cantaloupe melon. *Journal of Food Science,* **66:** 1283–1286.

[41] Becerra-Moreno, A., Redondo-Gil, M., Benavides, J., Nair, V., Cisneros-Zevallos, L. and Jacobo-Velázquez, D. A. (2015): Combined effect of water loss and wounding stress on gene activation of metabolic pathways associated with phenolic biosynthesis in carrot. *Frontiers in Plant Science,* Doi: 10.3389/fpls.2015.00837.

Table 1: Details of composite edible coatings applied on fresh-cut pineapple

Sr. No.	Treatments	Edible coating composition
1.	AG	Sodium alginate (1.29 %) + Olive oil (0.1%) + Cinnamic acid (0.1%)
2.	CG	Carrageenan (0.5 %) + Olive oil (0.1%) + Cinnamic acid (0.1%)
3.	XG	Xanthan gum (0.25 %) + Olive oil (0.1%) + Cinnamic acid (0.1%)
4.	Control	Distilled water

Table 2: Changes in color (*L and *b** values), firmness and weight loss percentage (WLP) in fresh-cut pineapple treated with composite edible coatings during storage at 5°C.**

Treatments	Storage period (Days)				
	0	4	8	12	16
			*L**		
AG	57.29±1.70^{a}	56.67±2.69^{a}	57.33±4.09^{a}	57.25±3.92^{a}	46.44±3.94^{b}
CG	57.29±1.70^{a}	58.25±2.49^{a}	57.14±3.63^{a}	53.86±4.30^{b}	51.50±2.33^{c}
XG	57.29±1.70^{b}	52.13±3.48^{c}	58.63±4.03^{b}	62.67±3.44^{a}	50.00±2.56^{d}
Control	57.29±1.70^{a}	51.57±3.05^{b}	42.57±5.26^{c}	40.89±5.60^{d}	42.38±3.78^{c}
			*b**		
AG	48.71±2.98^{a}	42.67±4.85^{b}	42.44±5.73^{b}	43.63±4.81^{b}	26.56±4.03^{c}
CG	48.71±2.98^{a}	45.63±3.46^{b}	39.29±3.35^{d}	41.57±2.22^{c}	20.38±2.50^{e}
XG	48.71±2.98^{a}	40.25±3.65^{c}	28.25±3.85^{d}	42.83±3.43^{b}	19.13±4.82^{e}
Control	48.71±2.98^{a}	23.86±4.67^{b}	25.43±4.20^{c}	18.67±8.22^{d}	16.75±6.58^{e}
			Firmness (Newton)		
AG	3.47±0.25^{a}	2.63±0.21^{b}	2.34±0.05^{b}	1.79±0.10^{c}	1.28±0.07^{c}
CG	3.47±0.25^{a}	2.70±0.20^{b}	2.62±0.39^{b}	1.50±0.10^{c}	1.29±0.08^{c}
XG	3.47±0.25^{a}	2.43±0.25^{b}	2.30±0.20^{b}	1.70±0.10^{c}	1.20±0.20^{c}
Control	3.47±0.25^{a}	2.07±0.15^{b}	1.38±0.14^{c}	1.03±0.25^{c}	1.00±0.10^{c}
			Weight loss percentage (%)		
AG	0.00±0.00^{d}	5.07±0.14^{c}	4.90±0.42c	11.97±0.09^{b}	15.86±0.51^{a}
CG	0.00±0.00^{d}	7.37±0.03^{c}	8.57±0.06^{c}	13.43±0.09^{b}	23.90±0.34^{a}
XG	0.00±0.00^{e}	6.73±0.15^{d}	16.30±0.04^{c}	18.97±0.09^{b}	37.42±0.03^{a}
Control	0.00±0.00^{d}	15.70±0.43^{c}	32.93±0.42^{b}	37.37±0.11^{a}	36.30±0.33^{a}

Means within the row represented by different superscript letters are significantly different at $p< 0.05$ using Tukey's Multiple Comparison Test. The values represented (a-d) in the results indicated the range from higher to lower rank. AG – Sodium alginate, CG - Carrageenan and XG – Xanthan gum.

Table 3: Changes in ascorbic acid, carotenoids, total phenolics and antioxidant activity in fresh-cut pineapple treated with composite edible coatings during storage at 5°C.

Treatments	Storage period (Days)				
	0	4	8	12	16
	Vitamin C (mg.100g^{-1})				
AG	67.36±1.59^{c}	63.19±9.85^{d}	61.80±6.33^{e}	73.26±2.76^{b}	84.03±5.41^{a}
CG	67.36±1.59^{c}	68.75±0.60^{c}	64.58±2.17^{d}	77.78±9.68^{b}	92.01±1.05^{a}
XG	67.36±1.59^{c}	67.71±4.17^{c}	66.67±10.05^{d}	70.83±2.08^{b}	96.18±10.49^{a}
Control	67.36±1.59^{e}	81.94±2.62^{d}	87.85±5.74^{c}	109.38±3.61^{a}	105.21±4.77^{b}
	Carotenoids (µg.g^{-1})				
AG	9.97±0.13^{b}	10.23±0.96^{a}	9.91±0.16^{b}	6.69±0.08^{c}	5.64±0.00^{d}
CG	9.97±0.13^{a}	9.27±0.36^{a}	5.29±0.19^{b}	3.47±0.06^{c}	3.00±0.08^{c}
XG	9.97±0.13^{a}	6.09±0.19^{b}	5.56±0.11^{c}	3.17±0.19^{d}	2.87±0.02^{e}
Control	9.97±0.13^{a}	8.75±0.16^{b}	5.91±0.10^{c}	5.15±0.16^{c}	3.04±0.04^{d}
	Total phenolics content (mg.g^{-1})				
AG	3.49±0.29^{b}	3.97±0.25^{b}	4.04±0.03^{a}	4.21±0.21^{a}	4.42±0.14^{a}
CG	3.49±0.29^{b}	3.46±0.39^{b}	3.97±0.01^{b}	4.43±0.23^{a}	3.96±0.11^{b}
XG	3.49±0.29^{b}	3.39±0.07^{b}	4.44±0.16^{a}	4.14±0.38^{a}	3.30±0.07^{b}
Control	3.49±0.29^{b}	4.24±0.26^{a}	3.72±0.25^{b}	3.55±0.12^{b}	4.62±0.16^{a}
	Antioxidant activity (%)				
AG	58.54±3.80^{b}	49.64±1.75^{c}	49.15±1.62^{c}	85.45±8.11^{a}	31.96±3.88^{c}
CG	58.54±3.80^{c}	48.82±3.93^{d}	63.92±6.59^{b}	73.42±5.21^{a}	26.91±1.78^{e}
XG	58.54±3.80^{c}	79.79±1.68^{b}	83.58±3.52^{a}	78.34±2.52^{b}	22.79±3.66^{d}
Control	58.54±3.80^{d}	92.55±1.43^{a}	79.29±2.48^{b}	68.94±4.16^{c}	33.59±1.89^{e}

Means within the row represented by different superscript letters are significantly different at $p< 0.05$ using Tukey's Multiple Comparison Test. The values represented (a-d) in the results indicated the range from higher to lower rank. AG – Sodium alginate, CG - Carrageenan and XG – Xanthan gum.

Table 4: Changes in sensory attributes in fresh-cut pineapple treated with composite edible coatings after 6 and 12 days of storage at 5°C.

Treatments	6th day of storage				
	Color	taste	texture	odor	overall acceptability
AG	8.03±0.50[a]	8.27±0.25[a]	7.73±0.40[a]	7.90±0.36[a]	7.98±0.25[a]
CG	7.27±0.25a	8.17±0.29[a]	7.80±0.26[a]	7.63±0.15[a]	7.72±0.17[a]
XG	7.37±0.12[a]	7.80±0.26[a]	7.60±0.36[a]	7.17±0.15[a]	7.48±0.17[a]
Control	2.83±0.29[b]	5.50±0.50[b]	4.67±0.29[b]	3.77±0.68[b]	4.19±0.39[b]
Treatments	**12th day of storage**				
	Color	taste	texture	odor	overall acceptability
AG	6.67±0.29[a]	7.53±0.25[a]	5.17±0.15[a]	6.27±0.25[a]	6.41±0.09[a]
CG	5.83±0.29[b]	7.67±0.32[a]	4.67±0.29[b]	6.07±0.12[b]	6.06±0.05[b]
XG	3.93±0.40[c]	3.27±0.25[b]	3.00±0.00[c]	4.83±0.29[c]	3.76±0.12[c]
Control	1.00±0.20[d]	0.00±0.00[c]	1.07±0.12[d]	0.83±0.15[d]	0.73±0.04[d]

Means within the column represented by different superscript letters are significantly different at $p< 0.05$ using Tukey's Multiple Comparison Test. The values represented (a-d) in the results indicated the range from higher to lower rank. AG – Sodium alginate, CG - Carrageenan and XG – Xanthan gum.

Table 5: Microbial contamination in fresh-cut pineapple treated with composite edible coatings after 6 and 12 days of storage at 5°C.

Treatments	Storage period (Days)		
	0	6	12
Total plate count (log CFU/g)			
AG	3.02±0.03[b]	3.48±0.02[ab]	4.07±0.03[a]
CG	3.02±0.03[b]	3.51±0.09[ab]	3.79±0.06[a]
XG	3.02±0.03[a]	3.56±0.08[a]	3.67±0.05[a]
Control	3.02±0.03[b]	3.92±0.04[ab]	4.21±0.01[a]
Yeasts and molds*			

Means within the row represented by different superscript letters are significantly different at $p<0.05$ using Tukey's Multiple Comparison Test. The values represented (a-d) in the results indicated the range from higher to lower rank. AG – Sodium alginate, CG - Carrageenan and XG – Xanthan gum.*Below the detection level.

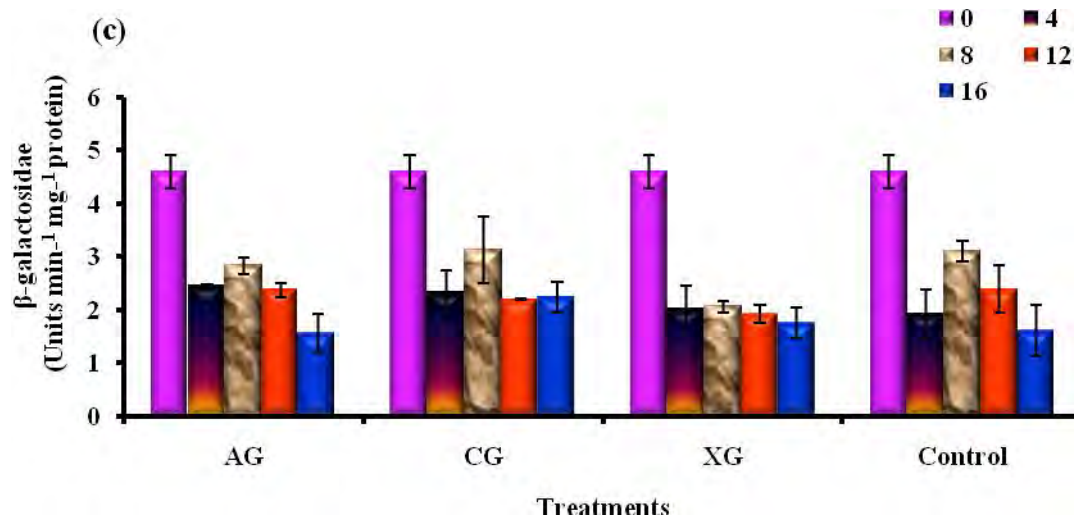
(c)
0
4
8
12
16
β-galactosidae (Units min-1 mg-1 protein)
0
1
2
3
4
5
6
AG
CG
XG
Control
Treatments

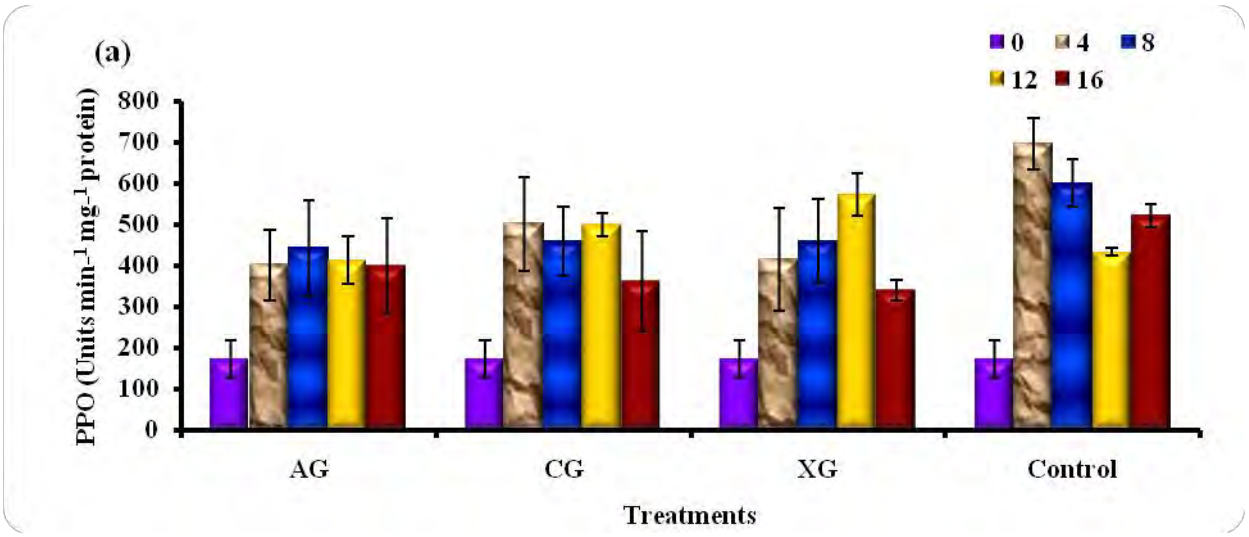
(a)
0
4
8
12
16
PPO (Units min-1 mg-1 protein)
0
100
200
300
400
500
600
700
800
AG
CG
XG
Control
Treatments

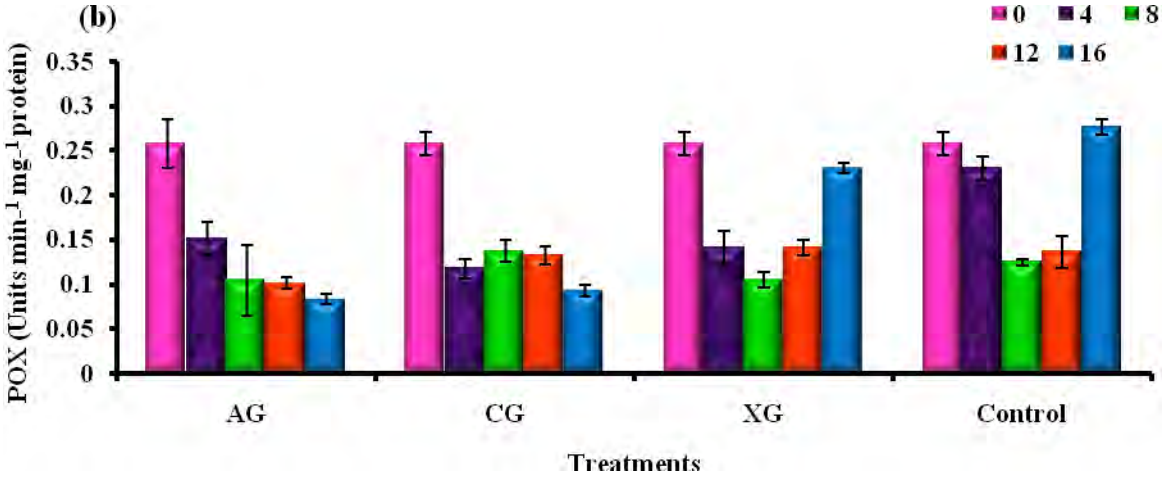
(b)
0
4
8
12
16
POX (Units min-1 mg-1 protein)
0
0.05
0.1
0.15
0.2
0.25
0.3
0.35
AG
CG
XG
Control
Treatments

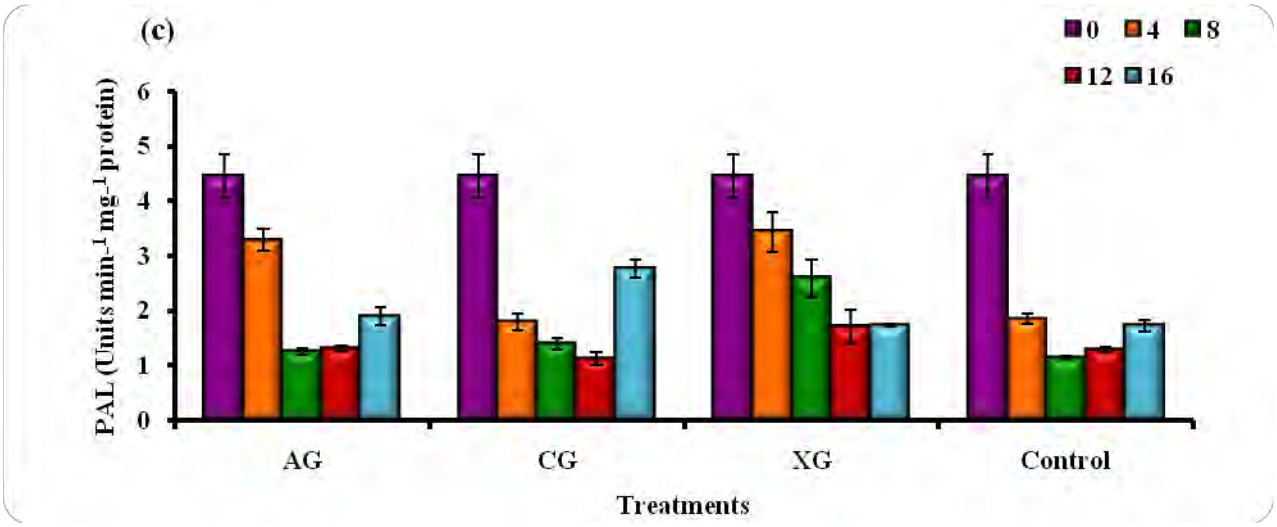

Figure 1 Changes in specific activity of (a) Polyphenol oxidase (PPO), (b) Peroxidase (POX) and (c) Phenylalanine ammonia lyase (PAL) in fresh-cut pineapple treated with composite edible coatings during storage at 5°C. Here, AG – Sodium alginate, CG - Carrageenan and XG – Xanthan gum.

PRAJÑĀ - Journal of Pure and Applied Sciences Vol. 26 : 24 – 37 (2018)
ISSN 0975 - 2595

IMPROVEMENT OF POSTHARVEST QUALITY AND SHELF LIFE OF CAPE GOOSEBERRY (*PHYSALIS PERUVIANA* L.) FRUIT WITH BIOACTIVE COMPOSITE COATINGS DURING LOW TEMPERATURE STORAGE

PINAL B. VYAS, T. V. RAMANA RAO* AND V. R. THAKKAR

Department of Biosciences, Sardar Patel University, Vallabh Vidyanagar – 388120, Gujarat

Email: tadapanenirao@yahoo.com

ABSTRACT

The functionality of xanthan gum and guar gum was evaluated individually and in combination with olive oil on the qualitative properties of cape gooseberry fruit stored at the lower temperature (10±1 ˚C) at a regular interval of 5 days. On the 10th day of the storage period, the maximum hardness (8 N) was seen in the cape gooseberry fruit treated with xanthan gum 0.5% (T1), whereas minimum (4.7 N) hardness occurred in untreated (C) cape gooseberry fruit. The lower activity of softening enzymes was noticed in cape gooseberry treated with xanthan gum followed by xanthan gum enriched with olive oil. The shelf life of uncoated fruits was up to 17 days, whereas fruits coated with xanthan gum had extended shelf life up to 9 days more. This study showed that 0.5% xanthan gum alone and its combination with olive oil delayed the ripening of cape gooseberries as compared to that of the control and other coated fruits.

Key words: Composite edible coating, Guar gum, Physalis peruviana L., Shelf life, Xanthan gum

INTRODUCTION

Cape gooseberries or golden berries (*Physalis peruviana*) are popular fruits known for their organoleptic properties such as flavor, odor, and color, nutritional value (vitamins A and C, potassium, phosphorous, and calcium), and health benefits [1].The fruit is named as cape gooseberry because it is first cultivated in the Cape of Good Hope in South Africa and in India it is commonly known as “Rasbhari” [1]. Cape gooseberries as reported to have more antioxidants than goji berries, broccoli, apples and pomegranates. Cape gooseberries contain twice the vitamin C of lemons hence they have magnificent antioxidants that help to fend off cardiovascular disease, strokes and cancer. The fruit is enclosed in a papery husk or calyx, and is around 2 cm wide, 4–5 g in weight, with a smooth, orange–yellow skin and juicy pulp containing abundant small yellowish seeds. During ripening the fruit color turns from green to orange due to the breakdown of chlorophyll and accumulation of carotenoid (mainly carotene for this berry), and progressive softening occurs [2]. When fully ripe, the fruit is sweet with a pleasant grape-like tang [3]. The fruit is eaten fresh, in cocktails or in salads, or cooked. The fruit is very high in pectin and makes excellent pies and jellies [4]. It has been introduced as a specialized culture in warm regions worldwide, particularly in some American countries as well as in specific areas of Oceania (Australia and New Zealand), Asia (India) and Central and South Africa [5].
Use of edible coatings is a technology which helps to extend the shelf life and to retain the nutritional properties of fruit. Thus, the application of edible composite coatings would be an effective measure for the postharvest shelf life improvement and avoid high product loss of cape gooseberry fruit.

Gums in edible forming preparation are used for their texturizing capabilities. All gums are polysaccharides composed of sugars other than glucose [6]. Guar gum is a polysaccharide composed of the sugars, galactose and mannose. Guar gum is more soluble and it is a better stabilizer. It is nonionic and hydro colloidal. Guar gum has been reported to extend the postharvest shelf life of apple, cucumber and tomato [7]. Xanthan gum, synthesized as an exo-polysaccharide by *Xanthomonas campestris* under unfavorable conditions, is a Generally

Recognized as Safe (GRAS) compound (FDA, 21CFR172.695, 2013) for its use as a stabilizer, thickener or emulsifier. It forms an extremely viscous solution in hot or cold water at low concentration with outstanding stability over a wide range of pH and temperature and it is also resistant to enzymatic degradation. Moreover, it facilitates the suspension of particulates, even in complex formulations for a long time [8]. It is widely used in foods because of its good solubility in either hot or cold solutions, high viscosity even at very low concentrations, and excellent thermal stability. Xanthan gum forms very viscous solutions and at sufficiently high polymer concentration, it exhibits frail gel-like properties [9]. For that reason, lipid component can be incorporated to enhance the film forming property of the xanthan gum to be used as a coating material. Olive oil is such lipid component which is composed of 56.3–86.5% monounsaturated fatty acids (MUFA) and extensively consumed due to its nutritional value and its organoleptic characteristics.

In view of the above reports, the current study has been undertaken to evaluate the potential of postharvest treatments of guar gum and xanthan gum and also their combinations with olive oil as a composite coating on the shelf life and physicochemical characteristics of cape gooseberry fruit during its substantial postharvest loss.

METHODOLOGY

Fruit Source

Cape gooseberry fruits used in the present study were purchased from the fruit market of Anand, Gujarat, India and they were graded for their uniformity in size, shape and color and the fruits free from any mechanical injury were selected.

Chemicals

Xanthan gum ($C_{35}H_{49}O_{29}$, monomer) and guar gum of Himedia brand, Mumbai (India) were procured through local chemical vendors; whereas the food-grade refined olive oil (92 % purity) was purchased from the local market of Anand town, Gujarat (India).

Methodology of Film-Forming Dispersions

Xanthan gum (0.5%, w/v) was initially dispersed in hot water and stirred at 80 °C for 2 hr. and this coating solution was labeled as T1. Guar gum was prepared by dissolving 0.5 g of powder in 100 ml of distilled water and stirred for 1 hr. at room temperature. Glycerol (0.75%) was added as a plasticizer and the solution was stirred for 10 min under the same conditions and labeled as a T2. To make the composite coating, xanthan gum (0.25%) and guar gum (0.25%) powder were added in distilled water and stirred for 2 hr. and labeled as T3. Olive oil 0.2% (v/v) was added separately to the solutions of xanthan gum (0.5%) and guar gum (0.5%) and stirred using a magnetic stirrer (2 MLH, Remi equipments, India), at 80 °C, for 30 min. and labeled as T4 and T5 respectively. To the composite coating of xanthan gum (0.25%) + guar gum (0.25%) olive oil was added and labeled as T6 (Table 1).

Application of Edible Coatings

Cape gooseberry fruits were surface disinfected by immersing them in 2% sodium hypochlorite solution for 2 min, washed, and air-dried for 30 min. at room temperature. The fruit were randomly categorized into seven groups, having 200 g in each, and each group was in two replicates. Six groups were assigned to coating treatments (T) as follows: Xanthan gum 0.5% (T1), Guar gum 0.5% (T2), Xanthan gum 0.25% + Guar gum 0.25% (T3), Xanthan gum 0.5% + Olive oil 0.2% (T4), Guar gum 0.5% + Olive oil 0.2% (T5), Xanthan gum 0.25% + Guar gum 0.25% + Olive oil 0.2% (T6) and fruit dipped in distilled water, designed as control (C) samples. The treatments include dipping of fruits for 3 min. in coating solutions. Residual solutions of fruit were allowed to drain off and the fruit were dried at 26±2 ˚C for 30min., and then these samples were placed in clamshells and were stored at 10±1 ˚ C and 40–45%

relative humidity (R.H.). The fruits of treatments as well as control were evaluated for the following quality attributes at the beginning of the experiment (i.e., 0 day) and after 5, 10, 15, and 20 days of their storage period. For control fruit, the data were recorded only up to 15 days of storage period, as subsequently, they began to decompose.

Determination of Physicochemical Attributes

Total Soluble Solids (TSS)

Total soluble solids (TSS) content of fruit was determined by using refractrometer (Atago Co., Tokyo, Japan). Homogenous sample was prepared by blending the cape gooseberry fruit. The sample was thoroughly mixed and a few drops of juicy fruit pulp were taken on prism of refractrometer and direct reading was taken by reading the scale in meter as described in AOAC [10].

Determination of Biochemical Attributes

Total sugars were estimated by following the phenol-sulphuric acid method cited by Thimmaiah [11]. Estimation of total phenolics content (TPC) was carried out according to the method described by Mc Donald *et al.* [12]. The quantitative analysis of ascorbic acid was carried by using dinitro-phenyl hydrazine (DNPH) method described by Roe and Kuether [13].

Determination of Firmness

Firmness was measured as the maximum penetration force (N) reached during tissue breakage, using a Texture Analyzer (Lloyd instruments ltd, type TG 34) with a 36 mm diameter flat probe. The penetration depth was 5 mm and the cross-head speed was 40 mm/min. Two replicates were used for each determination. The firmness was reported as peak force and expressed in Newton per gram (N/g) of the cape gooseberry sample [14].

Physiological weight loss (PLW)

The weight loss was calculated with the following formula:

$$Weight\ loss = \frac{[m0-m1]}{m0} \times 100 \qquad (1)$$

Where $m0$ is the initial weight and $m1$ is the weight measured during storage.

Enzyme Extraction and Assay of Polygalacturonase (PG) (EC 3.2.1.15) and Pectate lyase (PL) (EC 4.2.2.2)

Extraction of cell wall softening enzymes and assay was carried out by following the method cited by Lohani *et al.,* [15].

Postharvest Marketable (Shelf Life) Period

The shelf life of cape gooseberry fruit was calculated by counting the days required for them to attain the last stage of ripening, but up to the stage when they remained acceptable for marketability [16].

Statistical Analyses

The data presented in this paper was statistically analyzed by SPSS 17 software and the mean and standard deviation (SD) were calculated. The statistical significance of the data was assessed by one way analysis of variance and LSD test. Mean comparisons were performed using HSD of Tukey's test to examine if differences between treatments and storage time were significant at $P < 0.05$. The overall least significance difference (LSD; $p \leq 0.05$) was calculated and used to detect significant differences among all the treatments and control set [17].

RESULTS AND DISCUSSION

Effect of Edible Coatings on PLW

Cape gooseberries are extremely inclined to rapid water loss which results in shrinkage of fruit and weakening of the tissue due to their very thin skin, because weight loss

is associated with respiration and the transpiration processes of fruit. The effect of edible coating treatments on PLW of cape gooseberries stored at lower temperature was found to be significant ($p<0.05$) as shown in Figure 1a. The results of the current study suggest that during the storage period, the least PLW occurs on the 10th day in the fruits treated with T1 (15.6 %), while the higher level of it was observed in the control set of fruit on the 10th day (24.4 %) and on the 15th day (40%). In this regard, Rojas-Argudo [18] explained that the effectiveness of polysaccharide coatings as a water barrier can be enhanced by the incorporation of lipids. In the present study, addition of a lipid component such as olive oil and glycerol significantly enhanced the effectiveness of xanthan gum, indicating their regulation of the hydrophilic-hydrophobic balance, which would in turn; restrict the water loss from the fruit. Kittur *et al*. [19] reported the reduced weight loss in banana fruit coated with polysaccharide-based composite coatings as compared to that of uncoated. Thomas *et al.* [20] also noticed that the composite oil coating preserves the quality of fruit retarding ethylene emission and hence reduce PLW in pineapple fruits.

Effect of Coatings on TSS content and Total Sugars

The level of total soluble solids (ºBrix) of control and coated cape gooseberry fruits showed significant ($p<0.05$) difference (Table 2). Overall, a gradual increase in TSS was observed during the entire storage period. The TSS content in fresh cape gooseberry fruit (i.e. at day 0) was 0.73˚ brix and the amount of TSS had increased with the increase of storage period up to 25 days. The accumulation of TSS was found to be higher in the fruit of the control set during their 5th and 10th days of storage. This increase of TSS in control fruits might be due to hydrolysis of acids and deposition of polysaccharides during storage as reported by Trivedi *et al.,* [15]. The highest value of TSS (i.e.1.9 brix) was observed in the untreated (control) fruit after 10 days of the storage period, whereas fruits treated with T1 (i.e. 1.2 ˚brix) and T5 (1.3 ˚brix) showed lower accumulation of TSS content. In this regard, Debeaufort *et al.* [21] explained that the edible coatings are selective barriers to O_2 and CO_2 modifying internal atmospheres and slowing down the respiration rate of fruit. Vyas *et al.* [22] also reported that the polysaccharide-based coating of carboxymethyl cellulose slows down the accumulation of TSS in papaya fruit.

Total sugars are considered good index for the determination of storage life. The effect of edible coatings on the total sugar content of cape gooseberries was significant ($p<0.05$) as compared to control (Table 2). An increase in the content of total sugars was observed initially in both treated as well as untreated fruits. The total sugar content of cape gooseberry fruit at 0 days of storage period was 64.61 mg g^{-1}. The increasing trend of total sugars of fruits was observed up to 5 days of storage and then decreased under all treatments. This might be due to rapid conservation of polysaccharides into sugars in the earlier stage and later for utilization of sugars in respiration. However, the delayed increase was noticed in cape gooseberries coated with 0.5 % xanthan gum (70.58 mg g^{-1}) as compared to that of the control fruit (108.5 mg g^{-1}). The reason for higher total sugar content in the uncoated sample may be due to decreased rate of respiration in coated samples where the utilization of sugar as a respiratory substrate also decreases. In this regard, Rohani *et al.* [23] also reported that the slower respiration also slows down the synthesis and use of metabolites resulting in lower sugars in coated fruits.

Effect of Coatings on Cell Wall Softening Enzymes and its Relation with Firmness of Cape gooseberry Fruit

Softening is one of the main factors determining fruit quality, and it can induce the onset of infections and physical injuries. The effect of edible coating treatments on the

firmness of cape gooseberries stored at lower temperature was found to be significant ($p<0.05$), as shown in Figure 1b. Firmness of cape gooseberry fruit i.e. at 5 days of storage period, was observed lesser in untreated fruits (5.45 N/g), whereas higher firmness was noticed in cape gooseberry fruit treated with T1 (9.21N/g) Apparently, at end of the storage the higher firmness was retained in cape gooseberry fruit treated with T1 and T5 as compared to that of other treatments as well as control set of fruit. This is in agreement with Zapata *et al.* [24] who explained that the firmness retention in coated fruit could be due to a reduction in pectinesterase and polygalacturonase enzymatic activities, which are responsible for depolymerization or shortening of chain length of pectin substances at the cell wall and thus degradation of insoluble proto-pectins to the more soluble pectins and pectic acid. Low oxygen and high carbon dioxide concentrations reduce the activities of these enzymes and allow retention of the firmness during storage [25]. Hence, results of present study aptly support the findings by Pandey *et al.* [26] who reported that the composite edible coatings preserve the quality of fruits, retard ethylene emission and enhance texture. Rao *et al.* [27] also reported that the polysaccharide-based sodium alginate composite coating delays the decline of firmness of ber fruit compared to that of the control.

Enzymes involved in pectin degradation, are closely related to changes in pectins, which play an important role in the softening changes in fruit and vegetable tissues [28]. The dramatic changes associated with the pectin contents can be accredited to the reality that pectin is most subject to enzymatic changes and shows the highest water solubility among the polysaccharides during ripening and storage [29].

There was a significant ($p<0.05$) change in activity of PG of coated cape gooseberries as shown in Figure 2a. In the present study, the activity of PG enzyme of freshly harvested cape gooseberries was 0.0045 U/mg protein. On the 10^{th} day of the storage period the significant results were noticed in treated fruits. The activity of untreated cape gooseberry fruit was 0.08 U/mg protein, whereas the activity was lower in fruits treated with T1 and T3 (i.e. 0.04 U/mg protein and 0.043 U/mg protein). The interpretation is given by Yaman and Bayoindirli [30] supports the results of the present study. According to these authors, the low oxygen and high carbon dioxide concentrations reduces the activity of enzymes and allows retention of the firmness of fruits during storage. In this study, the relatively lower activities of PG and PL in the xanthan gum coated fruits contributed to the enhanced retention of firmness during storage.

Data presented in Figure 2b shows the activity of PL form 0 day to the end of the storage period. The activity of PL enzyme on 0 days (freshly harvested cape gooseberries) of storage period was 0.0041 U/mg protein. On the 5^{th} day of the storage period, the activity of the enzyme was noticed higher in untreated fruits (0.020 U/mg protein), whereas the lower activity was noticed in fruits treated with T1 and T2 (i.e. 0.017 U/mg protein and 0.018 U/mg protein respectively). As explained by Conforti and Zinck [31], the increases in senescence most likely speeds up the metabolic process which in turn may increase the activity level of the endogenous pectin-degrading enzymes.

Effect of Coatings on Bioactive Compounds of Cape gooseberry Fruit during its Storage at Low Temperature

Carotenoids

Carotenoids are one type of plant pigments responsible for the yellow color of the fruit. They contribute to the major nutritional value of cape gooseberry fruit. As the color index and maturity increase with storage and ripening, the amount of carotenoid accumulation also increase [32]. The statistical analysis showed that edible coating had a significant ($p<0.05$) effect on carotenoids of cape gooseberries during the storage period

(Table 3). In the present study, the level of carotene in cape gooseberry fruit was noticed to increase up to some extent and then started to decline towards the end of the storage period as presented in Table 3. Nevertheless, more amount of carotene was retained in the treated cape gooseberry fruit as compared to that of the untreated fruit of cape gooseberry. The amount of carotene in freshly harvested cape gooseberry fruit was 0.07 µg/g. The higher amount was observed in fruits treated with xanthan gum (0.5%) was 0.072 µg/g, whereas its amount in control fruits was 0.058 µg/g only. Guar gum and xanthan gum were effective in maintaining the quality of carotene in cape gooseberry fruit at low temperature storage. Similarly Saha *et al.* [7] also reported that persimmon fruit coated with 1% guar gum exhibit more retention of carotene as compared to that of the uncoated persimmon fruit.

TPC

There was a significant change in TPC content of coated cape gooseberries ($p<0.05$), as shown in Table 3. Phenolic compounds are beneficial compounds mainly found in fruits and vegetables. They have been implicated in the reduction of degenerative diseases in human beings, primarily because of their antioxidant potential. Phenols have been reported to exhibit antioxidant activity [33], and it is well known that total phenolic compounds contribute to fruit quality and nutritional value by modifying color, taste, aroma, and flavor and also by providing beneficial health effects. In the present study as shown in Table 3, the content of phenols in the treated as well as untreated fruits, were found to get increased during the early storage days and then decreased subsequently. Treated fruits showed a higher amount of phenols as compared to that of the untreated fruits indicating the positive effects of xanthan gum and guar gum. Among all the treatments, the fruits coated with T3 showed higher level of phenols, i.e., 0.959 mg/g on 5th days of storage period. As predictable, throughout the storage period, the least amount of phenolics was noticed in the control fruits. In addition, as guar gum contains a higher amount of phenols, it helped in enhancing the level of phenols in cape gooseberry fruits and therefore, extended their shelf life. The decreasing of phenolic compounds at the end of storage might be due to the breakdown of cell structure so as to senescence phenomena during storage [34]. Similarly, Carvalho *et al.* [35] noticed that the edible coating of sodium alginate preserves the total phenolic and carotenoid content during cold storage of cape gooseberries.

Ascorbic Acid

Ascorbic acid one of the most important nutritional quality factors is present in plant tissues undergoing active growth and development. It is easily oxidized, especially in aqueous solutions, and greatly favored by the presence of oxygen and the losses are enhanced by extended storage, higher temperature, low relative humidity, physical damage and chilling injury [36]. As the results of the present study revealed that the retention of the ascorbic acid content was extremely affected by the treatment with edible coating solutions and storage time. Although the ascorbic acid content of both coated as well as control samples decreased throughout their storage, the use of xanthan gum and guar gum coatings have significantly ($P < 0.05$) reduced the loss of the ascorbic acid content in cape gooseberry fruit (Table 3). The higher amount of ascorbic acid was noticed in fruits treated with T1 and T5 (i.e. 201.25 mg 100g^{-1} and 322.91 mg 100g^{-1}) on 15th days of storage period, whereas 125.62 mg 100g^{-1} amount was noticed in uncoated fruits. Similar ascorbic acid levels were previously indicated for cape gooseberry fruit [2]. These results revealed that at the end of the storage, amongst all of the coatings, the xanthan gum (0.5%) coating was showing potential of retaining of ascorbic acid at a higher level.

Effect of Coatings on Postharvest Shelf Life

During the course of the present study, the protective role of the composite coatings along with the olive oil could be observed in reducing the decay incidence and extending the shelf life of cape gooseberry fruit. Among all the treatments, the treatment T1 (Xanthan gum) was the best in maintaining the quality, whereas the T2, T3 and T4 showed the significant effect of decay control. Coating of xanthan gum (T1) extended the shelf life up to 9 days as compared to that of the uncoated fruit which had shelf life up to 17 days only. In this regard, Guilbert *et al.* [37] explained that an edible coating act as a barrier to the external elements (factors such as moisture, oil and vapor) and thus protect the product and extend the shelf-life. Maftoonazad and Ramaswamy [38] also stated that the coating slows down the respiration rate, reduces the color changes of skin and flesh and increases the shelf life of fruits. Baraiya *et al.* [39] also reported the advantage of xanthan gum coating enriched with olive oil in prolongation of the postharvest life of the grapes stored at low temperature.

CONCLUSION

During the course of the present study, the coating of xanthan gum and guar gum incorporated with olive oil had prolonged the shelf life with better quality than that of the control fruit. Delayed increase in TSS and total sugars suggest that the xanthan gum (T1), as a preservative material, could delay the ripening process by slowing down the respiration and metabolic rate in cape gooseberry fruit. Moreover, the use of guar gum was effective on TPC of cape gooseberries. Furthermore, xanthan gum alone and with olive oil not only extended the storage life of cape gooseberry fruit but also retained their firmness along with the activity of cell wall softening enzymes during their storage and delayed the ripening process. The best effect on quality maintenance was achieved with the xanthan gum alone with a carrier of olive oil. Therefore, the composite coating of xanthan gum enriched with olive oil is promising as a composite edible coating to be used to enhance the shelf life and quality of cape gooseberry fruit.

ACKNOWLEDGEMENTS

The authors express gratitude to the Head, Department of Biosciences, Sardar Patel University, Gujarat, INDIA for providing necessary facilities for carrying out this work. We are also grateful to Dr. A. S. Nandane, who helped us to carry out the texture analysis of our samples at A. D. Patel Institute of Technology, New Vallabh Vidyanagar.

REFERENCES

[1] Erkaya, T., Daodemir, E., and Engul, M. (2012) Influence of cape gooseberry (*Physalis peruviana* L.) addition on the chemical and sensory characteristics and mineral concentrations of ice cream. *Food Research International,* **45*:*** 331–335**.**

[2] Gutierrez, M.S., Trinchero, G.D., Cerri, A.M., Vilella, F. and Sozzi, G.O. (2008) Different responses of goldenberry fruit treated at four maturity stages with the ethylene antagonist 1-methylcyclopropene. *Postharvest Biology and Technology,* **48:** 199–205.

[3] Morton, J. (1987) Cape gooseberry. In: Morton, J.F. (Ed.), Fruits of Warm Climates. Miami, Florida, pp. 430–434.

[4] Mc Cain, R., (1993) Golden berry, passion fruit and white sapote: potential fruits for cool subtropical areas. In: Janick, J., Simon, J.E. (Eds.), New Crops. John Wiley & Sons Inc., New York, pp. 479–486.

[5] Klinac, D.J. (1986) Cape gooseberry (*Physalis peruviana*) production

systems. *New Zealand Journal of Experimental Agriculture,* **14:** 425–430.

[6] Williams, P. A.; Phillips, G. O. (2000) In Handbook of hydrocolloids; Ed.; pp 1-19. CRC Press, Cambridge, England.

[7] Saha A., Gupta R. K., Sharma R.R., Kumar, K. and Tyagi Y. (2015) Edible coating and its effect on shelf life and quality of 'Hachiya', an astringent variety of persimmon fruit. *Asian Journal of Biochemical and Pharmaceutical Research,* **3:**182-192.

[8] Sworn, G. (2009) Xanthan gum. In G. O. Phillips, & P. A. Williams (Eds.), Handbook of hydrocolloids (p. 186). CRC Press, Wood head Publishing Ltd. Cambridge, UK.

[9] Izydorczyk, M., Steve, W.C. and Wang, Q. (2005) Polysaccharide Gums: Structures, Functional Properties, and Applications, Food Carbohydrates, Chemistry, Physical Properties and Applications, Chapter 6. CRC Press, Taylor & Francis Group, Boca Raton, FL 33487-2742.

[10] Association of Official Analytical Chemists (AOAC International) (1994) Official Methods of Analysis.16th ed. Virginia, USA.

[11] Thimmaiah, S. (1999) Standard methods of Bio-chemical analysis. Kalyani Publishers, New Delhi, India.

[12] McDonald, S., Prenzler, P.D., Autolovich, M. and Robards K. (2001) Phenolic content and antioxidant activity of olive extracts. *Food Chemistry,* **73:**73-84.

[13] Roe, J.H. and Kuether, C.A. (1943) The determination of ascorbic acid in whole blood and urine through the 2, 4, Dinitrophenylhydrazine derivative of Dehydro Ascorbic acid. *Journal of Biological chemistry,* **147 (2):** 399-407.

[14] Munoz, P. H., Almenar E., Del Valle, V. and Gavara R. (2008) Effect of chitosan coating combined with postharvest calcium treatment on strawberry (*Fragaria ananassa L.*) quality during refrigerated storage. *Food Chemistry* **10 (2):** 428-435.

[15] Lohani, S., Trivedi, P.K. and Nath, P. (2004) Changes in activities of cell wall hydrolases during ethylene-induced ripening in banana: effect of 1-MCP, ABA and IAA. *Postharvest Biology and Technoogy,* **31***:* 119–126.

[16] Mondal, M.F. 2000. Production and Storage of Fruits (in Bangla). Published by Mrs. Afia Mondal. BAU Campus, Mymsningh-2202. pp. 312.

[17] Bico, S.L.S, Raposo M.F.J, Morais, R.M.S.C and Morais, A.M.M. (2009) Combined effects of chemical dip and/or carrageenan coating and/or controlled atmosphere on quality of fresh cut banana. *Food Control,* **20:**508–514.

[18] Rojas-Argudo, C, Del Río M.A. and Perez-Gago, M.B. (2009) Development and optimization of locust bean gum (LBG) based edible coatings for postharvest storage of Fortune mandarins. *Postharvest Biology and Technology,* **52:** 227–234.

[19] Kittur, F. S., Saroja, N., Habibunnisa, and Tharanathan, R. N. (2001) Polysaccharide based composite coating formulations for shelf-life extension of fresh banana and mango. *European Food Research Technology,* **213:** 306–311.

[20] Thomas, S.A., Molina, E-Bosques, Stolik, S. and Sanchez, F. (2005) Composite oil coating preserves the quality of pineapple fruits. *Journal of Physics,* **125:**889–892.

[21] Debeaufort, F.J., Quezada-Gallo, A. and Voilley, A. (1998) Edible films and coatings: tomorrow's packaging: a review. *Critical Review in Food Science and Nutrition,* **38***:* 299-313.

[22] Vyas, P.B., Gol, N.B. and Rao, T.V.R. (2014) Postharvest quality maintenance of papaya fruit by using polysaccharide based edible coatings. *International Journal of Fruit Science,* **14 (1):**81–94.

[23] Rohani, M. Y., Zaipun, M. Z. and Norhayati, M. (1997) Effect of modified atmosphere on the storage life and quality of Eksotika papaya. *Journal of Tropical Agriculture and Food Science,* **25:** 103–113.

[24] Zapata, P. J., Guille, F., Martinez-Romero, D., Castillo, S., Valero, D. and Serrano, M. (2008) Use of alginate or zein as edible coatings to delay postharvest ripening process and to maintain tomato (*Solanum lycopersicon* Mill) quality. *Journal of Food Science and Agriculture,* **88:** 1287–1293.

[25] Salunkhe, D. K., Boun, H. R. and Reddy, N. R. (1991) Storage processing and nutritional quality of fruits and vegetables, Vol. 1. Fresh Fruits and vegetables. CRC Press Inc. Bostan

[26] Pandey, S. K. Jean, Joshua, E. and Bisen, A. (2012) Influence of gamma irradiation, growth retardants and coatings on the shelf life of winter guava fruits (*Psidium guajava L.*). *Journal of Food Science and Technology,* **49 (6):** 753–759.

[27] Rao, T.V.R., Baraiya, N.S., Vyas, P B. and Patel, D.M. (2015) Composite coating of alginate-oilve oil enriched with antioxidants enhances postharvest quality and shelf life of ber fruit (*Ziziphus mauritiana* Lamk. Var. Gola). *Journal of Food Science and Technology,* **53 (1):** 748–756.

[28] Abu-Goukh, A. A. and Bashir, H. A. (2003) Changes in pectic enzymes and cellulose activity during guava fruit ripening. *Food Chemistry,* **83 (2):** 213–218.

[29] Fraeye, I., Roeck, A.D., Duvetter, T., Verlent, I., Hendrickx, M. and Loey, A.V. (2007) Influence of pectin properties and processing conditions on thermal pectin degradation. *Food Chemistry,* **105 (2):** 555–563.

[30] Yaman, O. and Bayoundrilli, L. (2002) Effects of an edible coating and cold storage on shelf-life and quality of cherries. *Journal of Food Engineering,* **35:** 146-150.

[31] Conforti, F.D. and Zinck, J.B. (2002) Hydrocolloid-lipid coating effect on weight loss, pectin content, and textural quality of green bell peppers. *Food Chemistry,* **67:** 1360–1363.

[32] Zhou C., Zhao, D. Sheng Y., Tao J. and Yang Y. (2011) Carotenoids in fruits of different Persimmon cultivars. *Molecules,* **16 (1):** 624-636.

[33] Howard, L. T., Talcott, S. T., Brenes, C. H. and Villalon, B. (2000) Changes in phytochemical and antioxidant activity of selected pepper cultivars (*Capsicum* species) as influenced by maturity. *Journal of Agricultural Food Chemistry,* **48:** 1713–1720.

[34] Macheix, J. J, Fleuriet A. and Billot J. (1990) Fruit phenolics. CRC Press, Inc. Florida.

[35] Carvalho, C. P., Villano D., Moreno D. A., Serrano M. and Valero D. (2015). Alginate edible coating and cold storage for improving the physicochemical quality of cape gooseberry (*Physalis peruviana* L.). *Journal of Food Science and Nutrition,* **1:** 002.

[36] Lee, S.K. and Kader, A.A. (2000) Pre harvest and postharvest factors influencing vitamin C content of horticultural crops. *Postharvest Biology and Technology,* **20 (3):** 207–220.

[37] Guilbert, S., Gontard, N. and Gorris, L.G.M. (1996) Prolongation of the shelf-life of perishable food products using biodegradable films and coatings. *LWT- Food Science and Technology,* **29:** 10–17.

[38] Maftoonazad, N. and Ramaswamy, H.S. (2005) Postharvest shelf-life extension of avocados using methyl-cellulose-based coating. *LWT-Food Science and Technology,* **38:** 617-624.

[39] Baraiya, N.S., Ramana Rao, T.V., and Thakkar, V. R. (2016) Composite coating as a carrier of antioxidants improves the postharvest shelf life and quality of table grapes (*Vitis vinifera* L. var. thompson seedless). *Journal of Agricultural Science and Technology,* **18:** 93-107.

Table-1: Formulations of edible coatings for cape gooseberry fruit

Coating treatments	Xanthan Gum (%)	Guar Gum (%)	Olive Oil (%)
T1	0.5	----	-----
T2	----	0.5	----
T3	0.25	0.25	----
T4	0.5	----	0.2
T5	----	0.5	0.2
T6	0.25	0.25	0.2
C	**----**	**----**	**----**

Table-2: Effect of edible coatings on TSS and Total sugars of cape gooseberry fruit stored at low temperature (10 ± 1˚C)

	Day 0	Day 5	Day 10	Day 15	Day 20	Day 25
Treatments			**Total soluble solids (°Brix)**			
T1	0.733±0.058^{d}	1.467±0.058^{ab}	1.200±0.000^{d}	0.900±0.000^{d}	1.50±0.00^{b}	2.00±0.00^{a}
T2	0.733±0.058^{d}	1.500±0.100^{a}	1.600±0.000^{bc}	1.533±0.058^{bc}	1.50±0.17^{b}	0.000±0.000
T3	0.733±0.058^{d}	1.333±0.115^{abc}	1.700±0.000^{b}	1.500±0.265^{bc}	1.90±0.00^{a}	1.83±0.38^{ab}
T4	0.733±0.058^{d}	1.300±0.000^{bc}	1.533±0.058^{c}	1.433±0.058^{c}	1.20±0.00^{c}	1.60±0.00^{ab}
T5	0.733±0.058^{d}	1.200±0.000^{c}	1.067±0.058^{d}	1.700±0.000^{abc}	1.13±0.12^{c}	1.53±0.06^{b}
T6	0.733±0.058^{d}	1.500±0.000^{a}	1.300±0.100^{b}	1.800±0.100^{ab}	0.000±0.000	0.000±0.000
C	0.733±0.058^{d}	1.500±0.000^{a}	1.900±0.000^{a}	1.900±0.000^{a}	0.000±0.000	0.000±0.000
Treatments			**Total Sugars (mg g^{-1})**			
T1	64.61±0.092	70.58±5.010^{g}	60.26±4.76^{g}	46.83±12.93^{g}	28.02±2.17	9.23±0.24^{b}
T2	64.61±0.092	93.32±12.33^{d}	73.23±5.11^{b}	67.48±9.88^{d}	35.71±0.94	0.000±0.000
T3	64.61±0.092	73.33±4.945^{f}	78.91±26.63^{f}	72.01±25.05^{e}	29.43±0.94	12.42±0.88^{a}
T4	64.61±0.092	76.63±10.31^{e}	72.92±2.82^{c}	89.31±28.40^{a}	35.61±1.87	11.52±1.71^{ab}
T5	64.61±0.092	99.05±37.42^{c}	77.32±15.44^{d}	84.14±4.82^{b}	12.13±2.02	12.79±1.09^{a}
T6	64.61±0.092	106.9±3.789^{b}	77.24±17.01^{e}	75.99±4.53^{c}	0.000±0.000	0.000±0.000
C	64.61±0.092	108.6±41.92^{a}	77.82±2.27^{a}	64.98±5.05^{f}	0.000±0.000	0.000±0.000

Values are mean ± standard deviation, n = 3. Values within treatments with different letters (a–d) in a column differ significantly ($P \leq 0.05$) with values from higher to lower.

Table-3: Effect of edible coatings on Carotenoid, TPC and Ascorbic acid of cape gooseberry fruit stored at low temperature (10 ± 1 ˚C)

	Day 0	Day 5	Day 10	Day 15	Day 20	Day 25
Treatments			**Carotenoids (μ g^{-1} FW)**			
T1	0.07±0.00	0.072±0.0008^{a}	0.055±0.003^{ab}	0.03±0.00^{b}	0.035±0.0005^{b}	0.031±0.002^{a}
T2	0.07±0.00	0.044±0.003^{d}	0.041±0.000^{e}	0.03±0.00^{b}	0.040±0.0001^{a}	0.000±0.000
T3	0.07±0.00	0.063±0.004^{bc}	0.047±0.000^{d}	0.04±0.00^{b}	0.042±0.0015^{a}	0.037±0.005^{ab}
T4	0.07±0.00	0.050±0.002^{d}	0.052±0.001^{bc}	0.05±0.00^{a}	0.032±0.0006^{b}	0.028±0.003^{b}
T5	0.07±0.00	0.067±0.001^{ab}	0.058±0.001^{a}	0.03±0.00^{b}	0.040±0.0017^{a}	0.024±0.006^{b}
T6	0.07±0.00	0.065±0.0009^{b}	0.052±0.000^{c}	0.03±0.00^{b}	0.000±0.000	0.000±0.000
C	0.07±0.00	0.058±0.0007^{c}	0.044±0.002^{de}	0.03±0.01^{b}	0.000±0.000	0.000±0.000
Treatments			**TPC (mg g^{-1})**			
T1	0.60±0.02^{d}	0.80±0.02^{b}	0.906±0.213^{ab}	0.749±0.059^{b}	0.882±0.066^{a}	0.982±0.078^{a}
T2	0.60±0.02^{d}	0.75±0.05^{b}	0.785±0.061^{abc}	0.551±0.027^{c}	0.842±0.123^{a}	0.000±0.000
T3	0.60±0.02^{d}	0.96±0.08^{a}	0.662±0.050^{bcd}	0.548±0.035^{d}	0.622±0.010^{b}	0.872±0.017^{a}
T4	0.60±0.02^{d}	0.86±0.03^{ab}	0.712±0.017^{bc}	0.789±0.177^{b}	0.652±0.030^{b}	0.805±0.120^{a}
T5	0.60±0.02^{d}	0.81±0.02^{b}	0.471±0.030^{d}	0.759±0.084^{b}	0.662±0.036^{b}	0.394±0.095^{b}
T6	0.60±0.02^{d}	0.72±0.09^{b}	0.585±0.049^{d}	0.996±0.391^{a}	0.000±0.000	0.000±0.000
C	0.60±0.02^{d}	0.76±0.02^{b}	1.023±0.175^{a}	0.591±0.053^{c}	0.000±0.000	0.000±0.000
Treatments			**Ascorbic acid (mg100g g^{-1})**			
T1	567.3±4.16^{a}	454.4±77.0^{ab}	325.0±5.3^{b}	201.3±3.8^{c}	210.4±14.5^{b}	236.9±13.5^{a}
T2	567.3±4.16^{a}	503.8±6.0^{a}	381.7±6.6^{a}	256.5±6.0^{b}	164.4±8.1^{c}	0.000±0.000
T3	567.3±4.16^{a}	304.2±70.2^{c}	256.3±10.3^{c}	131.5±5.6^{de}	109.0±10.5^{d}	95.8±31.8^{c}
T4	567.3±4.16^{a}	295.8±3.1^{c}	198.1±3.3^{d}	191.0±4.5^{c}	157.7±10.5^{c}	78.8±1.7^{c}
T5	567.3±4.16^{a}	121.7±80.1^{d}	387.7±5.6^{a}	322.9±2.5^{a}	267.5±6.0^{a}	188.3±1.0^{b}
T6	567.3±4.16^{a}	423.8±45.9^{abc}	189.6±3.1^{d}	136.7±0.4^{d}	0.000±0.000	0.000±0.000
C	567.3±4.16^{a}	323.3±3.0^{bc}	198.1±3.3^{d}	125.6±0.6^{e}	0.000±0.000	0.000±0.000

Values are mean ± standard deviation, n = 3. Values within treatments with different letters (a–d) in a column differ significantly ($P \leq 0.05$) with values from higher to lower.

Figure-1: Effect of edible coatings on (a) Physiological loss of weight (PLW) and (b) firmness of cape gooseberry fruit stored at low temperature (10 ± 1 ℃). Values are mean ± standard deviation, n = 3. Values within treatments with different letters (a–d) in a column differ significantly ($P \leq 0.05$) with values from higher to lower.

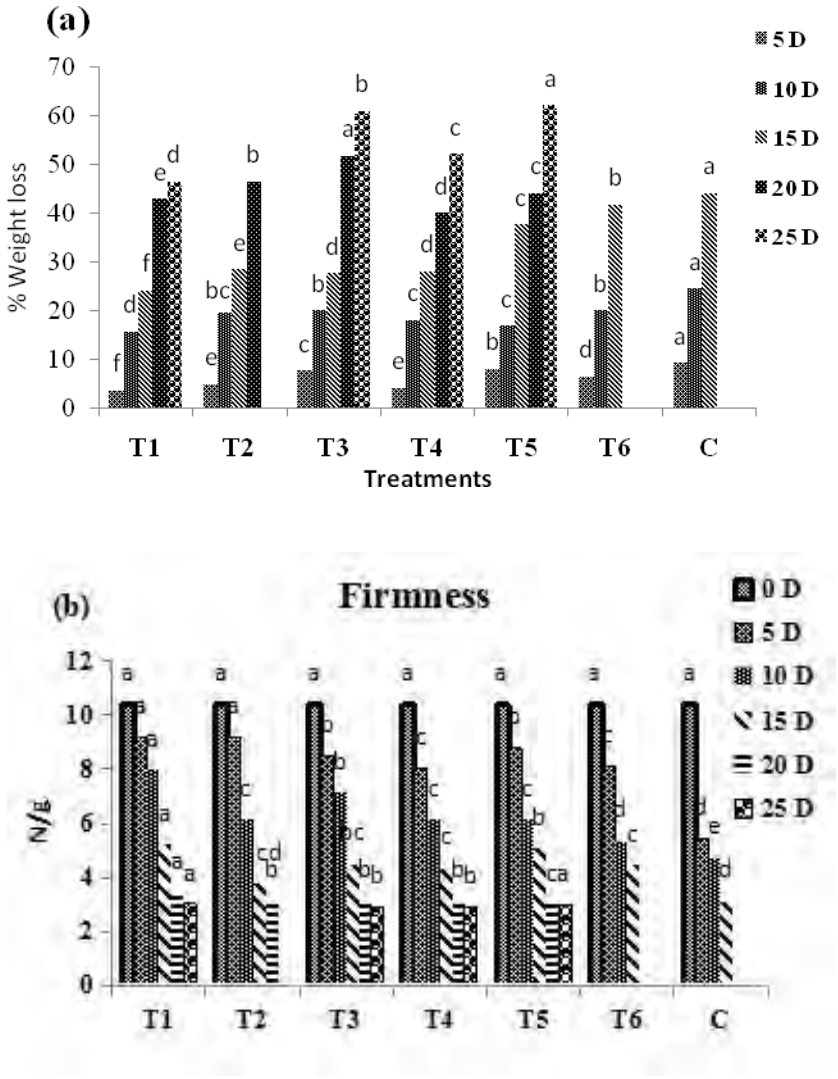

Figure-2: Effect of edible coatings on activity of (a) PG and (b) PL of cape gooseberry fruit stored at low temperature (10 ± 1 ℃). Values are mean ± standard deviation, $n = 3$. Values within treatments with different letters (a–d) in a column differ significantly ($P \leq 0.05$) with values from higher to lower.

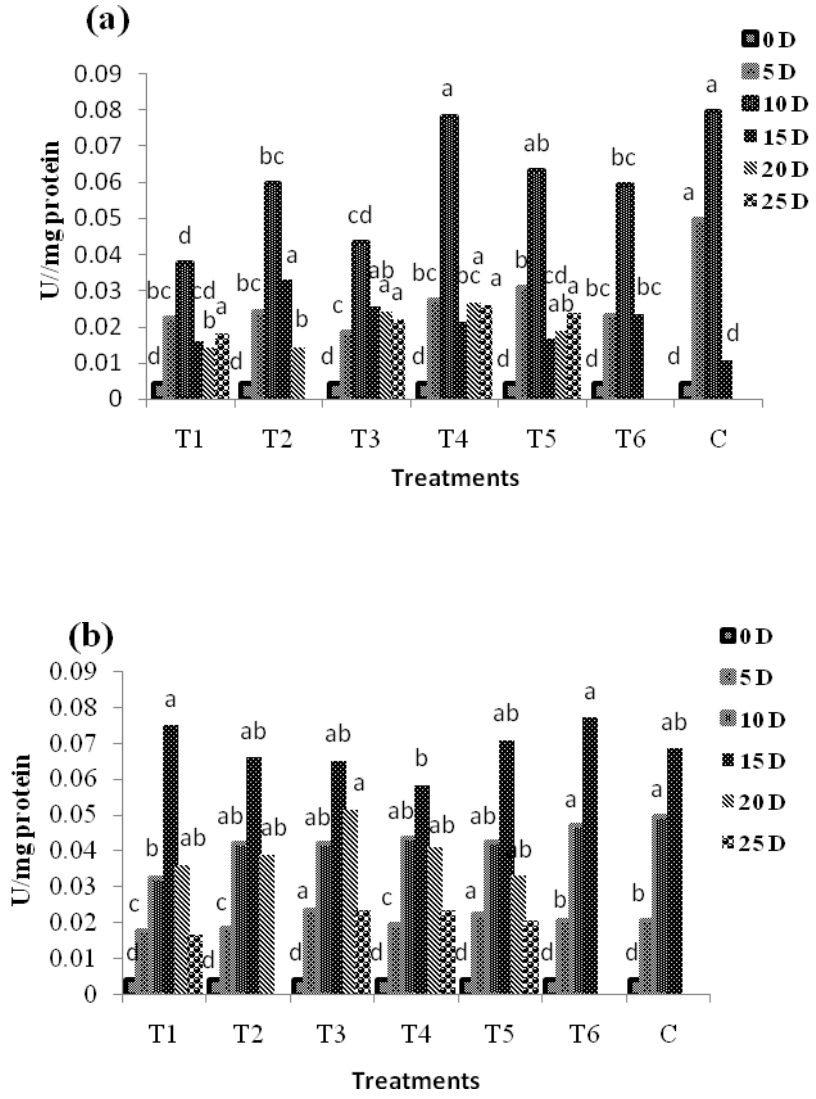

PRAJÑĀ - Journal of Pure and Applied Sciences Vol. 26 : 38 – 46 (2018)
ISSN 0975 - 2595

DATA SYNCHRONIZATION IN APPLICATION SOFTWARE

L. N. CHAVALI, P. N. OJHA AND C. RAM LOHITH

Technology Practitioners and Consultants, Hyderabad

Email: lnchavali@yahoo.com

ABSTRACT

It is a well known fact that the data in database is bound to have changes with the passage of time as it is designed for applications in real world. As world changes day by day, it is challenging to handle the changes in database and to transport them to different target data stores. In application software under discussion in this paper, these changes are being transported to target data store by ETL (Extract Transform Load) from State Data Centre (SDC) to National Data Centre (NDC) and by Customized Synchronization (Sync) framework using stored procedures from offline locations to SDC. The primary focus of this paper is on Customized Sync which is implemented as a multi-threaded sync server that will synchronize data to and from different offline servers to SDC in a transparent manner to the users.

Keywords: synchronization, blackout, thread, offline

INTRODUCTION

Communication topology and propagation strategy are two vital aspects of data synchronization. 'Communication topology' defines the pattern of communications among systems /or nodes whereas 'Propagation strategy' defines how frequently system /or nodes synchronize with one another [2]. The topologies range from central master, ad-hoc peer-to-peer, hierarchical etc. The propagation strategies vary from eager to lazy strategies. Eager strategy may help updating the data immediately while the update propagation may be delayed in lazy strategy. The eager may minimize or reduce the risk of conflicts in terms of stale reads and write conflicts whereas resolution is required to address these conflicts in lazy strategy because of delay in communication and of large write-logs. However, lazy propagation offers an advantage that the systems can be operated in a disconnected state.

There are many methods through which the data synchronization can happen. Some of them may include [3]**: -**

1. **Trigger method** – Insert, delete and modify triggers are used to sync data by activating triggers.
2. **Log Analysis method** – It is nothing but analysing the information of the database log to capture changes in sequence of synchronization objects.
3. **Time Stamp based method** – A method where in every table of the application has a timestamp field to record the modification time of each table.
4. **Trigger and Log Table method** – This is closer to realizing real time database synchronization by employing web services with event driven mechanism.

The rules to resolve conflicts may be domain independent or may depend on application semantics i.e. data driven reconciliation in which systems can trigger reconciliation often enough to avoid conflicts by using application-specific knowledge. If the users decide to trigger manual reconciliation, it is likely to increase delays because of volume of data and therefore may result in increase in conflict rates. However, the chief advantage of manual reconciliation is control and allows user to synchronize the data as and when needed.

The tools like Google *Gears* is an open source browser extension that lets developers create web applications that can run offline. Nevertheless, the goal of *Gears* is not just to enable offline application, but to bridge the gap between web application and desktop application [7]. The popular utility like *rsync* which is widely deployed on UNIX systems is used primarily for synchronizing files and directories from one location to another mostly in backing up systems [8].

There are many proven commercial frameworks that are available in the market as of today. Some of them are described below: -

1. Microsoft Sync Framework

It is a data synchronization platform from Microsoft that can be used to synchronize data across multiple data stores. Sync framework can be used for offline access to data, by working against a cached set of data and

submitting the changes to a master database in a batch, as well as to synchronize changes to a data source across all consumers (publish/subscribe sync) and peer-to-peer synchronization [1] of multiple data sources. Sync framework features built-in capabilities for conflict detection such as changes to the data that has already been updated, and can flag them for manual inspection or use defined policies to try to resolve the conflict. There is no unique way or unanimously agreed method for data synchronization. This task differs from case to case, and even data synchronizations that should be simple at first glance can be complicated, due to the complexity of data structures. The implementations of data synchronization are rarely optimal [10].

2. Open Sync Framework

OpenSync is a synchronization framework that is platform and distribution independent. It consists of a powerful sync-engine and several plug-ins that can be used to connect to devices. OpenSync is very flexible and capable of synchronizing any type of data, including contacts, calendar, tasks, notes and files (https://www.openhub.net/p/opensync).
OpenSync is a successor project of MultiSync. OpenSync's main and most practical goal is to create a solution to synchronize PIM (Personal Information Management - address book contacts, calendar events and tasks, personal notes, etc.) data between mobile devices like mobile phones, PDAs (Personal Digital Assistant), desktop computer PIM tools and services [4]. SymmetricDS (https://www.symmetricds.org/doc) is open source software for database and file synchronization, with support for multi-master replication, filtered synchronization, and transformation. It uses web and database technologies to replicate change data as a scheduled or near real-time operation, and it includes an initial load feature for full data loads. The software was designed to scale for a large number of nodes, work across low-bandwidth connections, and withstand periods of network outage.

3. Oracle GoldenGate Replication Framework

.

GoldenGate can synchronize two heterogeneous databases, by reading the real-time history of all transactional changes of the source database. The delta is then sent over to the other database, again in real-time. In technical language, this is called Change Data Capture (CDC). Simplicity is the feature of killer applications; GoldenGate guarantees transactional integrity when copying between source and target databases. With the simple deployment of GoldenGate between databases, one can build a High Available i.e. redundant architecture with each database holding accurate copies of each other's data. Most importantly, GoldenGate permits active-active database replication. Oracle GoldenGate guarantees that even in an unstable environment where networks and host servers occasionally drop out, transactions will never be missed or skipped [5].

There are many off-the-shelf products like Aspera Sync from IBM (https://www.asperasoft.com) and Attunity (https://www.attunity.com/data-replication-tool/) for replication or synchronization of data.

4. Customized Sync framework

In applications, any data that is entered at source (i.e. offline) is stored at source's server and this server in turn will communicate to target server hosted at data center for data synchronization over internet/SWAN/intranet links. However, the data exchange over internet between source and target will take place through Secure Socket Layer (SSL). The data will be synchronized between server at State Data Centre (SDC) and server at source without interrupting user operations.

The synchronization in applications under discussion is designed for MySQL / MSSQL database server at SDC and MySQL as offline server at remote locations. The sync server is built using Java Development Kit (JDK version 6.0 or above), and the databases at both ends should be running for Sync to operate. The database at SDC is configured for row level lock only. Fig 1 given below briefly depicts the sync framework and the functional flow of synchronization

Fig 1 – Synchronization Framework

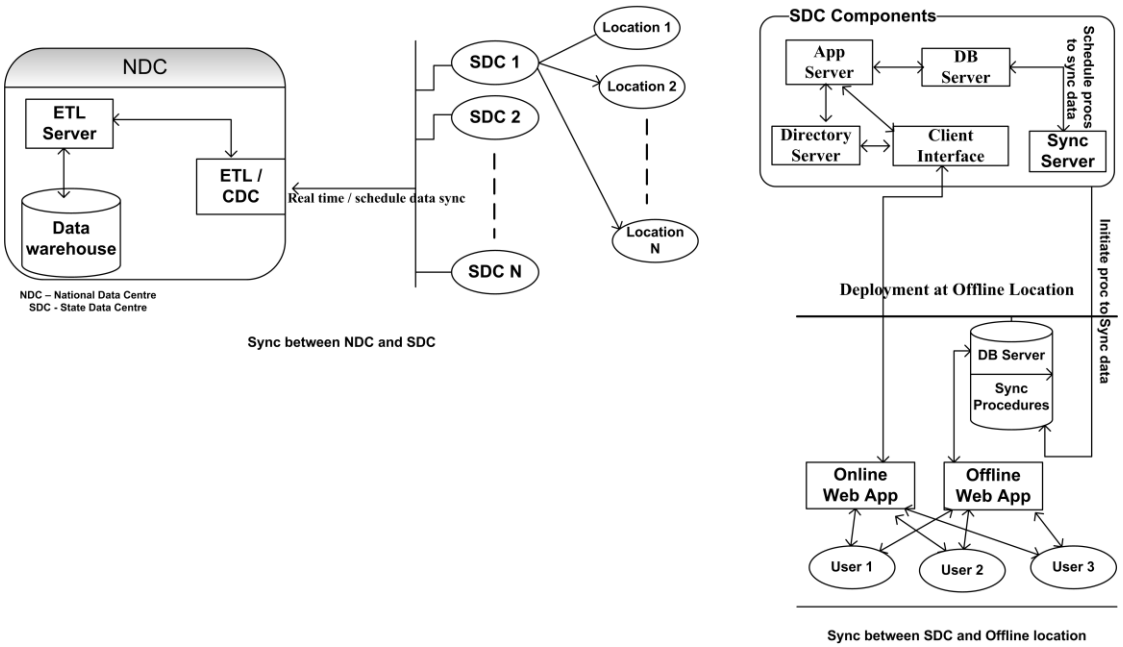

The table 1 describes the key feature comparison of custom sync with that of commercially available off-the-shelf products.

Table 1: Feature Comparison of different sync models

Key feature	Microsoft Sync	Oracle GoldenGate	Open sync	Custom Sync
Synchronize by using an n-tier or service-oriented architecture	Yes	Yes	Yes	No
Supports heterogeneous databases	Yes	Yes	Yes	Yes
Incremental change tracking	Yes	Yes	Yes	Yes
Conflict detection and resolution	Yes	Yes	Yes	Yes
Easily create data views on the client (UI)	Yes	Yes	No	No
Automatically initialize schema and data	Yes	Yes	No	Yes
Supports large data sets	Yes	Yes	No	Yes
Query processor is locally available	Yes	Yes	Yes	No
Use on devices	Yes	Yes	Yes	No

METHODOLOGY

1) Synchronization Model in Applications

In custom sync framework, the synchronization interval must be configured to sync the data between online resources and offline resources. If resource at the both ends is the database, then the data transmission is completed before purging the data from the offline database; and before reaching the database size limit.

Data Synchronization

Master data synchronization is done on the basis of client / server model. The data always moves from the server to the client, and therefore the synchronization is unidirectional. The data change i.e. incremental changes in masters is synchronized with offline database by stored procedures.

The custom sync framework supports two fold approaches viz.

a) Synchronize the metadata of online database i.e. database at SDC with that of offline database.
b) Bi-directional synchronization of the record or transactional data.

Method 1 – offline and online transmission of data over http links.
Method 2 – offline and online transmission of data over user socket.

The approach in this framework has a few limitations as briefly explained below.

1. When network connectivity is available, offline application is barred from operation.
2. When connection to the SDC server is re-established, user will be notified about the blackout period (i.e. no operation from online or offline) during which the background utility will synchronize the metadata, and subsequently, the record or transactional data will be synchronized. During the metadata synchronization, user is not allowed for any data submission from the application.

The given below figure illustrates various transition states of sync server.

Fig 2 – State diagram of Sync

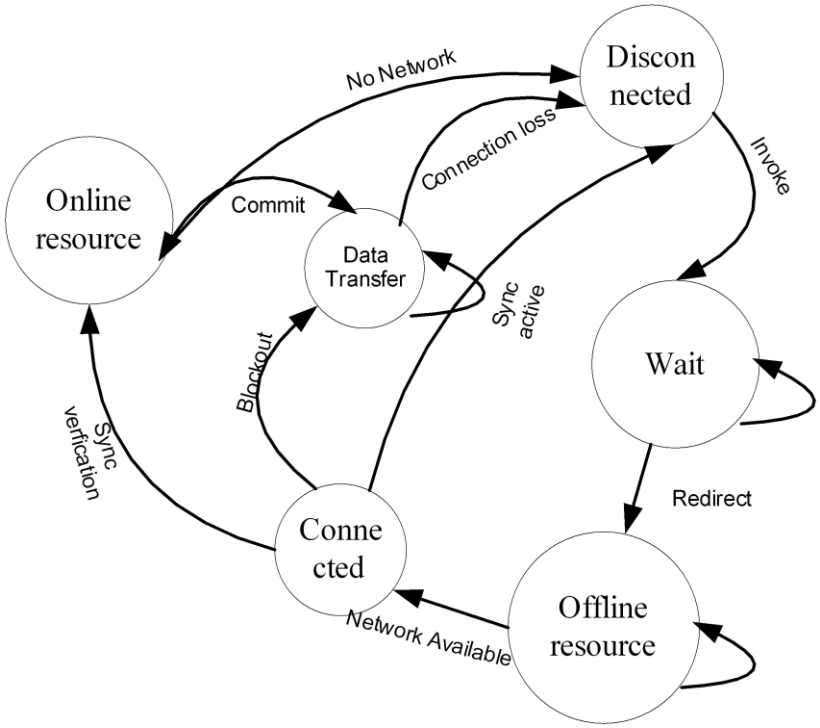

From Fig 2, the transition from offline to online happen only by having valid network connection, declaring blackout and performing data transfer. The transition from online to offline happened as and when there is a loss of network connectivity. The user operates the offline application and all transactional data will be put in offline database. It is to be noted that the metadata is synchronized only after declaring the '*blackout'* period during which the offline users cannot operate the application from offline or online.

2) Sync Server Implementation

The sync application is built as multi-threaded server which is run from SDC. It executes various procedures for synchronizing the data between SDC and offline server. Thread is a path of execution in the process. Threads allow multiple executions to take place in the same process environment, to a large degree independent of one another. The main reason for having threads in sync application is that multiple offline stations/servers are required to be synchronized for data. Therefore, in order to perform the data exchange with many offline servers simultaneously from SDC, the synchronization tasks are decomposed into multiple threads which run in parallel / quasi-

parallel to perform the tasks. When a multithreaded process is run on a single-CPU system, thread scheduling is one dimensional and CPU should decide in which thread it should run next. It takes turns to run multiple threads. The CPU switches rapidly back and forth among the threads providing the illusion that the threads are running in parallel. When threads are scheduled on multiple processors, scheduling is two dimensional as the scheduler has to decide the thread to run on which processor there by making it more complicated. In multiprocessor scenario, the threads run simultaneously on virtual processors associate with each CPU. The virtual processors can be taken back by kernel in order to assign them to other needy processes or threads. All threads in the process share resources of the process like open files, signals etc. It is not possible to have protection between threads in the process and it may not be necessary as threads are expected to collaborate and to work together to perform the tasks.

The sync server in software applications is organized as shown in Figure 3.

Fig 3 - Multi threaded sync server

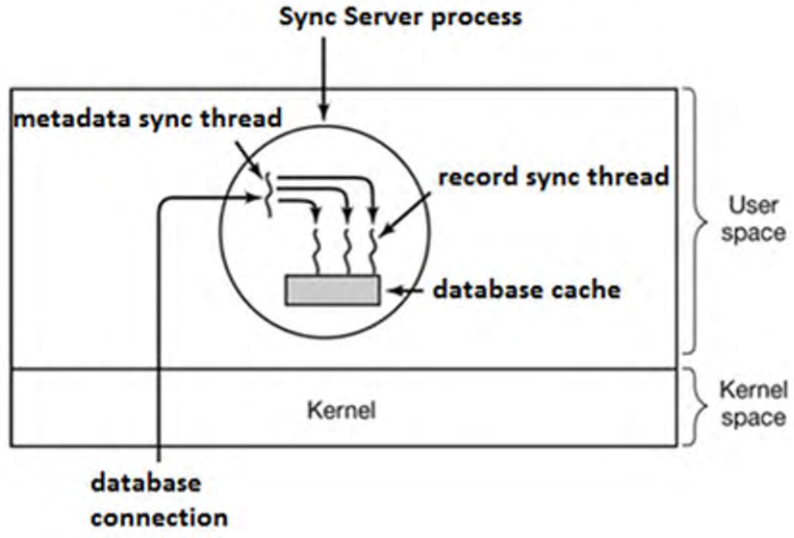

Sync server will have two threads per offline station apart from three other threads meant for logging, console and the main. The '*metadata sync*' thread checks the metadata at SDC and at offline for a module and synchronize offline metadata with that of SDC. '*record sync*' thread exchange all such records whose meta flags are verified by 'metadata sync' thread in both directions.
The pseudo code of the sync server is given below:

```
main ()
{

if (connection success from both DB)
{
/*Sync DB at SDC to offline DB */

                If
Establish Server Socket at port 19218;
If remote station code in host list == "true" && thread is not running)
{
//start the thread
while (1 == 1)
{
Start metadata sync thread; // may be referred in program as SDC to offline
Start record sync thread; // referred as offline to SDC
Establish the connection from Server DB at SDC;
Establish the connection from offline DB;

(RECORD_SYNC_ON = NULL)
{
Fetch Records of Server DB at SDC that are yet to be synchronized;
Convert the Records into XML format;
```

Insert XML records into offline DB;
Update Sync Flags at offline and SDC;
Commit;
}
/* Sync offline DB to Server DB at SDC */
If (RECORD_SYNC_ON = NULL)
{
Fetch Records of offline DB that are yet to be synchronized;
Convert the Records into XML format;
Insert XML records into Server DB at SDC;
Update Sync Flags at offline and SDC;
Commit;
}
} /* end of if - connection loop */
} /* end of while loop */
} /* end of if – thread */
Else no need to sync;
} /* end of program*/

The XML files which are created at run time for data transfer are deleted automatically at the end of the data transfer.

OBSERVATIONS

Deadlocks

Deadlock occurs when a group of threads have been granted exclusive access to some resources, and each one wants yet another resource that is being used by other thread in the group. All of them are blocked and none will ever run again.
It has been observed that whenever a new user is assigned in an offline application through Administrator, the new user is not visible in offline application, but it has shown up the previous user in offline. However, the new user works fine in online mode.

The above user problem is explained in Fig 4 to understand the deadlock scenario. This has been presented here for illustration purpose only.
In Fig 4, the sync flags of SDC and offline servers are allocated to metadata sync thread, data record to be updated is allocated to record sync thread and the record in cache is allocated to SQL procedure. The procedure is requesting for access to update the sync flags post data exchange whereas this is locked by metadata sync thread and thereby creating a deadlock.

Fig 4 – Deadlock situation

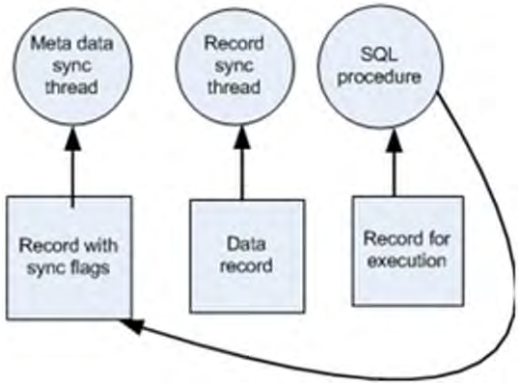

If procedure generates an exception, then the user threads will reschedule the data exchange after the schedule interval. However, if the procedure throws an exception again, then there is every possibility of a deadlock situation created.

There may be many reasons for a deadlock; nonetheless some well-known reasons for deadlock are listed below: -

1. Exhaustion of the thread table.
2. Limitation on the number of open files and finite swap space.
3. Contention for the shared resources.

Most of the errors observed in error table 2 may be indirectly related to contention of resources
Maintaining the data dependency across threads is vital. Disambiguating the addresses accessed by different threads, invalidating stale state in caches, making the state of a committing thread visible to all other threads, discarding incorrect state when a thread is squashed, and managing the speculative state of multiple threads in a single processor are important in speculative multithreading [6].

RESULT AND DISCUSSION

The configuration of the database server in the lab where sync is deployed and tested is Quad core and 20 GB RAM. Table 2 briefly lists out the errors that have been logged by Sync Server.

Table 2: Errors in sync log

S.No	Error type	Description
1	Procedure does not exist	Data sync from SDC to offline server A unable to locate the PROCEDURE "offline_db_sync_proc.PR_DS_UPDATE_PROP_EXT_SYNC_FLAG".
2	Duplicate Entry	Data sync from SDC to offline server B Duplicate entry '81121500213001501-99' for key 'PRIMARY'
3	Deadlock on locked resource	Data sync from DC to offline server A Transaction was deadlocked.
4	Station out of sink	Station C stop to sync automatically.
5	No operation allowed	Data sync from SDC to offline server D for Master update, user update and data entry. Connection was implicitly closed by the driver.

1. Performance Statistics

It is evident from Fig 4 that the memory consumption of db and sync servers is high, thereby forcing a restart of sync server. There is a marginal change in memory consumption and the number of threads as seen from Fig 5 and 6. Therefore, it can be concluded that only a few transactional activities are taking place. Out of all nine offline servers started, four offline servers were shut down for some reason during test and two offline servers out of the four were re-started. The number of threads at start up is 21. However, the base thread count remains the same despite reduction in the number of offline servers. On the contrary, it has been observed that the thread count is varying over the base count because of offline server's unstable connectivity.

Fig 5 – SQL memory versus Sync memory.

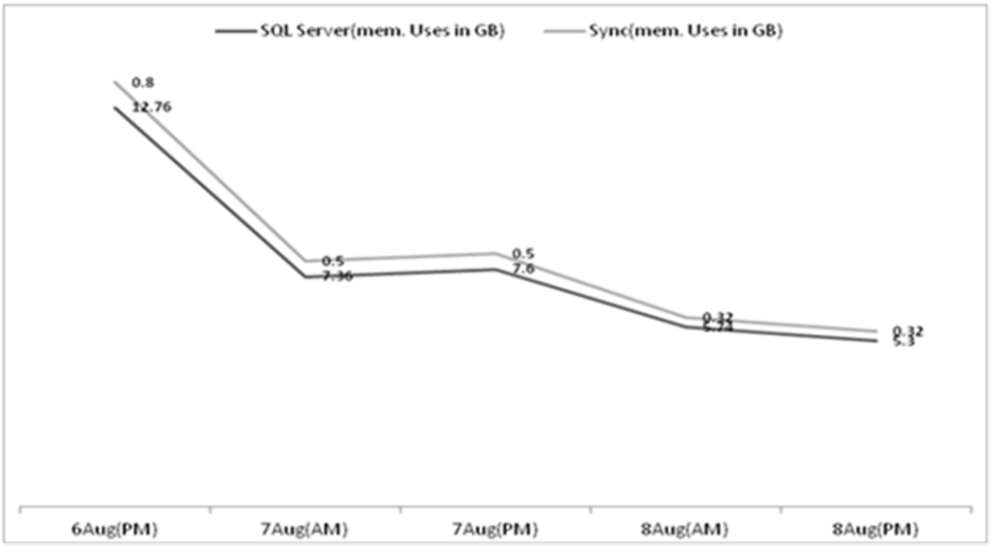

Fig 6 – Sync thread versus Sync memory

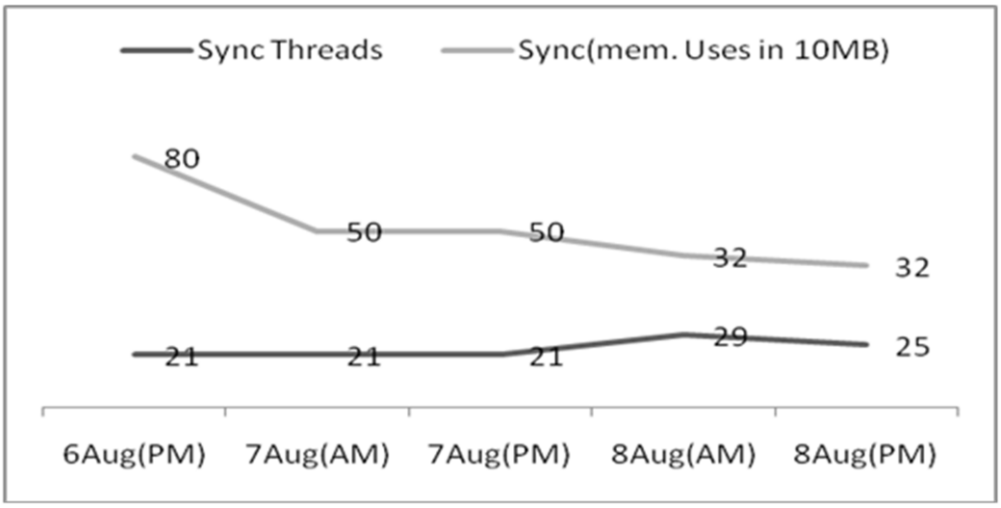

2. Query Response

The sync framework in application software replicates the data on transactional basis. There are 25 classes of transactions in the application software under test. Whenever synchronization happens for a specific transaction, it seems that all the related table data will be exchanged. Any new transactions outside the window of the existing set of transactions may not be synchronized.

The response times of five procedures that have been captured at two different instances during test are shown in Fig 7. The graph was generated with SQL profiler of Microsoft. It can be observed that the response time varies from 1.3 sec to 20 sec with few records in the database in the test lab. The expected user response time as per requirements at peak load is 3 sec. The query response times are based on the current execution plan. The same execution plan will deteriorate the response times for higher workload or higher volume of data.

3. Root Cause Analysis

It has been observed that in some of the transactions, the long running queries are holding the database locks thereby causing other resources waiting in the queue. This has resulted in longer transaction commits to the database.

LIKE operator is being used widely in procedures to generate the primary key for some of the tables, which has caused full table scan. Due to this, the performance has been impacted. As the procedures are re-used by other modules, it has resulted in long wait, lock wait and time out of the transactions.

To alleviate this problem, the number generation logic of the primary key has been changed and the execution times of stored procedure have improved by many folds. The concurrency is controlled by modifying the throttling parameter.

Fig 7 – Response times of procedures

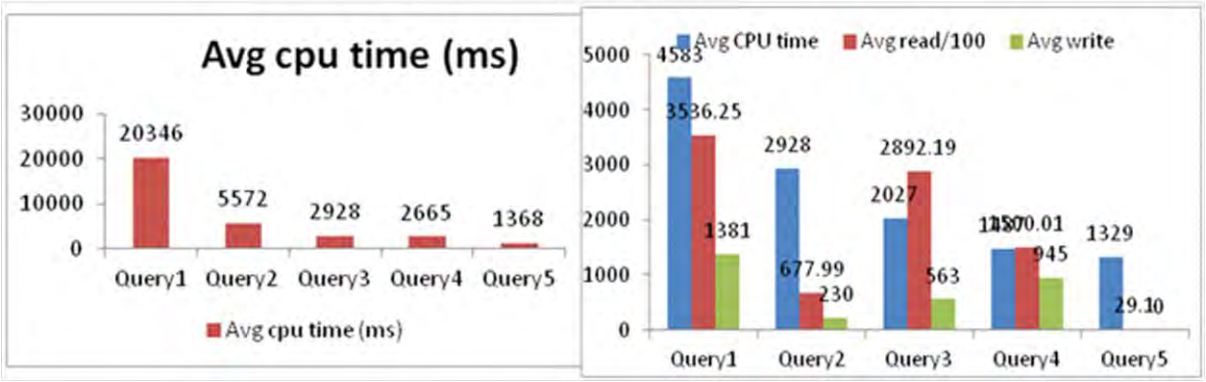

CONCLUSIONS

It is planned by design that the offline application is a contingency arrangement for no online access for any reason. In the custom model discussed in this paper, the tight coupling between offline and online is a cause of concern. Loss of data, different response times to the same transaction from different locations, performance impact on database due encryption or multi-lingual adaption are some of the bottlenecks which are yet to be addressed in the solution, possibly would be addressed in future releases of synchronization software. The customized framework is tailored to the customer requirements and will scale up easily as more and more locations are added. This framework is currently being used in one of the mission mode projects. The computing paradigm is slowly shifting from centralized to decentralized as evident with the advent of blockchain solutions. The emergence of distributed technologies has given birth to new ways of synchronizing data sets and files which is agnostic to the underlying transport. A new protocol viz. DAT is designed for syncing folders of data, even if they are large or changing constantly. DAT is a dataset synchronization protocol that supports public or private decentralized network and use public key cryptography for encryption [9]. The sync methods in future may become more decentralized and may replace the existing methods due to factors such as cost, vendor lock-in, speed, privacy and centralizatio.

REFERENCES

[1] Joe Kunk (2012): Database Synchronization with Microsoft Sync Framework, *Visual Studio magazine*, 34-38

[2] Mike Dahlin, Aslan Brooke, Muralidhar Narasimhan, Bruce Porter (2000): Database synchronization for distributed simulation, *European Simulation Interoperability Workshop*, pp 1-7

[3] A.F. Cardenas (1987): Heterogeneous distributed database management. The HD-DBMS, Proceeding of IEEE Volume 75(5):588 - 600

[4] Hui Ling Du, Benjamin C. Pierce (2009): Universal Data Synchronizer for Personal Calendars, *Conference Proceedings*, *Website*: https://pdfs.semanticscholar.org/

[5] Oracle Corporation (2018): Oracle Fusion Middleware Using Oracle GoldenGate for Heterogeneous Databases, 12c (12.3.0.1), Oracle Press USA, pp 15.1-22.4

[6] Luis Ceze, James Tuck, Calin Cas, Josep Torrellas. (2006): Disambiguation of Speculative Threads in Multiprocessors, IEEE 1063-6897/06

[7] Tushar Mohate, Vijay Rasal, Anil Panchal, Sarita Ambadekar (2015): Internet Data Synchronization Tool, IJCST Volume 3 Issue 2

[8] Salekul Islam and Mohammad Amanul Islam (2014): A Web-based Data Backup, Synchronization and System Administration, DOI: 10.5815/ijcnis.2014.09.01, *Website*: http://www.mecs-press.org/

[9] Maxwell Ogden, Karissa McKelvey, Mathias Buus Madsen (2017): Home page for Code for Science & Society. Retrieved from *Distributed Dataset Synchronization and Versioning, Website*: https://codeforscience.org

[10] Andrej Gajdos (2016): Home page for toptalTM, Retrieved from *Guide to Data Synchronization in Microsoft SQL*, toptalTM, *Website*: https://www.toptal.com/sql/

PRAJÑĀ - Journal of Pure and Applied Sciences Vol. 26 : 47 – 52 (2018)
ISSN 0975 - 2595

A FRAILTY MODEL APPROACH TO THE COMPLETELY RANDOM DESIGN

ASHOK SHANUBHOGUE AND NITIRAJ B. SHETE
Department of Statistics, Sardar Patel University

ABSTRACT

We have come across many cases where usual analysis of variance of data from completely randomized design fails to detect the difference in treatment effects which are apparent in the values of means of observations under different treatments. This may be due heterogeneity in variances or may be due some unexplained part of variation present in the data. We observed similar case in which there is an apparent difference in mean which was identified by the analysis of variance as chance variation. The purpose of this research paper is to identify the cause of extra variation with the help frailty variable Z incorporated in the variance of the error distribution and reducing unexplained part of variation. Thus, statistically ascertaining the apparently present significant differences of means.

Keywords: Heterogeneity, ANOVA, Leven's and Bartlett Test, AD test, CRD, Frailty

INTRODUCTION

In survival analysis the problem of heterogeneity is dealt by incorporating frailty random variable. The first univariate frailty model was suggested by Beard (1959), considering different mortality models. The same model was independently suggested by Vaupel (1979) and Lancaster (1979). Beard (1959) used longevity factor instead of the term frailty and later on the term frailty was introduced by Vaupel (1979) in the univariate case. We observe that same concept can be incorporated in other statistical studies suitable to solve some seemingly mysterious problems.

We have found many situations while testing homogeneity of treatment effects in completely randomized design that the apparent relatively larger differences in the treatment effects get masked due undue variation present in the data, i.e, due to larger unexplained part variation present in the data. Procedure to extract or give explanation to the variation present, researcher considered random effect model. We believe that the effects are fixed but there may be some other random variable which is not observable but it is acting as effect modifier or is masking the signal. Such random variable we call as effect modifier or frailty random variable. In this research paper, we provide an example where treatment effects are apparently different but regular analysis of variance (ANOVA) fails to detect. To circumvent this difficulty we propose a new error model in which the common variance is divided by a random variable Z. Further, conditional distribution of error ε given Z is normal. Under this assumption we develop entire theory of ANOVA under completely random design. The stimulating example is given below.

A fast food franchise is test marketing 3 new menu items. To find out if they are same popularity, 18 franchisee restaurants are randomly chosen for participation in the study. In accordance with the completely randomized design, 6 of the restaurants are randomly chosen to test market the first new menu item, another 6 for the second menu item, and the remaining 6 for the last menu item. Following table represents the sales figures of the 3 new menu items in the 18 restaurants after a week of test marketing. Can we say, at .05 level of significance, sales volumes for the 3 new menu items are same?

Sr. No.	Item1	Item2	Item3
1	22	52	16
2	42	33	24
3	44	8	19
4	52	47	18
5	45	43	34
6	37	32	39
Mean	40.33	35.83	25.00

The answer the above questions, we need to carryout ANOVA provided following assumptions are valid.

1. Homogeneity of variance between the groups
2. Error must be normally distributed.

Bartlett test is the commonly used test for the homogeneity of variance when errors are normal and the Leven test for any distribution, and one sample Kolmogorov-Smirnov test (KS-test) or Anderson Darling test (AD test) is used for normality. Using Minitab statistical software we carryout these two tests. Following are the outputs of Minitab.

Minitab Output

Test for Equal Variances: sale versus item

```
95% Bonferroni confidence intervals
for
standard deviations
item  N    Lower    StDev    Upper
   1  6  5.79451  10.2111  31.9009
   2  6  8.91791  15.7152  49.0964
   3  6  5.34750   9.4234  29.4399

Bartlett's Test (Normal Distribution)
Test statistic = 1.48, p-value = 0.477

Levene's Test (Any Continuous
Distribution)
Test statistic = 0.64, p-value = 0.540
```

Test for equality of means:

Source	DF	SS	MS	F	P
Item	2	745	373	2.54	**0.112**
Error	15	**2200**	147		
Total	17	2946			

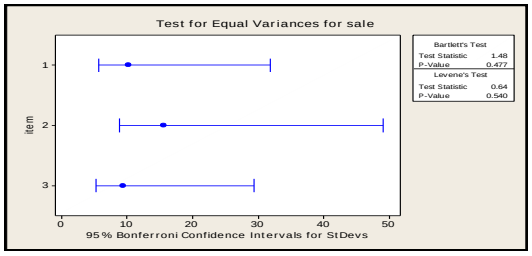

Fig: Test for Equal Variances

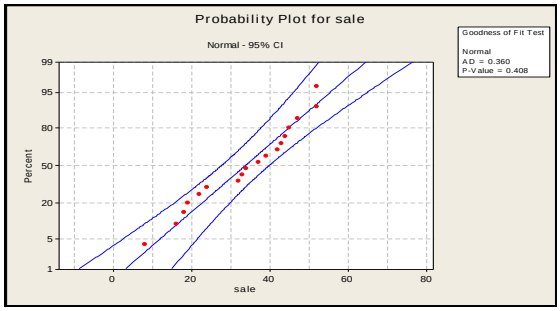

Fig. Test for Normality

Since the p-value of 0.112 is greater than the 0.05 significance level, we do not reject the null hypothesis that the mean sales volumes of the new menu items are all equal.

In this example we observe that error sum of squares contains some other un explained part variation along with random error which cause not to detect large difference present in the means of observations for three items. This needs to be extracted so that the signal can be rightly detected. The given below attempts model error differently by incorporating frailty and give explanation to the above situation.

Proposed Model for completely randomized design (CRD)

In CRD the homogeneous experimental units are randomly grouped and the treatments are assigned to each group randomly.. Let i^{th} treatment be replicated r_i times (i=1,2,3,…, ν) so that sum of all r_i equal to n; the total no. of observation. The linear model assuming various effects to be additive becomes;

$$y_{ij} = \mu + \alpha_i + \varepsilon_{ij} \quad \text{for all } i=1(\ )\nu \text{ and } j=1(\ )^{r_i} \qquad (1)$$

Where,

y_{ij} be the yield or response of j^{th} plot receiving i^{th} treatment

μ be the general mean effect

α_i be the effect due to i^{th} treatment

ε_{ij} be the error effect due to chance

We assume that;

i. The various effects are additive in nature

ii. ε_{ij} are i.i.d. $N(0, \sigma_e^2)$

Let us consider i.i.d continuous frailty random variable Z_{ij} associated with $(i,j)^{th}$ experimental unit. We assume that $\varepsilon_{ij}|z_{ij} \sim N(0, \frac{\sigma^2}{z_{ij}})$ for all i= 1,2,…., ν and j=1,2,…,r_i .Consequently, $Y_{ij}|Z_{ij}$ follows $N(\mu+\alpha_i, \frac{\sigma^2}{z_{ij}})$ for all i= 1,2,…., ν and j=1,2,…,r_i with the density function;

$$f(y_{ij}|z_{ij}) = \frac{(z_{ij})^{\frac{1}{2}}}{\sigma\sqrt{2\pi}} \exp\left\{-\frac{z_{ij}(y_{ij}-\mu-\alpha_i)^2}{2\sigma^2}\right\} \qquad (2)$$

We further assume that the distribution of Z_{ij} as standard exponential . That is,

$$g(z_{ij}) = \exp\{-z_{ij}\} \quad \forall \quad i,j \qquad (3)$$

Then, using (2) and (3), the joint distribution of Y_{ij} and Z_{ij} is,

$$f(y_{ij}, z_{ij}) = \frac{(z_{ij})^{\frac{1}{2}}}{\sigma\sqrt{2\pi}} \exp\left\{-\frac{z_{ij}\left((y_{ij}-\mu-\alpha_i)^2+2\sigma^2\right)}{2\sigma^2}\right\} \quad (4)$$

Integrating above with respect to Z_{ij} , we get,

$$f(y_{ij}) = \frac{\sigma^2}{\left((y_{ij}-\mu-\alpha_i)^2+2\sigma^2\right)^{\frac{3}{2}}} \quad (5)$$

Using (4) and (5) we get the following conditional distribution of Z_{ij} given Y_{ij}

$$f(z_{ij}|y_{ij}) = \frac{(z_{ij})^{\frac{1}{2}}\left((y_{ij}-\mu-\alpha_i)^2+2\sigma^2\right)^{\frac{3}{2}}}{\sigma^3\sqrt{2\pi}} \exp\left\{-\frac{z_{ij}\left((y_{ij}-\mu-\alpha_i)^2+2\sigma^2\right)}{2\sigma^2}\right\} \quad (6)$$

Therefore,

$$E(z_{ij}|y_{ij}) = \int_0^\infty z_{ij}\ f(z_{ij}|y_{ij})\, dz_{ij}$$

By solving above integral,

$$E(z_{ij}|y_{ij}) = \left(\frac{3\sigma^2}{(y_{ij}-\mu-\alpha_i)^2+2\sigma^2}\right) \quad (7)$$

It can be easily seen that $E\left(E(z_{ij}|y_{ij})\right) = 1$.

Maximum Likelihood Estimates:

From the joint distribution given in equation (4), the likelihood function is given by,

$$L(\mu, \alpha_i, \sigma|y_{ij}, z_{ij}) = \frac{(z_{ij})^{\frac{n}{2}}}{(\sigma\sqrt{2\pi})^n} \exp\left\{-\frac{\sum_{i,j}\left(z_{ij}\left((y_{ij}-\mu-\alpha_i)^2+2\sigma^2\right)\right)}{2\sigma^2}\right\} \quad (8)$$

Therefore the maximum likelihood estimates of the μ, α_i, σ^2 are given by the likelihood equations as

$$\frac{\partial(\log L)}{\partial\alpha_i} = 0$$

$$\Longrightarrow \hat{\alpha_i} = \frac{\sum_{j=1}^{r_i}(z_{ij}Y_{ij})}{z_{i.}} - \hat{\mu} \quad \forall\, i = 1,2,\dots,v \quad (9)$$

$$\frac{\partial(\log L)}{\partial\mu} = 0$$

$$\Longrightarrow \hat{\mu} = \frac{\sum_{i,j}(z_{ij}Y_{ij})}{z_{..}} \quad (10) \text{ provied that } \sum_i(\alpha_i z_{i.}) = 0$$

$$\frac{\partial(\log L)}{\partial\sigma^2} = 0$$

$$\Longrightarrow \widehat{\sigma^2} = \frac{\sum z_{ij}(y_{ij}-\hat{\mu}-\widehat{\alpha_i})^2}{n} \quad (11)$$

Where,

$z_{i.}$ = sumof all z_{ij} receiving i^{th}tratement $= \sum_j z_{ij} \quad \forall i = 1,2,3,\dots,v$

$z_{..}$ = Sum of all z_{ij} $= \sum_{i,j} z_{ij}$

Algorithm to compute $E(Z_{ij}|y_{ij})$:

i. Enter the values of y_{ij} in excel, in which column represents treatments.
ii. Initially consider all $z_{ij} = 1$. Also compute $z_{i.}$ as the i^{th} column total for all i=1,2,…,v and z.. as the sum of all z_{ij}.
iii. Use values of y_{ij} and z_{ij} to obtain maximum likelihood estimates of the model parameters α, μ and σ by using the equations (9), (10), and (11).
iv. Use the given y_{ij} and estimated values of model parameter and find $E(Z_{ij}|y_{ij})$ by using relation given in equation (7) and substituting the unknown parameter by their estimates.
v. Again use the $E(Z_{ij}|y_{ij})$ and compute the maximum likelihood estimates of the model parameters α, μ and σ for given y_{ij}.
vi. Repeat the (vi) until mean of all values of Z_{ij} is 1.
vii. Use these $E(Z_{ij}|Y_{ij})$ to construct ANOVA table.

Construction of ANOVA table:

Let us consider the linear model assumed in equation (1);

$y_{ij} = \mu + \alpha_i + \varepsilon_{ij}$ for all i= 1 ( ) v and j=1( ) r_i

As considered earlier, for given z_{ij} (obtained from algorithm) for all i= 1,2,…., ν and j=1,2,…,r_i , $\varepsilon_{ij}|z_{ij} = (Y_{ij} - (\mu + \alpha_i)) \sim N(0, \frac{\sigma^2}{z_{ij}})$ for all i= 1,2,…., ν and j=1,2,…,r_i.Then $\left(\frac{\epsilon_{ij}z_{ij}}{\sigma^2}\right) = \left(\frac{z_{ij}(y_{ij}-\mu-\alpha_i)}{\sigma^2}\right)$ follows N(0,1).Hence, $\left(\frac{z_{ij}\epsilon_{ij}^2}{\sigma^2}\right) \sim \chi^2_{(1)}$ and hence

$\sum_{(i,j)}\left(\frac{z_{ij}\in_{ij}^{2}}{\sigma^2}\right) \sim\chi^2_{(n-1)}$. Therefore the sum of squares due to error (SSE) is given by,

$$SSE = \sum_{(i,j)} z_{ij}\left(y_{ij} - \hat{\mu} - \hat{\alpha_i}\right)^2$$

$$= \sum_{(i,j)} Z_{ij}\left(y_{ij} - \hat{\mu} - \frac{\sum_{j=1}^{r_i}(z_{ij}Y_{ij})}{z_{i.}} - \hat{\mu}\right)^2 \quad (12)$$

Let us consider,

$$\overline{Y}^{w}_{..} = \hat{\mu} = \frac{\sum_{i,j}(z_{ij}Y_{ij})}{z_{..}}$$

and $\overline{Y}^{w}_{i.} = \frac{\sum_{j=1}^{r_i}(z_{ij}Y_{ij})}{z_{i.}} \quad \forall\, i = 1,2,\dots,v$

(13)

Using (13) in (12) and simplifying we get,

$$SSE = \sum_{(i,j)} z_{ij}\left(y_{ij} - \overline{Y}^{w}_{..}\right)^2 - \sum_{i} z_{i.}(\overline{Y}^{w}_{i.} - \overline{Y}^{w}_{..})^2$$

Therefore,

$$TSS = \sum_{(i,j)} z_{ij}\left(y_{ij} - \overline{Y}^{w}_{..}\right)^2 \text{ and}$$

$$SST = \sum_i z_{i.}(\overline{Y}^{w}_{i.} - \overline{Y}^{w}_{..})^2$$

(14)

For algebraic computation, we simplify the different SS given in equation (14) as follow,

$$TSS = \sum_{(i,j)} z_{ij}y_{ij}^2 - (CF)_w \text{ and}$$

$$SST = \sum_i \left(\frac{\left(\sum_j z_{ij}Y_{ij}\right)^2}{z_{i.}}\right) - (CF)_w$$

(15)

Where,

$$CF_w = \frac{G_w^{\,2}}{z_{..}} = \frac{\left(\sum_{(i,j)} z_{ij}Y_{ij}\right)^2}{z_{..}}$$

(16)

Our derivation, matches with the approach followed in general least square theory discussed in Rao(2001)

For example discussed above, sales of three new menu items for the 18 restaurants, the estimated values for the Z_{ij} using algorithm of $E(Z_{ij}|Y_{ij})$ is given as;

Sr. No.	$E(Z_{ij}\|Y_{ij})^*$		
	Item1	Item2	Item3
1	0.297923	0.624991	1.084483
2	1.496042	1.02937	1.460752
3	1.469408	0.139515	1.35638
4	0.806586	1.012475	1.272101
5	1.416915	1.374276	0.650644
6	1.160621	0.938014	0.409504
$Z_{i.}$	6.647495	5.118642	6.233863
$Z_{..}$	18		
α_i	7.73995	5.123684	-12.4606
μ	34.78564		

*$E(Z_{ij}|Y_{ij})$ obtained on 86 iteration

Using equation (15) and (16), and estimated frailty random variable Z_{ij}, we can compute different sum of squares. Therefore constructed ANOVA according to new criterion is given as follow;

ANOVA

SV	SS	d.f.	MSS	F-value	Sign.
Item	1501	2	750.2568	11.976	0.000779
Error	939.7	15	62.64899		
Total	2440	17			

Since the p-value of 0.000779 is less than significance level ($\alpha = 0.05$), we reject the null hypothesis. Therefore, mean sales volumes of new menu items are significantly different from each other. From above ANOVA, we can see that there is large difference between the mean sales for each menu as the p-value is much lesser than the significance level.

An Example where treatment effects are not apparent[5]:

The effective life testing of insulating fluids at an accelerated load of 35 kV is being studied. Test data have been obtained for three types of fluids. The results from a completely randomized experiment were as in following table. Can we say effective life of fluid for each fluid type is same?

Fluid Type	Effective Life					
Fluid 1	17.6	18.9	16.3	17.4	20.1	21.6
Fluid 2	16.9	15.3	18.6	17.1	19.5	20.3
Fluid 3	19.3	21.1	17.4	17.5	18.3	19.3

Regular ANOVA approach;

Minitab Output:

Test for Equal Variances: Life versus Fluid Type

```
95% Bonferroni confidence intervals
for
standard deviations

Fluid     N    Lower    StDev    Upper
type
Fluid 1   6  1.10781  1.95218  6.09888
Fluid 2   6  1.05235  1.85445  5.79357
Fluid 3   6  0.78992  1.39200  4.34881

Bartlett's Test (Normal Distribution)
Test statistic = 0.57, p-value = 0.754

Levene's Test (Any Continuous
Distribution)
Test statistic = 0.52, p-value = 0.604
```

Test for equality of means Fluid 1, Fluid 2, Fluid 3

```
Source  DF     SS    MS     F      P
Factor   2   2.54  1.27  0.41  0.668
Error   15  45.94  3.06
Total   17  48.48
```

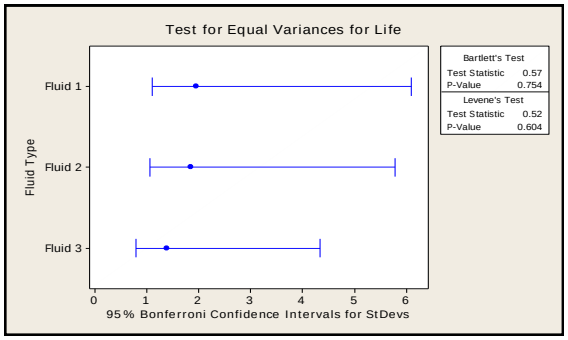

Fig: Test for Equal Variances

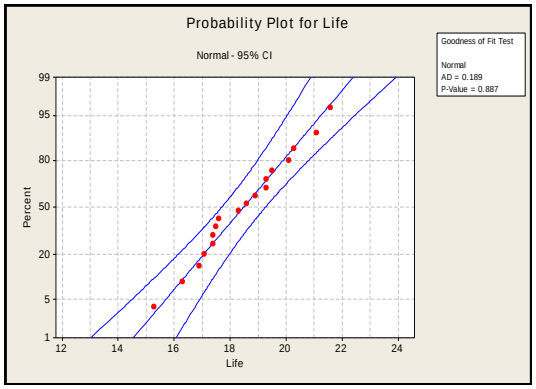

Fig. Test for Normality

So from the above minitab output, we can say that, there is no significant difference between the average effective life of fluid.

ANOVA construction through frailty random variable approach

The estimated values for z_{ij} using algorithm of $E(Z_{ij}|y_{ij})$ are given as;

Sr. No.	**E (Z_{ij}|Y_{ij})***		
	Fluid 1	Fluid 2	Fluid 3
1	1.311983	1.118577	1.333493
2	1.348964	0.478234	0.536131
3	0.684346	1.337415	1.017177
4	1.211225	1.224601	1.069834
5	0.755327	0.877381	1.444927
6	0.349067	0.567825	1.333493
Zi.	5.660912	5.604033	6.735055
Z..	18		
α_i	-0.0355	-0.36112	0.330316
μ	18.32556		

*$E(Z_{ij}|Y_{ij})$ obtained on 66 iteration

Constructed new ANOVA using frailty random variable approach is as follows,

ANOVA

SV	SS	d.f.	MSS	F-value	Sign.
Fluid Type	1.47	2	0.7363	0.3694	**0.6972**
Error	29.9	15	1.9936		
Total	31.38	17			

From above ANOVA table, we see that there is no significant difference between the averages of effective life of fluid.

CONCLUSION:

From the above study, we conclude that if we observe a relatively large error sum of squares compared to treatment sum of square then we should verify whether there is apparent difference in means of treatment effects. If yes, we suggest to use our approach and statistical ascertain the same. If not, our approach will also ascertain the same. Hence, we recommend to use our approach always to analyze CRD data.

REFERENCES:

1. Beard, R. E. (1959), "Note on some mathematical mortality models. The Lifespan of Animals. G.E.W. Wolstenholme, M.O'Conner (eds.),Ciba Foundation Colloquium on Ageing,Little, Brown,Boston,302–311.
2. Lancaster,T. (1979), "Econometric methods for the duration of unemployment",Econometrica 47, 939–956.
3. Vaupel, J. W., K. G. Manton and E. Stallard (1979), "The impact of heterogeneity in individual frailty on the dynamics of mortality", Demography 16, 439–454.
4. http://www.r-tutor.com/elementary-statistics/analysis-variance/completely-randomized-design.
5. Douglas C. Montogomery,(2012) "Design and Analysis of Experiments", 7th Ed, John Wiley.
6. C. Radhakrishnan Rao,(2001) "Linear Statistical Inference and It's Applications", Wiley.

PRAJÑĀ - Journal of Pure and Applied Sciences Vol. 26 : 53 – 61 (2018)
ISSN 0975 - 2595

CORROSION INHIBITION STUDY OF CITRUS AURANTIUM BARK (LEMON) POWDER AS GREEN INHIBITOR FOR MILD STEEL IN SULPHURIC ACID

AJAY N. PATEL, P. Y. DAVE AND G. M. MALIK
Department of Chemistry, Navyug science college, Surat.
Email: ajayupi_patel@yahoo.co.in, gmmalik2010@gmail.com

ABSTRACT

In this study, we report the study of the inhibition effect of Citrus aurantium bark powder on corrosion of mild steel in sulphuric acid using weight loss measurements and electrochemical techniques. The inhibitor efficiency of Citrus aurantium bark powder extract was found uniform for 24 h. Experimental results revealed that inhibition efficiency (I.E %) increased with increasing inhibitor concentration. As temperatures increased, percentage of inhibition decreases. Experimental results revealed that inhibition efficiency (I.E %) increased with increasing inhibitor concentration. The inhibitive and adsorptive characteristics of ethanol extract of Citrus aurantium bark powder for the corrosion of mild steel (MS) in 0.05 M H_2SO_4 solutions have been studied using following methods for monitoring corrosion. Ethanol extract of Citrus aurantium bark powder is a good adsorption inhibitor for the corrosion of mild steel in H_2SO_4.

The methods used were weight loss, effect of temperature, polarization and Electrochemical Impedance Spectroscopic (EIS). The inhibition efficiency(I.E.) increases with inhibitor concentration. The adsorption study of these compounds of mild steel surface found to obey Citrus aurantium bark powder adsorption isotherm. The value of free energy of adsorption (ΔG^0_{ads}), heat of adsorption (Q_{ads}), energy of activation (E_a), enthalpy of adsorption(ΔH^0_{ads}) and entropy of adsorption (ΔS^0_{ads}) were calculated. Present study indicates that Citrus aurantium bark powder extract is a good inhibitor for the corrosion of Mild steel in sulphuric acid medium.

Keywords : Mild steel-1, Sulphuric acid-2, Citrus aurantium bark powder-3, corrosion-4, inhibition effect-5.

INTRODUCTION

Metals undergo corrosion in the presence of oxygen and moisture and involve two electrochemical reactions. Oxidation occurs at anodic site and reduction occurs at cathodic site. Corrosion inhibitors reduce or prevent these reactions, they are adsorbed on the metal surface and act by forming barrier to oxygen, moisture and some of the inhibitors facilitate formation of passive film on the metal surface. The corrosion and inhibition behaviors of mild steel in sulfuric acid in the presence of *Citrus auran*tium bark extract have been studied using the electrochemical methods. It was found that the inhibition efficiency increased with Citrus aurantium bark extract concentration. The inhibition efficiency of *Citrus aurantium* bark was found to vary with concentration, temperature and immersion time. Good inhibition efficiency I.E.% was recorded in acid solution. The inhibition efficiency was found to be more than 90% in 0.05 M H_2SO_4 solution of 1 gm/Lit. inhibitor concentration. The adsorption study of these compounds on mild steel surface found to obey Temkin's adsorption isotherm. The potentiodynamic polarization results showed that the compound studied was mixed type inhibitor.

METHODOLOGY

Metal specimen and surface pretreatment: Rectangular specimens of the size 4.4 x 2.0 x 0.2 cm having an area of 0.2011sq. dm. of mild steel with small hole of 0.5 cm diameter near the upper edge, were used for the determination of corrosion rate. The specimens were cleaned by washing with distilled water, degreased by acetone for 1-2 minutes, then dried in warm air by air drier several times and are preserve in desiccators till use.

Preparation of extract: *Citrus aurantium* bark were collected in oven and dried at 50°C, dried leaves were ground to powder form. 10.0 g of the powder was digested in 100 ml of alcohol. Filter the solution and evaporate it in room temperature. The powder was used to prepare various concentrations as the inhibitor.

Weight loss measurements: In this method, the mild steel specimen having an area of approximately 0.2011 sq.dm. were each

suspended and completely immersed in 230 ml of sulphuric acid solution with different concentration like 0.05M, 0.1M and 0.5M solution without and with different concentration of *Citrus aurantium* bark for 24 hrs immersed period. After the test specimen washed with distilled water followed by acetone and dried with air dryer and reweighed. From the weight loss data, corrosion rate (CR) was calculated.

Surface coverage values are very useful in explaining the adsorption characteristics. The inhibition efficiency (η%) and degree of surface coverage (θ) at each concentration of inhibitors was calculated by comparing the corrosion loss in the absence (W_u) and presence of inhibitor (W_i) using the relationships:

$$\eta\% = \frac{W_u - W_i}{W_i} \times 100 \qquad \ldots\ldots\ldots\ldots \quad (1)$$

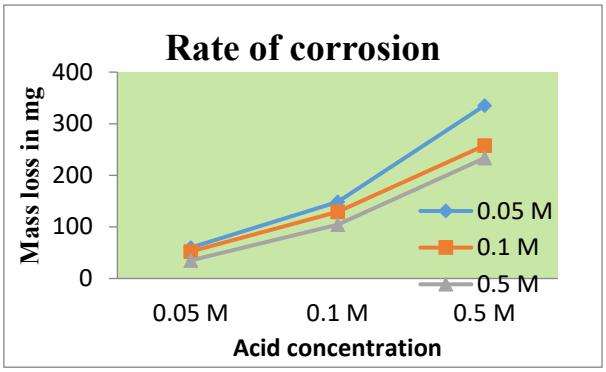

Figure 1: Corrosion rate of mild steel in **0.05 M H_2SO_4** in absence and presence of *Citrus aurantium* bark root for an immersion period of 24 h**.**

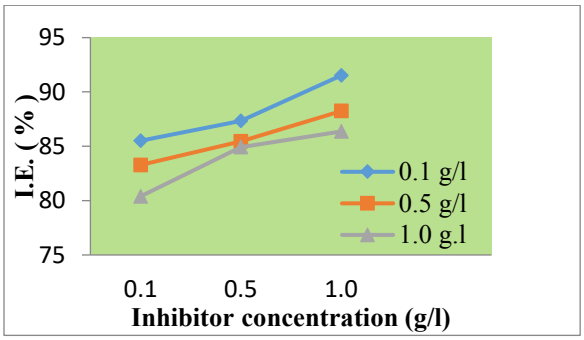

Figure 2: Rate of Inhibition efficiency of Mild steel in **0.05 M H_2SO_4** in absence and presence of *Citrus aurantium* bark root for an immersion period of 24 h**.**

Table-1: Effect of acid H_2SO_4 concentration on corrosion loss (CL) and inhibition efficiency (IE) of mild steel containing *Citrus aurantium bark* as inhibitor

Inhibitor conc.	Inhibitor	Time (h)							
1.0 gm/Lit		6h		12 h		18 h		24 h	
		mg dm^{-2} d^{-1}	I.E %	mg dm^{-2} d^{-1}	I.E %	mg $dm^{-2}d^{-1}$	I.E %	mg $dm^{-2}d^{-1}$	I.E %
	Blank	0.108	-	0.213	-	0.343	-	0.427	-
	Citrus aurantium	0.021	77.78	0.044	79.34	0.065	81.05	0.078	84.31

Table: 2 Inhibition efficiency (I E) of mild steel in different concentration of acid. Immersion period: 24h. Effective specimen area: 0.2011dm^2

Acid concentration							
Inhibitors	**Inhibitor Conc. (gm/Lit.)**	**0.05 M**		**0.1 M**		**0.5 M**	
		Mass loss (mg/dm^2)	I E (%)	Mass loss (mg/dm^2)	I E (%)	Mass loss (mg/dm^2)	I E (%)
Blank	-	413.19	-	887.45	-	1709.22	-
Citrus aurantium bark	0.1	58.89	85.51	148.42	83.28	335.13	80.39
	0.5	52.29	87.34	129.22	85.44	257.77	84.92
	1.0	35.06	91.51	104.38	88.24	233.22	86.36

Table: 3 Corrosion rate (Log ρ) of mild steel in **0.05 M H_2SO_4** in absence and presence of *Citrus aurantium* bark root for an immersion period of 24 h**.**

Inhibitor Conc. (gm/Lit)	**C.R (ρ)**	**Log ρ**	**I E (%)**	**Surface coverage (θ)**	**1-θ**	**Log (θ/1–θ)**
Blank	413.19	2.6161	-	-	-	-
0.1 gm/Lit	58.89	1.7774	85.51	0.8551	0.1449	0.7708
0.5 gm/Lit	52.29	1.7184	87.34	0.8734	0.1266	0.8390
1.0 gm/Lit	35.06	1.5448	91.51	0.9151	0.0849	1.0328

Table : 4 Corrosion rate (Log ρ) of mild steel in **0.1 M H_2SO_4** in absence and presence of *Citrus aurantium* bark root for an immersion period of 24 h**.**

Inhibitor Conc. (gm/Lit)	**C.R (ρ)**	**Log ρ**	**I E (%)**	**Surface coverage (θ)**	**1-θ**	**Log (θ/1–θ)**
Blank	887.45	2.9481	-			
0.1 gm/Lit	148.42	2.1715	83.28	0.8328	0.1642	0.6972
0.5 gm/Lit	129.22	2.1113	85.44	0.8544	0.1456	0.7685
1.0 gm/Lit	104.38	2.0186	88.24	0.8824	0.1176	0.8752

Table: 5 Corrosion rate (Log ρ) of mild steel in **0.5 M H_2SO_4** in absence and presence of *Citrus aurantium bark* root for an immersion period of 24 h**.**

Inhibitor Conc. (gm/Lit)	C R (ρ)	Log ρ	I E (%)	Surface coverage (θ)	1-θ	Log (θ/1–θ)
Blank	1709.22	3.2328	-	-	-	-
0.1 gm/Lit	335.13	2.5252	80.39	0.8039	0.1961	0.6128
0.5 gm/Lit	257.77	2.4112	84.92	0.8492	0.1508	0.7506
1.0 gm/Lit	233.22	2.3678	86.36	0.8636	0.1364	0.8013

OBSERVATION

Effect of temperature:

To study the effect of temperature on corrosion rate, the specimens was immersed in 230 mL in 0.05 M, 0.1 M, 0.5 M concentration of acid, with and without inhibitor at solution temperatures of 313, 323 and 333 K for a period of 2 hours.

Energy of activation (Ea) was calculated from the slopes of log ρ versus 1/T (ρ = corrosion rate, T = absolute temperature) and also with the help of Arrhenius equation.

$$\log\frac{\rho_2}{\rho_1}=\frac{Ea}{2.303R}\left(\frac{1}{T_1}-\frac{1}{T_2}\right) \quad \ldots\ldots\ldots\ldots (2)$$

where ρ_1 and ρ_2 are the corrosion rate at temperature T_1 and T_2 respectively.

The values of the free energy of adsorption (ΔG^0_{ads}) were calculated with slope of the following equation.

$$\log C = \log\left(\frac{\theta}{1-\theta}\right)-\log B \quad \ldots\ldots\ldots\ldots (3)$$

where $\log B = -1.74-\left(\frac{\Delta G^0_{ads}}{2.303RT}\right)$ and C is the inhibitor concentration. The values of heat of adsorption (Q_{ads}) calculated by the following equation.

$$Q_{ads}=2.303R\left[\log\left(\frac{\theta_2}{1-\theta_2}\right)-\log\left(\frac{\theta_1}{1-\theta_1}\right)\right]\times\frac{T_1T_2}{T_2-T_1} \quad \ldots\ldots\ldots\ldots (4)$$

Figure 3: Effect of temperature on corrosion rate

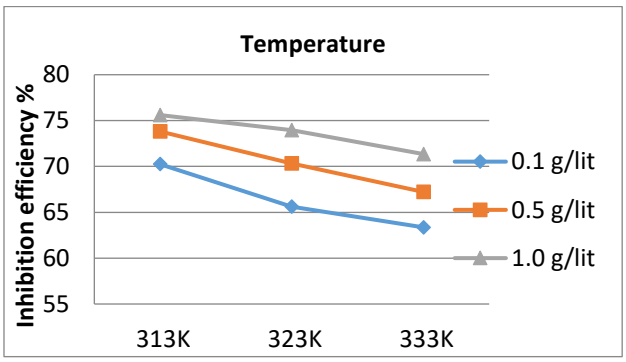

Effect of temperature on IE (%) for mild steel corrosion in 0.05 M H_2SO_4 at different inhibitor concentration of *Citrus aurantium* bark extract for immersion period of 2 h**.**

Effect of temperature on IE (%) for mild steel corrosion in 0.05 M H_2SO_4 at different inhibitor concentration of *Citrus aurantium* bark extract for immersion period of 2 h**.**

It was found that the value of Ea for inhibited system was higher than that of uninhibited system. It indicate that the inhibitors are more effective at lower temperature.

→ The enthalpy of adsorption (ΔH^0 ads) were calculated by using the equation.

ΔH^0_{ads} = Ea - RT (R = 8.314) …….. (5)

Where, Ea is activation energy at absolute temperature T in Kelvin and R is the gas constant.

→ The entropy of adsorption (ΔS^0 ads) were calculated by using the equation.

$$\Delta S^0_{ads} = (\Delta H^0_{ads} - \Delta G^0_{ads}) / T \quad \ldots. (6)$$

Polarization measurement

In the electrochemical cell Mild steel specimens having an area of 0.2011 sq.dm. was used as a

Table 6: Indicated that the value of I E% at difference temperature.

Inhibitor Concentration	Temperature K						(Ea) from equation (kJ/Mol)	(Ea) from Plot (kJ/Mol)
	313K		**323K**		**333K**			
	C R mg/dm²	I E %	C R mg/dm²	I E %	C R mg/dm²	I E %		
Blank	217.87	-	299.43	-	412.21	-	27.66	33.07
0.1 gm/Lit	68.14	68.72	101.23	66.19	159.38	61.34	36.94	42.19
0.5 gm/Lit	56.08	74.26	89.43	70.13	135.04	67.24	38.05	42.37
1.0 gm/Lit	51.38	76.42	81.28	72.86	119.32	71.05	36.45	39.88

working electrode, Ag / AgCl electrode as a reference electrode and platinum electrode as an auxiliary electrode and allowed to established a steady-state open circuit potential (OCP) for approximately 15 min. Polarization curves were plotted with potential against log current density

Electrochemical Impedance spectroscopy measurement (EIS) :

The typical Nyquist plots of Mild steel in the absence and presence of *Citrus aurantium* bark extract in 0.05M sulphuric acid solution was presented in figure. From the figure it was observed that the diameter of the semicircle increases in the case of inhibited acid solution, indicated an increase in corrosion resistance of system.

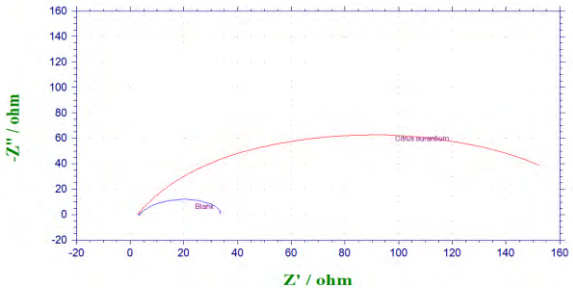

Figure 4: Nyquist plots of Mild steel in the absence and presence of *Citrus aurantium* bark

Tafel plot : Cathodic and anodic polarization curves give cathodic and anodic Tafel lines correspondingly. This technique is used to

measure the corrosion current(i_{corr}) so that the corrosion rate can be calculated. A Tafel plot can yield i_{corr} directly or it can yield the Tafel constants (βa and βc). The Tafel constants can then be used with the R_p value of calculate $i_{corr.}$

The inhibition efficiency IE (%) was evaluated from the Potentiodynamic polarization data of corrosion current density (i_{corr}) by the following formula.

$$IE\ (\%) = \frac{i_{corr}\ (uninhi) - i_{corr}\ (inhi)}{i_{corr}\ (uninhi)} \times 100 \quad .. (7)$$

Where , $i_{corr\ (uninhi)}$ and $i_{corr\ (inhi)}$ are corrosion current densities of metal in the absence and presence of inhibitors respectively.

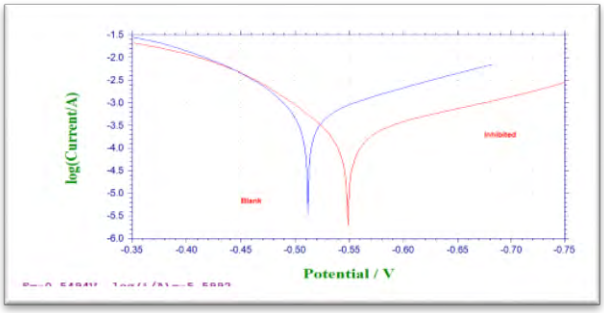

The double layer capacitance (Cdl) was calculated from the equation as below.

$$Cdl = \frac{1}{2\pi\ fmax\ Rct} \quad \ldots\ldots\ldots\ldots (8)$$

Where , f_{max} is the frequency at which the imaginary component of the impedance is maximum.

Table 7: Impedance parameters for corrosion of Mild steel in 0.05M sulphuric acid in the absence and presence of *Citrus aurantium* bark extract.

System	R_{ct} (Ω cm^2)	C_{dl} (μF/cm^2)	Inhibition efficiency (I.E %)	
			By EIS Method	By Mass Loss Method
Blank	30	44.2097	-	-
Citrus aurantium bark bark	149	1.7228	87.54 %	96.10 %

RESULTS AND DISCUSSION:

Weight loss studies

The values of inhibition efficiency (I.E %) and the corrosion rate (CR) obtained from the weight loss method at different concentrations of H_2SO_4 given in table-1.

Effect of temperature

The effect of temperature was studied in 0.05 M H_2SO_4 containing 1.0 gm/Lit. of inhibitor concentration at 313, 323 and 333 K temperature. The results showed corrosion loss increased with increase in temperature. Inhibition efficiency of inhibitors decreased with the rise in temperature.

Potential measurement

In 0.05 M H_2SO_4 the potential shifted to the negative direction from its initial value.

On addition of 1.0 g/lit of the inhibitor *Citrus aurantium* bark in 0.05 M H_2SO_4 the initial value of the OCP (open circuit potential) increased and settled at about within 5 minutes.

Polarization measurements

Anodic and cathodic polarization curves for mild steel in 0.05 M H_2SO_4 at 1.0 gm/Lit inhibitor concentration in the presence of inhibitors are shown in figure-1. The value of the corrosion potential with inhibitors were found more positive than without inhibitors as shown in figure-2. The semicircular nature of the plots indicates that the corrosion of mild steel is mainly controlled by charge transfer process.

Table 8: Potentiodynamic data and inhibition efficiency I.E (%) for mild steel in 0.05 M sulphuric acid at 1.0 g/l *Citrus aurantium* bark extract inhibitor.

System	E_{corr} (mV)	i_{corr} (µA)	Tafel Slop			Inhibition efficiency (I.E %)	
			Anodic +βa	Cathodic -βc	β (mV)	By Polarization Method	By Mass Loss Method
Blank	-0.548	85.6 x 10^{-4}	9.182	4.519	1.3167	-	-
Citrus aurantium bark	-0.567	17.6 x 10^{-4}	8.865	4.635	1.3233	86.45	91.51

CONCLUSION

Citrus aurantium bark was found as good eco-friendly inhibitor for the corrosion control of mild steel in H_2SO_4 solution. The inhibition efficiency increases with increase in *Citrus aurantium* bark concentration. *Citrus aurantium* bark adsorbed on metal surface follows Langmuir adsorption isotherm. Tafel plot indicates *Citrus aurantium* bark acts as a mixed type inhibitor.

REFERENCES

[1] George K.S. Investigation of carbon dioxide corrosion of mild steel in the presence of acetic acid. Corrosion science section – 178, NACE International Corrosion, 2007

[2] De Souza, F.S. and Spinelli, A., Caffeic acid as a green corrosion inhibitor for mild steel. Corrosion Science; 2009, 51(3): 642 649.

[3] Skryler LD, Streltsova EA and Skrylevo Tl. Inhibitory action of xylenol orange on aluminum corrosion in hydrochloric acid solution. Protection metals USSR. 1991; 27:755-758

[4] Vashi, R. T. and patel K.K. [Azadirachta indica extract as corrosion inhibitor for

copper in nitric acid,] *Research Journal of Chemical Sciences*, 2015,5(11), 59-66.

[5] Raicheva, S.N, Aleksiev, B.V. and Sokolove, E.I, The effect of the chemical structure of some nitrogen-containing and sulphur-containing organic compounds on their corrosion inhibiting action‖, Corrosion Science] *Corrosion science*, Vol.34 No.2, 1993, 34, 343-350.

[6] Swift A, Paul AJ and Vickerman JC. Investigation of the surface activity of corrosion inhibitors by XPS and time of flight SIMS. Surface interface analysis, 1993, 20, 27-35.

[7] Ejieh, C. and Dr. Ejimofor, R.A [Inhibition of corrosion on mild steel using piper guineense (uziza) extract in sulphuric acid medium of varying pH value,], 2016, 8, 3.

[8] Kumpawat N., Chaturvedi A. and Upadhyay R.K. Corrosion inhibition of mild steel by alkaloid extract of Ocimum sanctum in HCl and HNO3 solution. *Res. J. Chem. Sci*. 2012, 2(5),

[9] Abdel-Gaber A, Abd-El-Nabey B and Saadaway M. **(2009)**, "Inhibitive action of Cannabis plant extract on the corrosion of copper in 0.5M H2SO4", Corrosion Science. Vol.51, 1038

[10] Oguzie E E. **(2007)**, "Corrosion inhibition of mild steel in acidic and alkaline media by Sansevieria Trifasciata extract", Corrosion Science. Vol.49, 1527-1539

[11] Nnanna L A, Obasi V U, Nwadiuko O C, Mejeh K I, Ekekwe N D, Udensi S C. **(2012)**, "Inhibition by Newbouldia leavis leaf extract of the corrosion of mild steel in HCL and H2SO4 solution", Archives of Applied Science Research. Vol. 4(1), 207-217

[12] Deng S and X Li. **(2012)**, "Inhibition effect of Dendrocalamus Brandisii leaves extract on mild steel in HCL solution", Corrosion Science. Vol.65, 299-308

[13] Joshi H, Parle M. *Nelumbo nucifera petal* improves learning and memory in mice. J Med Food. 2006;9:113–8.

[14] Rao VS, Rao A, Karanth KS. Anticonvulsant and neurotoxicity profile of *Nelumbo nucifera petal* in rats. J Ethnopharmacol. 2005;102:351–6.

[15] Bagchi A, Oshima Y, Hikino H. Neolignans and Lignans of *Nelumbo nucifera petal* Roots1. Planta Med. 1991;57:96–7.

[16] Lyle N, Bhattacharyya D, Sur TK, Munshi S, Paul S, Chatterjee S, et al. Stress modulating antioxidant effect of *Nelumbo nucifera petal*. Indian J Biochem Biophys. 2009;46:93–8.

[17] Sharma P, Chaturvedi A, Upadhyay R K and Parashar P. **(2008)**, "Study of corrosion inhibition efficiency of naturally occurring Argenmone Mexicana on mild steel in HCL solution", Journal of Technology Research Chemistry. Vol.15(1), 21

[18] Al-Turkustani A M, Arab S T and Aldahiri R H. **(2010)**, "Aloe plant extract as an environmentally friendly inhibitor

on the corrosion of mild steel in HCL in absence and presence of Iodide ions", Journal of Modern Applied Science. Vol.4, 105-124

[19] James A O and Etela A O. **(2008)**, "Aloe-vera an inhibitor of mild steel corrosion in HCL", Journal of Pure and Applied Chemistry. Vol.3(3), 159-163

[20] Oguzie E E. **(2007)**, "Corrosion inhibition of mild steel in acidic and alkaline media by Sansevieria Trifasciata extract", Corrosion Science. Vol.49, 1527-1539

[21] Nnanna L A, Obasi V U, Nwadiuko O C, Mejeh K I, Ekekwe N D, Udensi S C. **(2012)**, "Inhibition by Newbouldia leavis leaf extract of the corrosion of mild steel in HCL and H2SO4 solution", Archives of Applied Science Research. Vol. 4(1), 207-217

[22] K. Zarrad, A. B. Hamouda, I. Chaieb, A. Laarif, and J. M.-B. Jemâa, "Chemical composition, fumigant and anti-acetylcholinesterase activity of the *Tunisian Citrus aurantium* L. essential oils," *Industrial Crops and Products*, vol. 76, pp. 121–127, 2015.

[23] A. Sanei-Dehkordi, M. M. Sedaghat, H. Vatandoost, and M. R. Abai, "Chemical compositions of the peel essential oil of *Citrus aurantium* and its natural larvicidal activity against the malaria vector Anopheles stephensi (Diptera: Culicidae) in comparison with Citrus paradisi," *Journal of Arthropod-Borne Diseases*, vol. 10, no. 4, pp. 577–585, 2016.

[24] P. Kang, K.-H. Ryu, J.-M. Lee, H.-K. Kim, and G. H. Seol, "Endothelium- and smooth muscle-dependent vasodilator effects of *Citrus aurantium* L. var. amara: focus on Ca^{2+} modulation," *Biomedicine and Pharmacotherapy*, vol. 82, pp. 467–471, 2016.

[25] X.-L. Zhang, W.-F. Xu, G. Chen, H.-F. Wang, and Y.-H. Pei, " Two new phenolic glycosides isolated from the fruits of *Citrus aurantium*," *Chinese Journal of Natural Medicines*, vol. 15, no. 1, pp. 41–44, 2017.

[26] F. Pellati, S. Benvenuti, and M. Melegari, " High-performance liquid chromatography methods for the analysis of adrenergic amines and flavanones in *Citrus aurantium* L. var. amara," Phytochemical Analysis, vol. 15, no. 4, pp. 220–225, 2004.

PRAJÑĀ - Journal of Pure and Applied Sciences Vol. 26 : 62 – 68 (2018)
ISSN 0975 - 2595

STUDY OF ANILINE AND ITS DERIVATIVES AS A CORROSION INHIBITORS IN HYDROCHLORIC ACID SOLUTION

M. B. MAPARA.
Department of Chemistry, M. B. Patel Science College, Anand. Gujarat -388001

ABSTRACT

Corrosion is a multi-billion dollar, world-wide problem and the current knowledge of corrosion and corrosion prevention is never adequate and there is a persistent need for further research to complement technical developments. Mild steel is frequently used as a construction material in different industries due to its low cost and high mechanical strength. However, corrosion data are less readily available in many of these environments. The main purpose of this study is to examine effect of acid, strength and additive concentrations on the corrosion resistance of mild-steel. In this study, weight-loss and thermometric techniques have been employed.

Key words: Hydrochloric acid, aniline derivatives, Weight-loss Measurements, Thermometric Measurements

INTRODUCTION

Corrosion behaviour of mild-steel in plain hydrochloric acids has been reported since long. The main purpose of this study is to examine the effect of - (i) acid concentration, (ii) additive concentration on the corrosion resistance of mild-steel, and (iii) mechanism of protective action. For the purpose of study - conventional weight-loss method and thermometric techniques were employed.

Corrosion is a natural phenomenon, which degrades the metallic properties of metal/alloys and renders them to be rejected from the specific structures of industrial importance. Country like India suffers very much in its economical growth due to the destructive phenomena of corrosion because of the tropical climate. The problem of corrosion is very serious in various industries because of the losses that occur due to shut-down and failures of industrial operations are of the colossal properties. Most common constructional of the structural metallic material steel is effectively an alloy of iron and carbon with minor incidental elements like silicon, manganese, sulphur and phosphorous. However, it is prone to corrosion in aqueous environment, especially acidic solution, which is usually involved in industrial exercises such as acid pickling, industrial acid cleaning, acid descaling and oil well acidizing processes[1,2]. Heterocyclic compounds have been reported as effective corrosion inhibitors because they can easily adsorb on metallic surface via their π- and non-bonding electrons, aromatic rings and polar functional groups, which act as adsorption centers[3,4,5,6,7,8,9].

EXPERIMENTAL

(1) Weight-loss Measurements:

Mild-steel with the composition of S-0.05%, P-0.02%, Mn-0.70%, C-0.27%, Si-0.35% is used. For complete immersion test the test specimens of size 5.5 cms x 2.5 cms x 0.2 cms were completely immersed in 250 ml of corrosive electrolyte solution. The concentration of plain hydrochloric acid solution studied were 0.1 M, 0.5 M, 1.0 M and 2.0 M. The effect of different concentrations (1, 5, 10 and 25 mM) of substituted derivatives i.e. p-toluidine, o-toluidine, p-chloroaniline, o-chloroaniline, aniline, p-nitroaniline and m-nitroaniline were

studied to understand the corrosion behaviour in presence of these compounds. The immersion period was ranging from 60 minutes to 24 hours in different acid concentrations. Total immersion tests were carried out at 30ºC with and without aniline and its derivatives. All the chemicals used were of Analytical Reagents (A.R) grade. From the results of weight-loss measurements - (i) corrosion rate (mdd), (ii) inhibition efficiency (IE%), (iii) surface coverage (θ) were calculated.

(2) Thermometric Measurements:

Test specimen of size 2.5 cms x 1.0 cm x 0.2 cm was immersed in 20 ml of acid solution for the thermometric study. The test were carried out in the concentration of 1.0 M and 2.0 M acid solutions, using 1, 5, 10 and 25 mM of aniline and its derivatives. Digital thermometer with 0.01ºC precision was used in Dewar flask. The changes in temperature were recorded at the regular interval of time. The results were used to calculate reaction number (RN) and inhibition efficiency (IE%).

RESULTS:

Weight-loss Measurements:

Corrosion behaviour of mild-steel in hydrochloric acid solution at different concentration were studied by weight-loss measurements. It has been observed that the corrosion rate increases with increase in the acid concentration. The corrosion rate increases from 603.25 mdd (0.1 M HCl) to 120.23×10^2 mdd (2.0 M HCl). The values of corrosion rate (mdd) and inhibition efficiency (IE%) for the inhibitors were calculated and reported in tables-1.

Addition of aniline and its derivatives reduces the corrosion rate.

The value of surface coverage was calculated directly from percentage inhibition efficiency by weight-loss method.

Thermometric Measurements:

Results of thermometric technique are presented in tables-2. It can be seen from the data that time to reach maximum temperature (T_{max}) has increased gradually and the temperature difference (ΔT) of the system has gradually decreased with increase in additive concentration.

The plots of time (minute) versus temperature (ºC) are given in figures-1 and 3 and reaction number (ºC min^{-1}) versus log C (M) is given in figures-2 and 4. Table 2 also include the comparison of inhibition efficiency arrived by thermometric and weight-loss method.

DISCUSSION:

Corrosion in hydrochloric acid solution is of great importance in many chemical processes. The present work was carried out in different concentrations of hydrochloric acid. As it is evident from the result presented that there was considerably low corrosion rate in lower concentration of acid solution and the corrosion rate gets increased with increase in acid concentration. It has already been established that at higher concentration of acid solution, corrosion behaviour of mild-steel can be considered to be predominantly chemical in nature. The dissolution rate for steel in various acids depends on the surface finish of the steel, type and concentration of the acid, temperature and the presence or absence of

impurities that can either promote or inhibit corrosion. Generally, the corrosion rate of mild-steel in hydrochloric acid increases with increase in acid concentration.

Decrease in corrosion rate with increase in additive concentration may be attributed to the decrease in the transport of oxygen and other reducible species which otherwise affect cathodic reaction adversely. At lower concentration, adsorbed layer of the additive may be incomplete. Inhibitive action of aniline and its derivatives on the dissolution character of ferrous material can be attributed to interaction between the additive and the metal surface. Though that may be the first stage of inhibition process. These aniline and its derivatives might have formed a bond with metal and the molecule might have been chemisorbed at the metal surface.

The results presented in tables-1 and 2 and figures-2 and 4 indicate successive decrease in reaction number (RN) and temperature difference (ΔT). Which suggest decrease in corrosion rate in presence of aniline and its derivatives. Higher reaction number (RN) in plain acid solution suggests dissolution of mild-steel. Decrease in reaction number (RN) with increase in aniline and its derivatives concentration suggest adsorption of the compound on the corroding surface. Furthermore, temperature difference (ΔT) values also decrease which suggest inhibition in presence of the additives used. The extent of inhibition depends on the degree of the coverage of the metal surface with the adsorbate. It can be said that when inhibitor is added, induction period is increased. It can also be concluded that strongly adsorbed inhibitors caused increase in time to reach T_{max}. Inhibitor efficiency can be very well judged by knowing the extent to which reaction number (RN) is affected. It is clear from the figures-2 and 4, that the curves are characterized by an initial period during which the temperature remain constant or varies vary slightly. The part of the curves can be described as incubation period in which pre-immersion oxide film protects the metal from acid attack or an induction period suggests time required the break-down of the film and start of attack. Plots of reaction number (RN) versus log C give straight lines indicating the fact that all the compounds used form chemisorbed monolayer protective film on the corroding surface.

The narrow difference in percentage inhibition on comparison of thermo- metric data with weight-loss measurements established the usefulness of this method.

Generally, inhibition efficiency of aniline can be correlated to its basic character by virtue of the amino group. In acid solutions, nitrogen atom of the amino group with its lone pair of electrons neutralizes acidic character of corrosive solutions to some extent and this is responsible for the corrosion inhibiting behaviour of aniline.

Introduction of a nitro group into the aniline molecule reduces its efficiency as an inhibitor. This could be due to the electron withdrawing tendency of the nitro group which weakens the basic nature of the parent compound as is evident from their pKb values. Among the nitro derivatives of aniline examined, p-nitroaniline was found to be a relatively

better corrosion inhibitor than m-nitroaniline. Presence of nitro group at meta-position to the amino group in the case of m-nitroaniline retards its portion not only due to electron withdrawing tendency but also due to steric hinderance. In p-nitroaniline steric hinderance is much reduced due to the greater separation of the amino group and nitro groups, undergoes protonation relatively easily and thereby neutralizing a greater amount of the acid than its meta isomer. P-Nitroaniline is hence more effective as an inhibitor compared to m-nitroaniline and its inhibition efficiency increases with increase in concentration.

Introduction of chlorine atom into aniline molecule was found to improve its inhibition efficiency. As is known, that any factor that enhances the basic character of aniline boosts its ability to reduce the concentration of the corroding acid through neutralization and promotes its inhibitive capacity. The trend observed for the chloro derivatives of anilines were thus as expected. Chlorine with its (+) I-inductive effect enable the enhancement of electron density over the amino nitrogen atom of aniline and thereby increasing its basic character.

The different isomeric toluidines viz. o-toluidine and p-toluidine showed a trend similar to what as observed for the corresponding chloroanilines. Toluidines were found to be more efficient inhibitors compared to the chloroanilines under similar experimental conditions. This was expected considering the greater electron donating tendency [(+) I-inductive effect] of methyl group with respect to that of the chlorine atom in chloroanilines. The following order of corrosion inhibition capacity in acidic media was observed for the isomeric toluidines:

p-toluidine > o-toluidine > p-chloroaniline > o-chloroaniline > aniline >p-nitroaniline > m-nitroaniline.

CONCLUSION:

From the above discussion, the following conclusions can be drawn:

(1) The corrosion rate of mild-steel increases with increase in acid concentration. The behaviour is predominantly chemical in nature.

(2) The corrosion rates are affected by nature of complex reaction taking place and also by the nature of the protective film.

(3) The extent of inhibition by aniline derivatives increases with the increase in concentration of additives.

(4) p-toluidine is found more effective compared to other organic additives.

(5) The order of inhibition efficiency the compounds examined can be given as under:
p-toluidine > o-toluidine > p-chloroaniline > o-chloroaniline > aniline >
p-nitroaniline > m-nitroaniline.

(6) Linearity of the plots of log (θ/1-θ) versus log C in presence of all the organic compounds suggests that they function through adsorption which can be explained using Langmuir isotherm model.

(7) Somewhat less anodic polarization, but more cathodic polarization in inhibited acid suggests that these compounds function through general adsorption at cathodic as

well as anodic region of the metal surface.

(8) There was good agreement in the value of inhibition efficiency calculated using polarization technique and thermometric results.

(9) Reaction number (RN) drops to a considerable extent and time to reach T_{max} gets prolonged in presence of the all inhibitor studied.

References

[1] Yadav M., Behera D. & Sharma U. Nontoxic corrosion inhibitors for N80 steel in hydrochloric acid. Arabian J. Chem. 9**(2)**, S1487–S1495 (2016).

[2] Zhao J. et al. . Cigarette Butts and Their Application in Corrosion Inhibition for N80 Steel at 90 °C in a Hydrochloric Acid Solution. Ind. Eng. Chem. Res. 49, 3986–3991 (2010).

[3] Yadav M., Sharma U. & Yadav P. N. Isatin compounds as corrosion inhibitors for N80 steel in 15% HCl. Egyptian J. Petrol. 22, 335–344 (2013).

[4] Migahed M. A. & Nassar I. F. Corrosion inhibition of Tubing steel during acidization of oil and gas wells. Electrochim. Acta. 53, 2877–2882 (2008).

[5] Chauhan L. R. & Gunasekaran G. Corrosion inhibition of mild steel by plant extract in dilute HCl medium. Corros. Sci. 49, 1143–1161 (2007).

[6] Yuce A. O. & Kardas G. Adsorption and inhibition effect of 2-thiohydantoin on mild steel corrosion in 0.1 M HCl. Corros. Sci. 58, 86–94 (2012).

[7] Abdallah M., Asghar B. H., Zaafarany I. & Fouda A. S. The inhibition of carbon steel corrosion in hydrochloric acid solution using some phenolic compounds. Int. J. Electrochem. Sci. 7, 282–304 (2012).

[8] Verma C., Ebenso E. E., Olasunkanmi L. O., Quraishi M. A. & Obot I. B. Adsorption Behavior of Glucosamine Based Pyrimidine-fused Heterocycles as Green Corrosion Inhibitors for Mild Steel: Experimental and Theoretical Studies, J. Phys. Chem. C. 120, 11598–11611 (2016).

[9] Ahamad I., Prasad R. & Quraishi M. A. Adsorption and inhibitive properties of some new Mannich bases of Isatin derivatives on corrosion of mild steel in acidic media. Corros. Sci. 52, 1472–1481 (2010).

TABLE- 1: Influence of different concentration of aniline and its derivatives on corrosion rate (mdd), inhibition efficiency (IE%) and surface coverage (θ) of mild-steel in 2.0 M HCl solution. Specimen area : 30.70 sq.cm. Immersion period : 1 hr.

Temperature : 30 ± 1°C

Inhibitor and its concentration (mM)		Corrosion Rate (mdd) (mgm/dm^2/day)	Inhibition Efficiency (IE%)	Surface Coverage (θ)	Log (θ/1-θ)
Blank		12023.45	-	-	-
1. p-Toluidine	1	6340.06	47.24	0.4724	-0.0479
	5	5573.94	53.61	0.5361	0.0628
	10	5269.05	56.12	0.5612	0.1068
	25	4792.18	60.08	0.6008	0.1775
2. o-Toluidine	1	6973.28	41.98	0.4198	-0.1405
	5	6058.62	49.57	0.4957	-0.0079
	10	6575.57	52.79	0.5279	0.0485
	25	5136.15	57.23	0.5723	0.1264
3. p-Chloroaniline	1	7637.78	36.42	0.3642	-0.2419
	5	6762.21	43.71	0.4371	-0.1098
	10	6363.51	47.05	0.4705	-0.0513
	25	5863.19	51.18	0.5118	0.0205
4. o-Chloroaniline	1	8302.28	30.89	0.3089	-0.3497
	5	7356.35	38.81	0.3881	-0.1977
	10	6918.56	42.42	0.4242	-0.1327
	25	6355.70	47.13	0.4713	-0.0499
5. Aniline	1	8990.22	25.22	0.2522	-0.4720
	5	8044.29	33.07	0.3307	-0.3061
	10	7614.33	36.61	0.3661	-0.2384
	25	7051.46	41.32	0.4132	-0.1532
6. p-Nitroaniline	1	9357.65	22.14	0.2214	-0.5461
	5	8677.52	27.78	0.2778	-0.4149
	10	8302.28	30.91	0.3091	-0.3493
	25	7911.40	34.16	0.3416	-0.2849
7. m-Nitroaniline	1	9834.52	18.17	0.1817	-0.6535
	5	9201.30	23.45	0.2345	-0.5138
	10	8935.50	25.66	0.2566	-0.4619
	25	8544.62	28.88	0.2888	-0.3913

TABLE- 2 : Influence of aniline and its derivatives on temperature difference (ΔT), time to reach maximum temperature (Δt), reaction number (RN) and inhibition efficiency (IE%) during corrosion of mild-steel in 2.0 M HCl solution.

Surface area of specimen : 3.2 sq.cm. Temperature : 30 ± 1°C

Inhibitor and its concentration (mM)		Temp. difference T_{max} (ΔT) °C	Time to reach (Δt) Min.	Reaction number (RN) °C Min^{-1}	Inhibition Efficiency (IE%) calculated from	
					Thermo-metric method	Weight-loss method
Blank		26.3	150	0.1754	-	-
1. p-Toluidine	1	19.8	215	0.0925	47.26	47.24
	5	17.8	220	0.0812	53.70	53.67
	10	17.6	230	0.0766	56.33	56.31
	25	16.8	240	0.0700	60.10	60.09
2. o-Toluidine	1	21.3	210	0.1015	42.13	42.12
	5	19.1	215	0.0889	49.53	49.30
	10	18.5	225	0.0824	53.02	52.67
	25	17.2	230	0.0749	57.30	57.28
3. p-Chloroaniline	1	22.3	200	0.1115	36.43	36.41
	5	20.6	210	0.0984	43.90	43.87
	10	19.9	215	0.0927	47.14	47.13
	25	18.8	220	0.0855	51.25	51.25
4. o-Chloroaniline	1	22.9	190	0.1204	31.36	31.33
	5	21.3	200	0.1066	39.22	39.20
	10	20.5	205	0.1004	42.75	42.74
	25	19.1	210	0.0912	48.00	47.96
5. Aniline	1	23.5	180	0.1304	25.66	25.61
	5	22.2	190	0.1171	33.24	33.22
	10	21.6	195	0.1110	36.72	36.67
	25	20.6	200	0.1033	41.11	41.05
6. p-Nitroaniline	1	23.7	175	0.1355	22.75	22.71
	5	22.6	180	0.1255	28.45	28.42
	10	22.8	190	0.1201	31.53	31.50
	25	22.3	195	0.1146	34.66	34.62
7. m-Nitroaniline	1	24.2	170	0.1428	18.59	18.53
	5	23.4	175	0.1342	23.49	23.48
	10	23.9	185	0.1297	26.05	26.00
	25	23.5	190	0.1242	29.19	29.15

PRAJÑĀ - Journal of Pure and Applied Sciences Vol. 26 : 69 – 77 (2018)
ISSN 0975 - 2595

SYNTHESIS, CHARACTERIZATION AND BIOLOGICAL APPLICATIONS OF OSMIUM(IV) COMPLEXES

BHARAT H. PURSUWANI, REENA R. VARMA AND MOHAN N. PATEL*
Department of Chemistry, Sardar Patel University,
Vallabh Vidyanagar–388 120, Gujarat, India.
Corresponding author. Tel.: +91 2692 226856
E-mail: jeenen@gmail.com

ABSTRACT

A series of osmium(IV) complexes of types [Os(L^{1-5})$(Br)_4$] (where L^1=2-benzoyl pyridine , L^2=di-pyridyl amine, L^3=2, 9-dimethyl-4,7-diphenyl-1,10-phenanthroline, L^4=o-phenylenediamine, L^5= di-pyridyl ketone) have been synthesized and characterized by electronic spectra, conductance measurements, magnetic measurement, LC-MS and FT-IR spectroscopy. An octahedral geometry around osmium(IV) has been assigned for all complexes. All complexes have been investigated for their interaction with Herring Sperm (HS) DNA utilizing the absorption titration and viscosity measurement study. The DNA-binding property of the osmium(IV) complexes have been also investigated theoretically using molecular docking study. The cleavage study on pUC19 DNA has been monitored by agarose gel electrophoresis. The results indicate that the osmium(IV) complexes can effectively promote the cleavage of plasmid DNA. The complexes have also been screened for their in vitro antibacterial and cytotoxicity activities. All complexes exhibited good antibacterial and cytotoxic activities.

Keywords: Osmium(IV), DNA-binding, Agarose gel electrophoresis, Cytotoxicity.

INTRODUCTION

Osmium metal have tendency to exhibit varying oxidation states, and due to such characteristics, it has been widely used in solar applications [1]. Attachment of heterocyclic moieties to the osmium metal brings up drastic changes in its applications to biological world. The heterocyclic environment around osmium metal could vary its reactivity as well as stability [2]. Osmium tetroxide is being used in hydroxylation of olefins [3]. But its salts bring ups a new look towards development of efficient and active complexes which could be important for biological studies. Complexes of different N-donor and O-donor ligands are of particular importance. Chemistry of osmium complexes is of keen importance. Osmium binding with P- and O- donor ligands has been studied widely. But, there is a thrust to study osmium metal with ligands having N-donor atoms.

There is a great potential of osmium in cancer treatment due to its unique chemical properties. So far, great promise has been shown in treating different types of cancer cells including colon and ovarian cancers that have developed and tested in the labs [4]. Complexes of osmium with phosphorus donor atoms have also been reported earlier [5]. Osmium complexes with phosphorous and arsenic donor atoms have been synthesized earlier and their spectral and electrochemical studies have been carried out [6]. Osmium metal binding with tris derivatives of bipyridyl ligands have been reported earlier [7].

Platinum compounds has been studied from decades. There is a need to explore chemistry of other metals. So we have synthesized Os(IV) complex of ligands with different donor atoms and have been characterized by mass spectroscopy, IR spectroscopy, electronic spectra, and magnetic measurement and conductance measurements. Biological studies of synthesized complexes i.e. DNA interaction activities, hydrodynamic volume measurement, absorption titration and molecular docking studies. Moreover antibacterial activity, cytotoxic activities if Os(IV) complex have been evaluated.

EXPERIMENTAL

Material and reagents

All chemicals used were of high purity were borrowed from Sigma Aldrich (Osmium tetroxide, ammonium bromide, hydrobromic

acid, orthophenylene diamine, 2-benzoyl pyridine, dipyridyl amine, dipyridyl ketone, 2,9-dimethyl-4,7-diphenyl-1,10-phehanthroline) were procured from Sigma Chemical Co.(India) (EtBr)and Lurea broath), from MTCC, India.

Physical measurements

FT-IR ABB Bomen MB 3000 spectrophotometer was used for taking IR spectra in; ῡ in cm^{-1}; range 4000–400 cm^{-1}. LC-MS spectra were taken using spectrophotometer which works thermally (United States of America). Electronic spectroscopy results were taken using Ultra Viloet-160A photometer operating on Shimadzu software (Japan). Gel electrophoresis was carried out using AlphaDigiDoc™ software.

SYNTHESIS

Synthesis and characterization of $(NH_4)_2OsBr_6$ salt

In round bottom flask, OsO_4 (0.001mmol) was mixed with 47% HBr and was refluxed for 2 hrs. The solution was decanted into 50 mL beaker and flask was rinsed with 9 mL HBr solution. To the hot beaker, 0.75gm NH_4Br (0.075mol) was added. After solid gets dissolved, the mixture was cooled at room temperature followed by addition of ethanol (12.5mL) with stirring. The solution was allowed to settle until dense black solid was obtained. Residue was transferred to sintered glass filter and was washed with ethanol till free from bromide. The product was kept in deep freezer at 2-4°C and successive filtrate were collected after each day. The salt was collected and again was evaporated to some level and kept under same condition again [8-9].

Synthesis and characterization of tetrabromido(2-benzoylpyridine)osmium(IV) (1)

$(NH_4)_2OsBr_6$ (0.2gm,0.46mmol) and 2-benzoylpyridine ligand (0.17gm,0.92mol) were dissolved and added in 10 mL methanol and refluxed for 45min.The reaction mass was cooled at RT followed by extraction with help of ethyl ethanoate. The compound was soluble in ethyl acetate and was collected by evaporating the solvent and excess salt left as residue was recovered and collected. The brownish precipitate formed were dried and washed with excess solvent.. Yield: 50%; M.p: (>300°c); Mol.Wt. : 693.06gm mol^{-1}; Magnetic Moment: 2.74 B.M ; ESI-MS (70eV) : m/z : 692.08(M^+), 614.5, 539.06, 458.06, 377.05, 183.2 (Base Peak); IR (KBr, cm^{-1}): 3070 ν(C-H); 1597 ν(C=O); 1450 ν(C=C); 1087,ν(C-N); 524 ν(Os-Br), 578 ν(Os-N). Conductance: 24 Ʊ mol^{-1} cm^2. UV-Vis (DMSO, $c = 10^{-4}$ mol dm^{-3}): λ_{max} (ε) = 276 nm (15,750 $mol^{-1}dm^3$ cm^{-1}).

Synthesis and characterization of tetrabromido(dipyridylamine)osmium(IV) (2)

It was synthesized using dipyridylamine by above procedure mentioned in *2.3.2*. Yield: 66.66%; M.p: (>300°c); Mol.Wt. : 681.05gm mol^{-1}; Magnetic Moment: 2.74 B.M ; IR (KBr, cm^{-1}): 3379 ν(C-H); 1365 ν(C=C); 1080 ν(C-N); 532.35 ν(Os-N); 354.90 ν(Os-Br). Conductance: 24 Ʊ mol^{-1} cm^2. UV-Vis (DMSO, $c = 10^{-4}$ mol dm^{-3}): λ_{max} (ε = 432 nm (75,550 $mol^{-1}dm^3$ cm^{-1}).

Synthesis and characterization of tetrabromido(2,9-dimethyl-4,7-diphenyl-1,10-phenanthroline)osmium(IV) (3)

It was synthesized using 2,9-dimethyl-4,7-diphenyl-1,10-phenanthroline by procedure mentioned in the section 2.3.2. Yield: 75%; M.p: (>300°c); Mol.Wt. : 694.04gm mol^{-1}; Magnetic Moment: 2.74 B.M; ESI-MS (70eV): m/z: 870.31(M^+), 795.60, 714.40, 636.40, 554.40, 360.60 (Base Peak), 78.40($C_6H_5^+$); IR (KBr, cm^{-1}): 3055 $\nu(C\text{-}H)_{ar.stretching}$; 1404 ν(C=C); 1033 ν(C-N); 393 ν(Os-Br); 540.07 ν(Os-N). Conductance: 24 Ʊ mol^{-1} cm^2. UV-Vis (DMSO, $c = 10^{-4}$ mol dm^{-3}): λ_{max} (ε) = 272 nm (25,800 $mol^{-1}dm^3$ cm^{-1}).

Synthesis and characterization of tetrabromido(orthophenylenediamine)osmium(IV) (4)

It was synthesized using orthophenylenediamine by above procedure mentioned in *2.3.2*. Yield: 33.33%; M.p: (>300°c); Mol.Wt. : 617.99gm mol^{-1}; Magnetic Moment: 2.74 B.M; IR (KBr, cm^{-1}): 3055.24 ν(C-H); 1450.77 ν(C=C); 1010 ν(C-N); 570 ν(Os-N), 378.05 ν(Os-Br). Conductance: 24 Ʊ mol^{-1} cm^2. UV-Vis (DMSO, $c = 10^{-4}$ mol dm^{-3}): λ_{max} (ε) = 432 nm (16,000 $mol^{-1}dm^3$ cm^{-1}).

Synthesis and characterization of tetrabromido(dipyridylketone)osmium(IV) (5)

It was synthesized using one mole of dipyridylketone by above procedure mentioned in *2.3.2*.Yield: 50%; M.p: (>300°c); Mol.Wt. : 694.04gm mol^{-1}; Magnetic Moment: 2.74 B.M; IR (KBr, cm^{-1}): 3078 ν(C-H); 1604,ν(C=O); 1033 ν(C-N); 1442 ν(C=C) , 686.66 ν(Os-N); 362 ν(Os-Br). Conductance: 24 Ʊ mol^{-1} cm^2. UV-Vis (DMSO, $c = 10^{-4}$ mol dm^{-3}): λ_{max} (ε) =270.50 nm (22,900 $mol^{-1}dm^3$ cm^{-1}).

BIOLOGICAL STUDY

***In-vitro* bacteriostatic activity**

MIC study was carried out on $Gram^+$ and $Gram^-$ microorganisms [10].

Brine shrimp toxicity screening

The activity was performed as described in literature method [11].

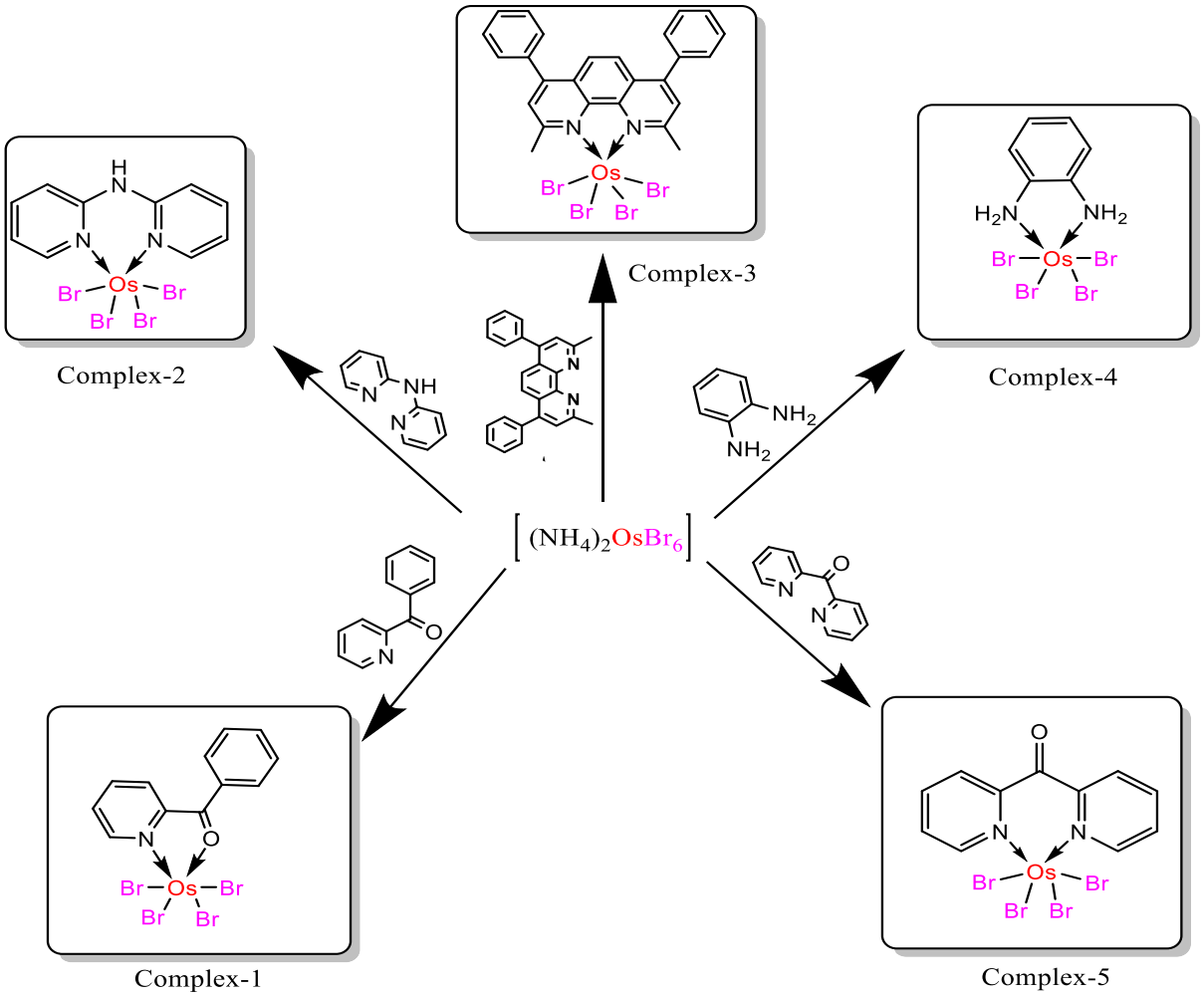

Absorption titration study of complex to HS DNA

This experiment was carried out using constant complex concentration in DMSO and varying HS-DNA concentration. [12-13].

Hydrodynamic volume measurement for complex to HS-DNA interaction

Hydrodynamic measurements were carried out by calculating time elapsed for complex-DNA solution to flow [14].

Molecular docking with B-DNA

HEX 8.0.0 software used to study docking interaction with B-DNA. [15-16].

Interaction of Os(IV) complexes with plasmid (pUC19) DNA by electrophoresis

Experiment was carried out using pUC19 DNA [17].

***In-vivo* cytotoxicity**

Schizosaccharomyces pombe cells were used for *in-vivo* cytotoxicity study [18-19].

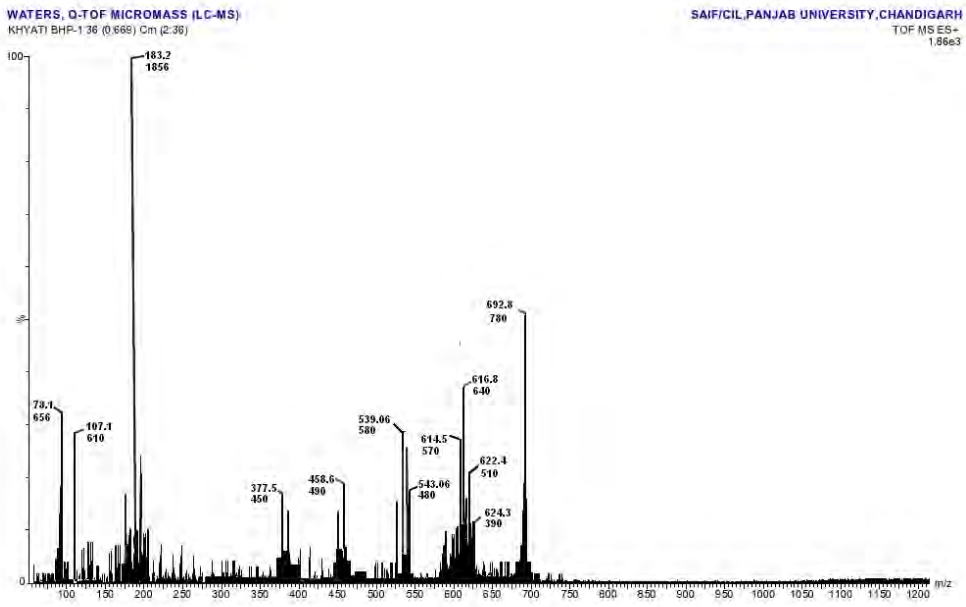

Figure 1. Mass spectra of *tetrabromido(2-benzoylpyridine)osmium(IV)* (1)

RESULTS AND DISCUSSION

Synthesis and characterization

Synthesized complexes have 2.74 BM magnetic moment value which is equivalent to theoretical spin value of octahedral complexes indicating paramagnetic behavior. Infrared spectra of complex 1 shows ν(C-H) at 3070 cm^{-1}, ν(C-O) at 1597 cm^{-1}, ν(C-C) at 1450 cm^{-1}, ν(Os-O) at 918 cm^{-1}, ν(Os-N) at 578 cm^{-1} and ν(Os-Br) at 524 cm^{-1} shown in supplementary material 1. Further there is peak at frequency 655.80 which is of N-Os-Br linkage showing comparatively higher value than ν(Os-N) [20-22]. MS of compound 1 exhibits $[M^+]$ at 692.08 m/z, Ph^+ at 78.10 m/z, $[C_6H_5CO^+]$ at 107.10 m/z justifying the structure of synthesized complexes shown in figure 1. Electronic spectra of Os(IV) have been recorded in DMSO solvent. The general spectral range of all the complexes fall between 271-432 nm which depict "metal-to-ligand charge-transfer" MLCT. All the complexes show non

electrolytic behavior having conductance value of 24 Ω^{-1} mol^{-1} cm^2.

In-vitro bacteriostatic activity

Broth dilution technique was used for carrying out to study activity of synthesized osmium(IV) complexes. It was performed against three $Gram^{-ve}$ and two $Gram^{+ve}$ bacteria.The values are effective in case of all the complexes as shown in Figure 2.

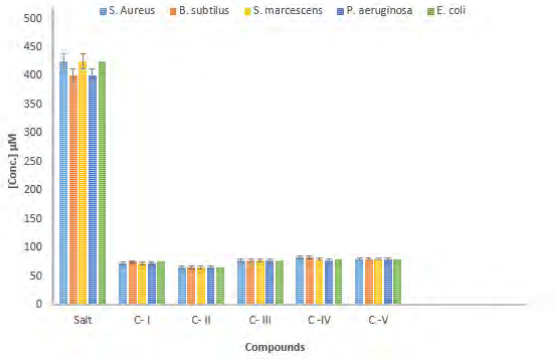

Figure 2. Minimum inhibitory concentration of Os(IV) complexes: The Os(IV) complexes are exposed at different concentrations overnight and the minimum inhibitory concentration of each complex is given by considering control sets gave null values

Brine shrimp toxicity screening

Brine shrimp lethality bioassay is used to study pharmacological activities and cytotoxicity by screening procedure of compounds having active biological moieties. Procedure deals with screening the synthesized compounds and calculating LC_{50} values (µg/ml). It is concluded that compound having least LC_{50} value is considered to be more potent. The values of different synthesized osmium(IV) complexes i.e. complexes 1, 2, 3, 4 and 5 are 15.62, 15.77, 6.58, 12.99, 15.92 µg/ml respectively. It could be concluded that complexes with ketonic group or carbonyl moiety which comprise electron withdrawing tendency bears more potent value compare to one with amine functionality.

Absorption titration study of complex to HS DNA interaction

Absorption titration study was carried out in presence of DMSO as a solvent and varying concentration of *HS DNA*. Complexes bind to DNA base pairs which shows Hypochromism shift as depicted in figure. The affinity of binding is calculated by following equation.

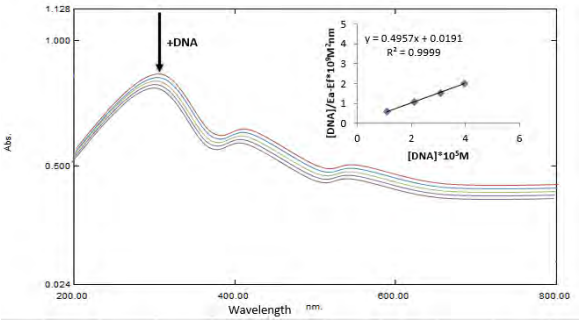

Figure 3. Absorption spectral changes on addition of HS DNA to the solution of complex III (after incubating it for 10 min. at room temperature in phosphate buffer. Graph: plot of $[DNA]/(\varepsilon_a-\varepsilon_f)$ vs. [DNA]. (Arrow shows the change in absorption with increase in concentration of DNA) amount of complexes and EtBr at 27±0.1 °C in phosphate buffer (pH 7.2)

where [DNA], ε_a, ε_f and ε_b are concentration of Deoxy ribonucleic acid, apparent absorption coefficient with respect to compound concentration, extinction coefficient and molar extinction coefficient respectively. From the graph of $[DNA]/(\varepsilon_a - \varepsilon_f)$ versus [DNA], intrinsic binding constant K_b is calculated from the slope. The Kb values of complexes 1, 2, 3, 4 and 5 are $0.23 \times 10^5\ M^{-1}$, $0.43 \times 10^5\ M^{-1}$, $0.22 \times 10^5\ M^{-1}$, $0.48 \times 10^5\ M^{-1}$

$$[DNA]/(\varepsilon_a - \varepsilon_f) = [DNA]/(\varepsilon_b - \varepsilon_f) + 1/K_b(\varepsilon_b - \varepsilon_f)$$

and $0.16 \times 10^5\ M^{-1}$, respectively. The successive order of values is 4 > 2 > 1 > 3 >5. Figure 3 Shows absorption spectral changes on addition of increasing amount of complex concentration.

Hydrodynamic volume measurement for complex to HS DNA interaction

Viscosity data gives the information about mode of complexes to DNA interaction.

The graph shows that the relative viscosity of the HS-DNA increases upon the addition of varying concentration of complexes suggesting partial intercalative mode of binding. Complexes 1, 2, 5 shows partial intercalative mode of binding whereas complexes 3 and 4 shows groove mode of binding that could be attributed due to planarity of phenyl ring in phenathrolene moiety in complex 3 and orthophenylenediamine ligand in complex 5 as shown in Figure 4. Due to planarity that could easily insert into binding site and show decrease in viscosity values hence showing groove mode of binding with the HS- DNA.

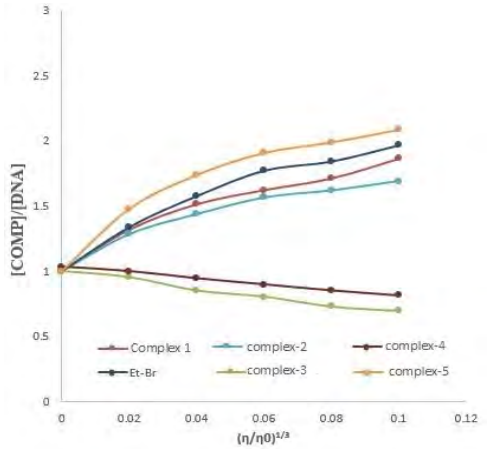

Figure 4. Plot of effect on relative viscosity of HS- DNA under the influence of increasing

Molecular docking with B-DNA

Molecular docking energy levels of complexes (1-5) are -301.07, -232.99, -287.73, -192.41 and -261.55 kJmol^{-1} respectively. The energy values clearly reflect interaction of complexes with DNA indicating effective binding. This also indicate effectiveness of presence of osmium as metal in complexes which shows binding ability. Again here we conclude that complex bearing phenyl moiety has more effective energy value compare to other complexes due to planarity and ease of insertion inside the groove. The figure 5 shows docked structure of complex 3 bearing phenanthrolene moiety. Due to planarity of phenyl rings it can easily insert inside the DNA showing effective docking energy value.

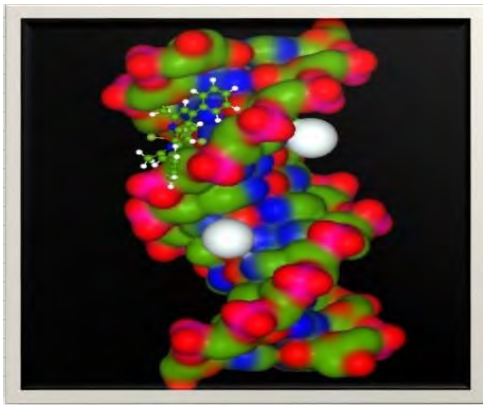

Figure 5. Docked structure of complex IV with B DNA

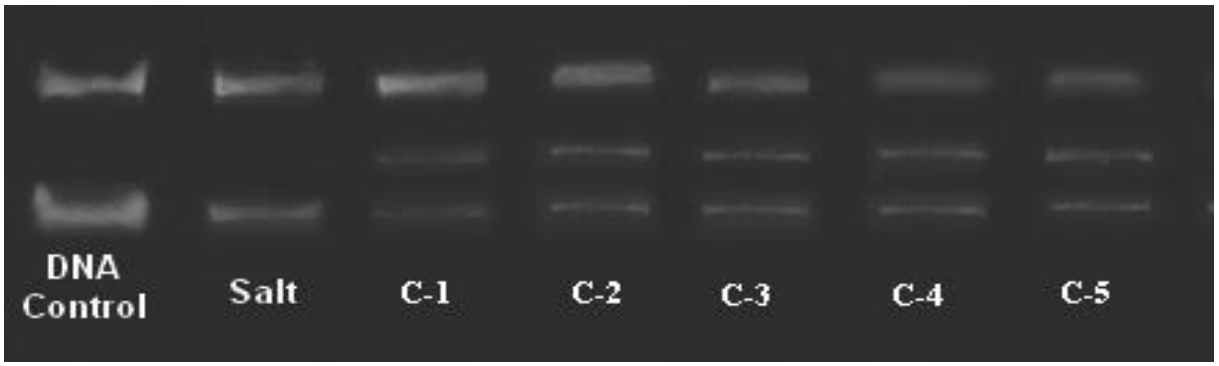

Figure 6. Photogenic view of cleavage of pUC19 DNA (50μM) with series of Os (IV) complexes (200 μ M) using 1% agarose gel containing 0.5 μgcm^{-3} ethidium bromide. All reactions were incubated in TAE buffer (pH 8) in a final volume of 15 mm^3, for 3 h. at 37 ^{o}

Interaction of Os(IV) complexes with plasmid (pUC19) DNA by electrophoresis

Gel electrophoresis property of ligands varies according to environment of surrounding ligands and complexes. Since our work consists of some planner and non-planner ligands surrounding metal salts, the cleavage properties varies accordingly. Complex having bipyridyl ketone moiety shows highest percentage of cleavage whereas complex with 2-benzoyl pyridine ring shows least. The successive order of cleavage of complexes is 2> 4 >3 > 5 >1.

In other words, high percentage of metal containing complex has good cleavage property to other. Photographed image figure 6 shows the cleavage of plasmid DNA in complexes and metal salt. The data are presented in Table 1.

***In-vivo* cytotoxicity**

For studying cell biology and cytotoxic effect, DNA of Schizosaccharomyces pombe cells is used. This are eukaryotic cells of big size. The selective activity of synthesized complexes is in order 3 >1 >4 >5 >2.. The complex with phenathrolene ring is more potent compare to others which could be attributed due to more planner structure of phenanthrolene ring to site into DNA of cells effectively

Table 1 DNA cleavage study

	Name	Form I	Form II	Form III	% Cleavage
1	DNA Control	83.3	16.7		
2	Salt	43.5	56.5		47.77
3	Complex 1	10.6	61.4	28	87.27
4	Complex 2	3.8	59.7	36.5	95.43
5	Complex 3	18.2	70.7	11.1	83.03
6	Complex 4	29.8	38.3	31.9	64.22
7	Complex 5	8.2	79.9	10.5	90.15

CONCLUSION

A series of heterocyclic ligand based osmium(IV) are studied. Biological activities of synthesized complexes have been studied. Spectral studies reveal that complexes exhibit Octahedral geometry.With comparison to osmium salt, complexes showed higher antibacterial activity. From absorption titration and viscosity data we conclude that complexes 1, 4 and 5 shows partial intercalative mode of binding whereas complexes 2 and 3 show groove mode of binding. Docking studies lead to conclusion of binding mode between osmium compounds and base pairs of DNA which shows intercalation. Further, cleavage tendency of complexes were good compared to osmium salt.

ACKNOWLEDGEMENTS

The authors thankful to the HOD, Chemistry, Sardar Patel University, VVN, Gujarat, India, for providing the laboratory facilities, UGC, New Delhi for providing financial support of UGC BSR grant, “UGC One Time Grant” scheme.

REFERENCES

[1] Kuciauskas D, Freund M. S, Gray H. B, Winkler J. R, and Lewis N. S, (2001) : Electron Transfer Dynamics in Nanocrystalline Titanium Dioxide Solar Cells Sensitized with Ruthenium or Osmium Polypyridyl Complexes, *J. Phys. Chem. B*, **105 (2),** 392–403.

[2] Dasa A, Basulia F, Peng S. M, and Bhattacharya S, (1999): Chemistry of osmium in $N_2P_2Br_2$ coordination sphere: Synthesis, structure and reactivities, *Polyhedron,* **18**, 2729–2736.

[3]Milas N. A, Trepagnier J. H, Nolan Jr. J. T, and Iliopulos MI, (1959): A Study of the Hydroxylation of Olefins and the Reaction of Osmium Tetroxide with 1,2-Glycols, *J. Am. Chem. Soc*., **81 (17)** , 4730–4733.

[4] Hanif M, Babak M. V and Hartinger C. G, (2014): Development of anticancer agents: wizardry with osmium, *Drug Discovery Today*, **19**, 10.

[5] Rickard C. E. F, Roper W. R, Woodgate S. D, Wright L. J, (2002): Tris(N-pyrrolyl)phosphine complexes of osmium(II) and osmium(0), *Journal of Organometallic Chemistry*, **643-644**, 168–173.

[6] Champness N. R, Frampton C. S, Levason W, Preece S. R, (1995): Synthesis, spectroscopic and electrochemical studies of iodo complexes of osmium(II), (III) and (IV) with phosphorus and arsenic donor ligands, *Inorganica Chimica Acta*, **3,** 43-50.

[7] Boonyavonga N, Suwanrujia P, Hannongbuaa S, Lib F, Sunc L, Karpkirda T. M, (2000): Synthesis, electrochemistry and photo-induced electron transfer of unsymmetrical dinuclear ruthenium osmium 2,2′-bipyridine complexes, *Journal of Photochemistry and Photobiology A: Chemistry,* 2014, 287, 40–48.

[8]Ley P. A, Sargeson A. M, (1992): Tris (l, 2 ethanediamine) complexes of osmium(IV), osmium(III) and osmium(II): oxidative dehydrogenation reactions, *Inorganica Chimica Acta.*, 198-200 449-460.

[9] Maruyama K, Mishima Y, Minagawa K, Motonaka J, (2001): Electrochemical and DNA-binding properties of dipyridophenazine complexes of osmium(II). *Journal of Electroanalytical Chemistry,* **510,** 96–102.

[10] Mehta J. V, Gajera S. B, Thakor P, Thakkar V. R and Patel M. N, (2015) :Synthesis of 1,3,5-trisubstituted pyrazoline derivatives and their applications, , *RSC Adv.,* **5,** 85350.

[11] Gajera S. B, Mehta J. V and Patel M. N, (2016): Metal-based biologically active compounds: design, synthesis, medicinal, toxicity and DNA interaction assay, *Med Chem Res.,* **25,** 526-537.

[12] Chu W , Wang Y , Liu S ,Yang X ,Wanga S, Li S ,Zhou G, Qin X , Zhou C and Zhang J, (2013): Synthesis, cytotoxicity and DNA-binding properties of Pd(II), Cu(II) and Zn(II) complexes with 4′-(4-(2-(piperidin-1-yl)ethoxy)phenyl)-2,2′:6′,2″-terpyridine. *Bioorganic & Medicinal Chemistry Letters,* **23,** 5487-5491.

[13] Mishima Y, Motonaka J, Maruyama K, Minagawa K and Ikeda S, Detection of DNA segment utilizing an immobilized DNA electrode and an osmium complex, *Sensors and Actuators B.,* **65,** 340–342.

[14] Mehta J. V, Gajera S. B and Patel M. N, (2016): Biological applications of pyrazoline-based half-sandwich ruthenium (III) coordination compounds. Journal of Bimolecular Structure and Dynamics. 35, 1599-1607.

[15] Banuppriya G, Sribalan R and Padmini V, (2018): Synthesis and characterization of curcumin-sulfonamide hybrids: Biological evaluation and molecular docking studies, *Journal of Molecular Structure,* **1155,** 90-100.

[16] Mandegani Z, Asadi Z, Asadi M, Karbalaei-Heidari HR, and Rastegari B, (2016): Synthesis, characterization, DNA

binding, cleavage activity, cytotoxicity and molecular docking of new nano water-soluble [M(5-CH2PPh3-3,4-salpyr)](ClO4)2 (M = Ni, Zn) complexes. *Dalton Trans,* **45,** 6592.

[17] Thakor K. P, Lunagariya M. V, Waghela BN, Vaidya FU, Pathak C and Patel MN, Design, (2018): synthesis, MTT assay, DNA interaction studies of platinum(II) complexes, *Journal of Bimolecular Structure and dynamics,*, 36, 14-31.

[18] Scalese G , Correia I , Benítez J, Rostán S , Marques F , Mendes F, Matos AP , Pessoa JC, Gambino D, (2017): Evaluation of cellular uptake, cytotoxicity and cellular ultrastructural effects of heteroleptic oxidovanadium(IV) complexes of salicylaldimines and polypyridyl ligands, *Journal of Inorganic Chemistry,* ,**66,** 162-172.

[19] Gajera S. B, Mehta J. V, Thakor P, Thakkar V. R, Chudasama P. C, Patel J. S and Patel M. N, (2016): Half-sandwich iridium III complexes with pyrazole-substituted heterocyclic frameworks and their biological applications, *New J. Chem*., **40,** 9968.

[20] Constable E. C and Housecraft C. E, (1993): Osmium, *Coordination Chemistry*. **124**, 183-216.

[21] Araneo A, Valenti V and Franco C, (1970): New osmium nitrosyl compounds, *J. Inorg. Nucl. Chem.,* **32,** 1877-1883

[22] Lewsi J and Wilkinson G. J, (1958): Infra-red spectra of osmium-nitrogen compounds, *Inorg. Nucl.Chem.*, **6,** 12-13.

PRAJÑĀ - Journal of Pure and Applied Sciences Vol. 26 : 78 – 85 (2018)
ISSN 0975 - 2595

SYNTHESIS, CHARACTERIZATION AND BIOLOGICAL EVALUATION OF *IN VITRO* ANTIBACTERIAL, SOD-MIMIC AND CYTOTOXIC ACTIVITIES OF GATIFLOXACIN BASED SQUARE PYRAMIDAL COPPER(II) COMPLEXES

DIVYANG H. GANDHI AND BHUPESH S. BHATT
[1]C. U. Shah University, Wadhwancity-363035, Gujarat (INDIA)
[2]Department of Chemistry, Sardar Patel University,
Vallabh Vidyanagar–388 120, Gujarat (INDIA)
Corresponding address: bhupeshbhatt31@gmail.com

Abstract

There is a worldwide agreement over the present need to develop novel agents to treat bacterial infections that have become increasingly unresponsive to standard antibacterial therapy. Emergence of bacteria resistance to a number of antimicrobial agents is becoming a major health problem. A series of isatin derivatives and their square pyramidal copper(II) complexes with fourth generation fluoroquinolone drug gatifloxacin were synthesized. The drug based copper(II) complexes were characterized by various spectroscopic (FT-IR, Mass, UV-visible spectroscopy) and analytical methods (magnetic measurement, conductivity measurement). The metal complexes were checked for various biological activities. In vitro antibacterial activity of complexes were checked against three Gram$^{(-ve)}$ and two Gram$^{(+ve)}$ microorganisms in terms of minimum inhibitory concentration and the data were in good agreement with the standard drug data. The effect of complexation reflects on antibacterial activity. Synthesized metal complexes were also screened for SOD mimic activity in terms of IC_{50} value. Superoxide dismutase (SOD) is a class of enzymes that catalyze the dismutation of superoxide into oxygen and hydrogen peroxide. The geometry at the central metal ion provides a site for binding of superoxide anion responsible for the high SOD mimic activity. The brine shrimp bioassay was also carried out to study the in vitro cytotoxic properties of the synthesized metal complexes.

Introduction

The transition metal complexes as active biological agents represents one of the most successful applications of bioinorganic and medicinal chemistry [1], in which transition metal serve as the agents of responsible synergic effect, when coordinated with organic molecules. Some important examples of transition metal complexes, particularly used in medicinal applications are platinum containing anticancer [2], gold containing antiarthritic [3] and bismuth containing antiulcer drugs [4]. Such advances make obvious choice for medicinal chemistry researchers to explore the therapeutic applications of other metals. So the recent research studies focus on evaluating biological activities of metal complexes, to explore their mechanism of action, their interaction with different biomolecules, biotransformation study and to study their toxic effects. The medicinal inorganic chemistry may be divided into three major categories, (i) organic molecules as drug which target metal ion in biological system, (ii) metal based drugs and (iii) radio nuclides used as imaging agents.

Copper ion is an essential micronutrient for human health [5]. It is incorporated into a variety of biochemical functions (RBC formation, iron absorption and utilization, glucose and cholesterol metabolism), and the central metal of various proteins and metalloenzymes associated with metabolic functions. It is also required for the proper growth, development, and maintenance of body organs (connective tissue, bone, heart, brain etc.) [6]. It also function to release and synthesize some life-sustaining enzymes and proteins, which in turn produce cellular energy and regulate oxygen transport, nerve

transmission and blood clotting [6]. Copper has healing properties, it helps to fight infections by boosting the human immune system, and helps to scavenge and neutralize reactive oxygen species produced during cellular processes, which can damage the cells. The deficiency of copper can lead to serious medical complications. Due to broad biological applications, the researchers took attention towards exploring biological applications of copper complexes. The literatures of past few years have plenty of information about medicinal applications of copper complexes, which includes antimicrobial, anti-inflammatory, antiviral, antitumor, chemical nuclease, enzyme inhibitors etc. [7].

After the successful applications of nalidixic acid in the curing of urinary tract infections [8], many generations of fluoroquinolone family drugs were researched and some of them are currently used as potential antibacterial drugs. The fluoroquinolone family drugs are used to cure infections such as lower respiratory tract infections, urinary tract infections, skin and soft tissue infections, cervical and urethral gonococcal infections, typhoid, acute sinusitis, prostatitis, bone-joint and pneumoccocal infections [9]. The ability of fluoroquinolone family drugs to block bacterial enzymes Topoisomerase II and Topoisomerase IV activity is the mechanism of antibacterial action [10]. So we synthesized fourth generation fluoroquinolone drug gatifloxacin based neutral copper(II) complexes with isatin derivatives. The Cu(II) mixed ligand complexes were characterized by conductivity measurement, magnetic moment measurement, LC-MS, IR and electronic spectroscopy. The complexes were checked for diverse biological application like antibacterial, SOD-mimic and cytotoxic activity.

Experimental

Material and methods

Analytical grade chemicals and solvents were used for all the studies. Isatin, *p*-chloroaniline, *m*-chloroaniline, *o*-chloroaniline, *p*-bromoaniline, *m*-nitroaniline, *p*-nitroaniline, *p*-hydroxybenzoic acid, *p*-methoxyaniline and *p*-toluidine were procured from Sigma Aldrich (India). PMS, NADH, NBT and Luria Broth were procured from Himedia (India).

IR spectra were obtained on a FT-IR Shimadzu instrument in the range 4000–400 cm^{-1} and sample was prepared as KBr pellets. The electronic spectra were obtained on a UV-160A, Shimadzu (Japan) UV-visible spectrophotometer. The Gouy's balance was used for magnetic moment measurement.

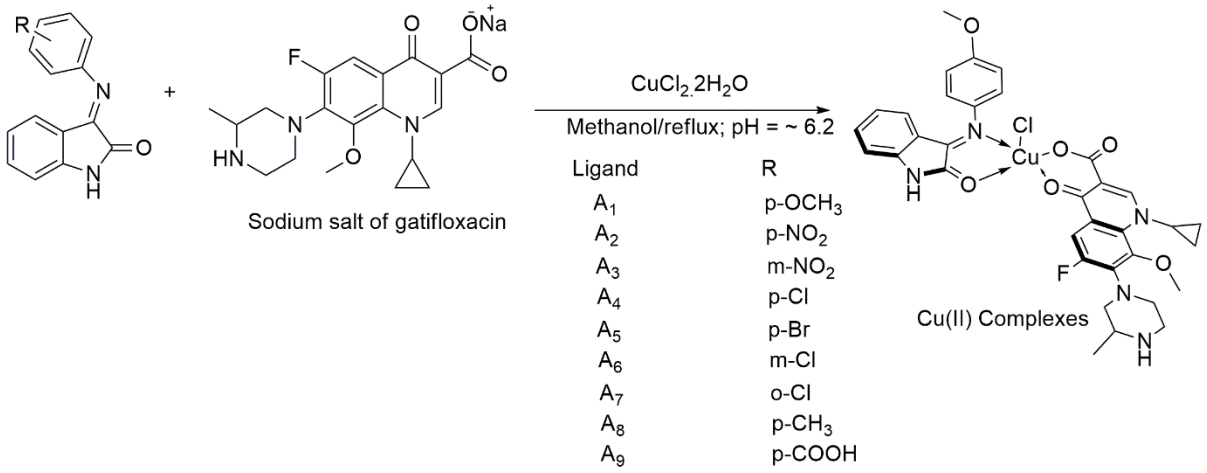

Scheme 1: Reaction scheme for synthesis of metal complexes.

Synthesis

The ligands (isatin derivatives) were synthesized according to the reported procedure [11]. The Cu(II) complexes [Cu(GFL)(A^n)Cl] were synthesized by taking the methanolic solution of $CuCl_2 \cdot 2H_2O$ (1.5 mmol) and the methanolic solution of neutral bidentate isatin derivative (A^n) (1.5 mmol) in a RBF, followed by addition of gatifloxacin (GFLH) solution (1.5 mmol, methanolic solution in presence of sodium methoxide) in methanol and the pH was adjusted to 6.2. The reaction mixture was refluxed for 1 h on a steam bath. After completion of reaction as monitored by TLC, the reaction mass was concentrated, filtered, washed by dichloromethane and dried to obtain amorphous product of green color (Scheme 1).

***In vitro* antibacterial assay**

The *in vitro* bacteriostatic activity of the metal salt, gatifloxacin (standard) and complexes against two $Gram^{(-ve)}$ *Escherichia coli, Serratia marcescens,* and two $Gram^{(+ve)}$ *Bacillus subtilis, Staphylococcus aureus*, microorganisms were evaluated in terms of minimum inhibitory concentration (MIC) using double dilution technique as reported procedure [12]. The bacterial culture were incubated in Luria Broth as media at 37° C, and bacterial growth was monitored by measuring the turbidity in solution after 18 h, in presence and absence of metal salt, standard and samples. The lowest concentration of compounds at which bacterial growth inhibited, was considered as the MIC value.

SOD-like activity

The assay is based on a fact that nitroblue tetrazolium (NBT) can be photoreduced to produce $O_2^{\bullet -}$, and the ability of complexes to scavenge $O_2^{\bullet -}$ at their vacant site can be the indicator of their SOD-mimic activity. The complex (0.25 to 5.0 µM), NADH (79 µM), NBT (75 µM), and PMS (30 µM) solution in phosphate buffer (pH 7.8) were used in this assay. The generated superoxide anion by this system were spectrophotometrically detected at 560 nm by monoformazan formation. The reduction rate of NBT was estimated in the presence and absence of the complexes after 5 min. The concentration of complexes responsible for 50% inhibition of NBT reduction was considered as IC_{50} value of complexes [12].

Brine shrimp lethality assay

Artemia Cysts eggs were hatched in artificial seawater for two days. A sample stock solution was preared by dissolving 10 mg complex in 10 mL DMSO. From this, solution were transferred to 18 different vials to make 2, 4, 8, 12, 16 and 20 µg mL^{-1} final concentrations of complexes, three vials were kept with DMSO as control only. The 10 nauplii in 1 mL of seawater were added and the volume was adjusted to 2.5 mL per vial with seawater. After 24 h, the survivor numbers were counted. The log of sample concentrations were plotted against %mortality of nauplii and LC_{50} value was determined [13].

Result and discussion

Characterization

The complexes were characterized by various spectroscopic (LC-MS, IR, electronic spectra) and analytical (magnetic and conductivity measurement) methods. The physical parameters are given in Table 1.

Table 1. Physical characterization data of complexes.

Complexes	Empirical formula	Formula weight	%Cu		m.p. /^{0}C	μ_{eff} /B.M.
			Theoritical	Experimental		
[Cu(GFL)(A^1)Cl] (1)	$C_{34}H_{33}ClCuFN_5O_6$	725.65	8.76	8.55	>250	1.82
[Cu(GFL)(A^2)Cl] (2)	$C_{33}H_{30}ClCuFN_6O_7$	740.62	8.58	8.21	243	1.84
[Cu(GFL)(A^3)Cl] (3)	$C_{33}H_{30}ClCuFN_6O_7$	740.62	8.58	8.25	239	1.89
[Cu(GFL)(A^4)Cl] (4)	$C_{33}H_{30}Cl_2CuFN_5O_5$	730.07	8.70	8.44	235	1.85
[Cu(GFL)(A^5)Cl] (5)	$C_{33}H_{30}BrClCuFN_5O_5$	774.52	8.20	7.98	240	1.88
[Cu(GFL)(A^6)Cl] (6)	$C_{33}H_{30}Cl_2CuFN_5O_5$	730.07	8.70	8.53	230	1.91
[Cu(GFL)(A^7)Cl] (7)	$C_{33}H_{30}Cl_2CuFN_5O_5$	730.07	8.70	8.48	232	1.84
[Cu(GFL)(A^8)Cl] (8)	$C_{34}H_{33}ClCuFN_5O_5$	709.65	8.95	8.70	>250	1.86
[Cu(GFL)(A^9)Cl] (9)	$C_{34}H_{31}ClCuFN_5O_7$	739.64	8.59	8.39	>250	1.91

The copper content was estimated using reported spectrophotometric titration method [14]. The data obtained were in a good agreement with the theoretical percentage of copper. In the IR spectra, the ν(C=O) pyridine band of gatifloxacin shifts from 1718 cm^{-1} to 1616-1634 cm^{-1} in the complexes, which clearly indicate the participation of pyridine carbonyl oxygen atom in the coordination with metal (Table 2). The difference Δν for the complexes lies in the range 186-209 cm^{-1}, which suggests unidentate behavior of coordination with carboxylic oxygen atom. Also additional bands in the IR spectra of complexes in the range 542-554 cm^{-1} and 508-522 cm^{-1} can be assigned to ν(M-N) and ν(M-O) stretching frequency, respectively. The

mass spectra of complex-1 shows molecular ion peak at expected m/z value (Figure 1). The μ_{eff} values of complexes are in the range 1.82-1.91 BM (Table 1), which shows presence of one unpaired electron with the copper metal ion in complexes.

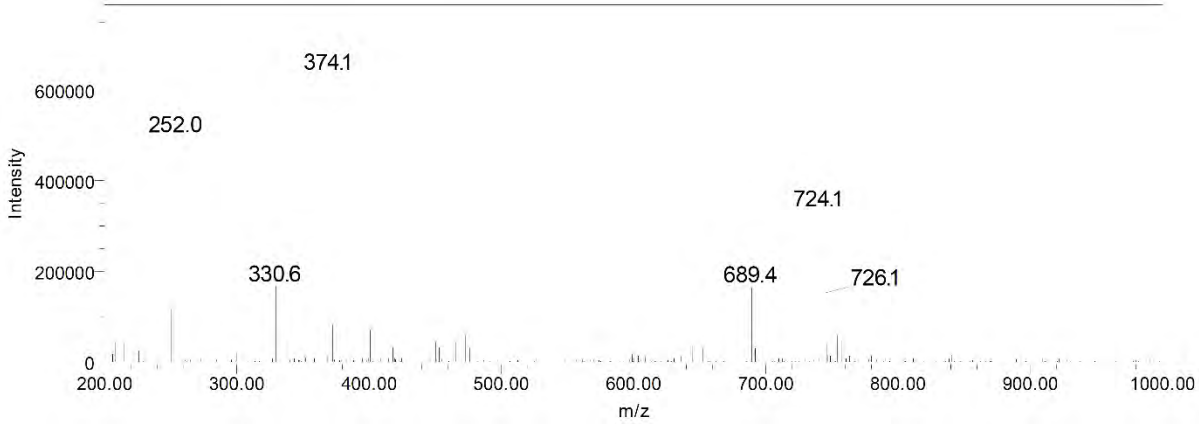

Figure 1: Mass spectra of complex -1.

Table 2. IR spectra data

Complexes	ν(C=O) pyridone /cm^{-1}	ν(COO)$_{as}$ /cm^{-1}	ν(COO)$_{s}$ /cm^{-1}	Δν /cm^{-1}	ν(M-N) /cm^{-1}	ν(M-O) /cm^{-1}
Gatifloxacin	1718	1611	1332	279		-
1	1625	1565	1362	203	545	520
2	1632	1577	1377	200	554	521
3	1634	1556	1362	194	540	519
4	1618	1564	1378	186	542	522
5	1626	1570	1360	210	544	510
6	1619	1566	1358	208	549	517
7	1620	1570	1371	199	546	520
8	1617	1575	1366	209	548	508
9	1616	1575	1373	202	550	511

***In vitro* antibacterial activity**

The emerging problem of drug resistance acquired by bacteria is a global threat to human and challenge for medicinal chemistry researchers. Many of the drugs have become obsolete due to decrease in their effectiveness to treat some common diseases. So novel strategies are required to combat with this issue. Chelation of drug could be a better choice to adopt since chelation of drug can alter the mechanism of drug action, also increase the lipophilicity of drugs, and so the permeability. So we checked the bacteriostatic activity of gatifloxacin based Cu(II) complexes by double dilution

method, against two gram(+ve) and two gram(-ve) pathogens. The results concerning *in vitro* antibacterial activity shows that all the metal complexes are far more potent than metal salt, also complexes are more potent than gatifloxacin (standard) against all tested pathogens (Table 3). Among all, the complexes containing electron withdrawing group especially shows exceptional potency against all the microorganism. The Tweedy's chelation theory can explain such a higher potency of metal complexes. Upon chelation, π-electrons delocalizes over the whole chelate ring, also metal ion share its partial positive charge with the ligand orbital, and this overlapping reduces the polarity of the complexes, and so there is increase in lipophilicity of metal complexes [15]. The increase in lipophilicity enhances the metal complex penetration into lipid membranes and block the metal binding site of enzyme. Another mechanism could be restricting the protein synthesis by disturbing respiration process of organism cell which lead to its growth inhibition.

Table 3 Biological activities data of metal complexes

Compounds	Antibacterial activity (MIC, μM)				SOD-*mimic* activity (IC_{50}, μM)	Cytotoxic activity (LC_{50}, μM)
	Gram positive		Gram negative			
	S. aureus	*B. subtilis*	*S. marcescens*	*E. coli*		
$CuCl_2 \cdot 2H_2O$	2698.0	2815.0	2756.0	3402.0	-	-
Gatifloxacin	5.1	4.0	2.9	2.9	-	-
1	1.8	1.8	2.5	1.3	1.9	11.2
2	0.7	0.8	0.8	1.1	0.9	5.3
3	0.9	1.3	1.4	1.5	1.2	6.3
4	1.2	1.6	1.9	1.8	1.2	6.7
5	1.8	2.0	2.1	1.9	1.4	6.5
6	1.9	1.5	1.7	1.5	1.8	8.9
7	1.6	1.8	1.4	1.5	1.7	7.3
8	2.2	1.9	0.9	1.7	1.7	9.8
9	0.9	1.3	0.9	1.4	1.2	5.7

SOD-*mimic* activity

Reactive oxygen species (ROS) generated in various biochemical reactions in aerobic and anaerobic organism are responsible for oxidative stress in aging process and in some diseases like inflammation, neurological disorders [16]. Superoxide dismutase is an enzyme that scavenge ROS produced during biological processes and act as antioxidant defence system. The ROS detoxification mechanism includes dismutation of superoxide radical anion $O_2^{\bullet -}$ into molecular oxygen and hydrogen peroxide, in which metalloenzyme SOD plays the role of catalyst. All the organism have this defence system having any of the type of SODs, which differs by the metal centre (Ni, Mn, Fe or Cu-Zn) present in the active site. In our experiment, we studied ability of Cu(II) complexes to mimic the SOD enzyme and ability to scavenge superoxide radical anion $O_2^{\bullet -}$ generated by NBT reduction [17]. The data of SOD mimic activity of complexes are shown in

Table 3 in terms of IC_{50} values, which suggest that all the square pyramidal complexes can effectively scavenge $O_2^{\bullet-}$ at their vacant coordinating site. The % inhibition of formazan formation at various complex concentrations with time was monitored at 560 nm and straight line curve (Y = mX + C) was plotted. Among all, complex-3 has least IC_{50} value, which can be attributed to the fact that presence of electron withdrawing nitro group can delocalize the extra charge produced on chelate ring due to presence of $O_2^{\bullet-}$.

Cytotoxic activity

Brine shrimp lethality bioassay is a simple cytotoxicity test and widely used for checking toxicity of natural plant extracts, heavy metals, medicines and pesticides on a simple zoological organism- *Artemia cysts*. It's a preliminary toxicity screen test for further experiments on animal models [18]. The cytotoxicity data (LC_{50} values) are shown in Table 3. The observed LC_{50} values show that all complexes are potent cytotoxic agents.

Conclusion

In the article, gatifloxacin based Cu(II) complexes of isatin derivatives were synthesized and characterized by various analytical and spectroscopic techniques. The shift in IR frequencies of gatifloxacin suggests pyridine and carboxylic oxygen as the coordinating atoms. Also appearance of additional ν(M-N) bond suggests coordination of azomethine nitrogen atom of isatin as the coordinating atom. The magnetic moment measurement suggest presence of one unpaired electron and conductivity measurement suggests neutral nature of complexes. The UV-visible spectroscopy suggests square pyramidal geometry of complexes. The complexes were tested for various biological applications such as antibacterial, SOD-mimic and cytotoxic activities. The MIC values show that complexes are potent bacteriostatic agents even more than standard drug gatifloxacin, and chelation could be the possible reason behind such a high activity, which increases the lipophilicity of drug and so the biopermeability. The SOD-mimic activity show that complexes can be served as potent antioxidant agents by scavenging superoxide radical anion to their vacant coordination site. The LC_{50} value evaluated on brine shrimp suggest potent cytotoxic nature of complexes.

Acknowledgement

Authors are thankful to the authority of C. U. Shah university for providing necessary research facility and giving permission to carry out the research work.

References

[1] C. Orvig, M.J. Abrams, Medicinal inorganic chemistry: introduction, Chemical Reviews, 99 (1999) 2201-2204.

[2] E. Wong, C.M. Giandomenico, Current status of platinum-based antitumor drugs, Chemical reviews, 99 (1999) 2451-2466.

[3] R. Rudkowski, G.G. Graham, G.D. Champion, J.B. Ziegler, The activation of gold complexes by cyanide produced by polymorphonuclear leukocytes—I: The effects of aurocyanide on the oxidative burst of polymorphonuclear leukocytes, Biochemical pharmacology, 39 (1990) 1687-1695.

[4] G.G. Briand, N. Burford, Bismuth compounds and preparations with biological or medicinal relevance,

Chemical reviews, 99 (1999) 2601-2658.

[5] A.N. Besold, E.M. Culbertson, V.C. Culotta, The Yin and Yang of copper during infection, JBIC Journal of Biological Inorganic Chemistry, 21 (2016) 137-144.

[6] M.C. Linder, Biochemistry of copper, Springer Science & Business Media, 2013.

[7] I. Iakovidis, I. Delimaris, S.M. Piperakis, Copper and its complexes in medicine: a biochemical approach, Molecular biology international, 2011 (2011).

[8] M. Zupančič, I. Arčon, P. Bukovec, A. Kodre, A physico-chemical study of the interaction of cobalt (II) ion with ciprofloxacin, Croatica Chemica Acta, 75 (2002) 1-12.

[9] H. Neu, Ciprofloxacin: an overview and prospective appraisal, The American journal of medicine, 82 (1987) 395-404.

[10] C.M. Perry, J.A.B. Balfour, H.M. Lamb, Gatifloxacin, Drugs, 58 (1999) 683-696.

[11] M. Verma, S.N. Pandeya, K.N. Singh, J.P. Stables, Anticonvulsant activity of Schiff bases of isatin derivatives, Acta Pharmaceutica, 54 (2004) 49-56.

[12] M.N. Patel, B.S. Bhatt, P.A. Dosi, Spectroscopic study of DNA hydrolysis, DNA intercalative, and electrostatic interaction activity exerted by drug based coordination compounds, Zeitschrift für anorganische und allgemeine Chemie, 638 (2012) 152-162.

[13] M.R. Islam, S.R. Islam, A.S.M. Noman, J.A. Khanam, S.M.M. Ali, S. Alam, M.W. Lee, Biological screening of a novel nickel (II) tyrosine complex, Mycobiology, 35 (2007) 25-29.

[14] M.N. Patel, P.A. Parmar, D.S. Gandhi, Square pyramidal copper (II) complexes with forth generation fluoroquinolone and neutral bidentate ligand: structure, antibacterial, SOD mimic and DNA-interaction studies, Bioorganic & medicinal chemistry, 18 (2010) 1227-1235.

[15] U.K. Mazumder, M. Gupta, S.S. Karki, S. Bhattacharya, S. Rathinasamy, S. Thangavel, Synthesis, anticancer and antibacterial activity of some novel mononuclear Ru (II) complexes, Chemical and pharmaceutical bulletin, 52 (2004) 178-185.

[16] V. Nivière, M. Fontecave, Discovery of superoxide reductase: an historical perspective, JBIC Journal of Biological Inorganic Chemistry, 9 (2004) 119-123.

[17] R. Buchtík, Z. Trávníček, J. Vančo, In vitro cytotoxicity, DNA cleavage and SOD-mimic activity of copper (II) mixed-ligand quinolinonato complexes, Journal of inorganic biochemistry, 116 (2012) 163-171.

[18] C. Wu, An important player in brine shrimp lethality bioassay: The solvent, Journal of advanced pharmaceutical technology & research, 5 (2014) 57.

PRAJÑĀ - Journal of Pure and Applied Sciences Vol. 26 : 86 – 95 (2018)
ISSN 0975 - 2595

CLEANING STRATEGIES FOR FLUX RECOVERY OF NANOFILTRATION MEMBRANE FOR ETHYLENE GLYCOL-SALT--WATER TERNARY MIXTURE

TEJAL M PATEL*, HARESH K DAVE AND KAUSHIK NATH
Department of Chemical Engineering, G H Patel College of Engineering & Technology
Vallabh Vidyanagar-388120, Gujarat, India
Email: tejalpatel@gcet.ac.in

Abstract

The success of a membrane filtration process largely depends on employing an effective and efficient membrane cleaning method. Different cleaning strategies are explored in the present work to recover the permeate flux of a flat sheet nanofiltration membrane employed in the separation of ethythelne glycol from industrial wastewater. Chemical cleaning was carried out with 2% each of citric acid, EDTA and STPP solutions. The effectiveness of these chemicals as a cleaning agent was studied and flux recovery was calculated. The flux recovery after cleaning with citric acid, EDTA and STPP solutions were found out to be 69.84, 55.77., and 47.85% respectively. The surface morphology and functionality of the pristine and used membrane samples were also characterized by SEM, FTIR and AFM analysis.

Keywords: membrane fouling, flux decline, concentration polarization, chemical cleaning

1. Introduction

Endowed with a number of advantages to its credit, membrane technology has become one of the most important industrial separation techniques to be applied extensively to various fields including the recovery of valuable products from wastewater. Among various pressure driven membrane processes nanofiltration in particular, has led to significant innovation in the recent past for the treatment of large amount of aqueous stream, which contain many different components with low molecular weight ranging from hundreds to thousands of Daltons such as inorganic/organic salts, amino acids and peptides, oligosaccharides, molasses, reactive dyes and so on [1,2,3]. Although the membranes can be operated at their optimal operating conditions, the fouling at a membrane surface seems to be an unavoidable phenomenon. Thus the success of a membrane filtration process largely depends on employing an effective and efficient membrane cleaning method. Membrane cleaning is of critical importance for the efficient recovery of the membrane's flux (throughput) and selectivity – the two most important performance indices of membrane separation [4, 5]. Cleaning also ensures the reuse of membrane for long term cost effective operation. The limited thermal and chemical robustness of membranes constrain cleaning methods to avoid frequent membrane replacement. There are quite a few numbers of physical and chemical cleaning methods depending upon the nature of the feed or foulants [6].

Physical cleaning of porous membranes includes hydraulic cleaning which consists of flushing (forward) and backwashing or backpulsing. This is one of the easiest cleaning methods, and nowadays is widely used in membrane bio reactors (MBR) and other cross flow operations [7, 8]. Regular intermittent backwash leads to the lift-off of deposited particles from the membrane surface and minimizes the extent of concentration polarization. Forward flushing can be undertaken during the filtration cycle with a backwash to improve shear and remove particle concentration build-ups. Backpulsing (also called backshocking) is a more rapid backwash with a forward filtration step and followed by a reversed filtration step. The pneumatic cleaning of the membrane consists of air sparging, air lifting, air scouring, and air bubbling [9, 10]. Air or inert gas is applied for direct cleaning or to enhance flux in the filtration step. This process has the advantage of low maintenance cost, ease of integration with the existing system, and elimination of cleaning chemicals. However, the disadvantages of air sparging include limited effectiveness in cleaning and the high pumping cost [11, 12]. The combined cleaning of air sparging and hydraulic backflush is also applied in many processes. Low frequency ultrasound irradiation (up to 40 kHz) is an effective cleaning strategy for fouled membranes. Ultrasonic waves create cavitation

and induce acoustic streaming, which provide vigorous mixing to breaking concentration polarization and cake layer on the membrane surface [13, 14].

When selecting cleaning conditions, one of the most important considerations is if the conditions for cleaning are compatible with membrane media and other components of the membrane filters and systems. Chemical compatibility of membrane and other filter components and systems limits the type and the maximum allowable concentration of a chemical to be used during cleaning [7]. Membranes made from materials with high chemical resistance allow more flexible selections of the type and the concentrations of cleaning chemicals in dealing with various types of fouling problems. Concentration of cleaning chemicals can affect both the equilibrium and the rate of reaction. Unlike reactions occurred in liquid phase, reactions between cleaning chemicals and fouling materials occur in the interface of liquid and a (solid) fouling layer. The concentration profile of cleaning chemicals within the fouling layer is a function of the concentration of cleaning chemicals in the bulk liquid phase. Therefore, the concentration of cleaning chemicals not only needs to maintain the reasonable reaction rate, but also needs to overcome mass transfer barrier imposed by the fouling layer [15]. In general, 5-20% of the operating costs of a large plant are associated to membrane cleaning procedures (Madaeni et al., 2001) [16]. Therefore, an intense research work is being done to develop new cleaning methods

A current practice of membrane cleaning is based on recommendations from membrane manufacturers which may consume more cleaning chemicals since the recommendations are given based on feed water quality, and are not based on severity of fouling. In addition, these chemicals are also quite costly [7, 17]. Membrane cleaning processes are not well automated and there is an opportunity to develop an advanced tool for estimating effectiveness of the membrane cleaning and optimizing of the cleaning operation. Therefore, a simple alternative method to identify the effectiveness of the membrane cleaning would be helpful. By estimating the effectiveness of the membrane cleaning, the cleaning chemical consumption and the plant down time can be minimized. Keeping this in mind different cleaning strategies were explored in the present work for a flat sheet nanofiltration membrane after using in the separation of ethylene glycol from wastewater. Chemical cleaning was carried out using citric acid, EDTA and sodoium tripolyphosphate. Physical cleaning methods involved were back and forward flushing with water and low frequency ultrasonic irradiation. Flux recovery was evaluated after each cleaning cycle to assess the reusability of the membrane. The pristine and fouled membranes were also analyzed using scanning electron microscopy, Fourier-transform infrared spectroscopy, and atomic force microscopy.

2. Materials and methods

2.1 Chemicals and reagents

Citric acid (pH: 2.5), ethylene diamine tetra-acetic acid (EDTA) (pH: 8), and sodium tripolyphosphate (STPP) (pH: 9.8) were the cleaning reagents for the present study. Ethylene glycol (EG) containing wastewater was procured from M/s PCP Chemicals Pvt Limited, Mumbai, India. The important composition of wastewater is presented in Table 1. All the chemicals used in this study were of AR grade, supplied by Merck, India and were used as received without further purification. Deionized water (resistivity18 $M\Omega \cdot cm^{-1}$ at 25°C) was used for preparing stock solution.

2.2 Membrane

Hydrophilized polyamide (PA-NF) membrane having molecular weight cut-off of 150 was used in the present study. The membrane was supplied by M/s Permionics Membrane Pvt. Ltd, Baroda, India. PA-NF membrane has three layers, which are fabric backed polysulfone UF support, interfacially coated with polyamide layer and then hydrophilized using Permionics proprietary additives. The average pore sizes and effective area of the membrane were 6±1 nm and 0.016 m^2 respectively. The key physico-chemical and performance properties of the PA-NF

membrane are listed in Table 2. The water permeability of the membrane was estimated to be 2.99×10^{-11} m^3/m^2sPa.

2.3 Experimental set-up and operating conditions

The details of experimental setup and the schematic diagram are available elsewhere[18].Wastewater sample, diluted 5 times using deionised water, was passed through the membrane module at 490 kPa trans-membrane pressure for 90 minutes. The volume of feed solution was 25 l in the feed tank. Permeate samples were collected at fixed time intervals and concentration of the same were measured using Karl Fisher Apparatus. TDS and Conductivity of the samples were also measured using TDS meter (Hanna Instruments, Taiwan). All the experiments were conducted at the prevailing ambient temperature of 32±2°C.

2.4 Chemical Cleaning

Membrane cleaning was performed by immersing used membrane in the cleaning solution at ambient temperature kept overnight. The cleaning solution involved 2% by vol of citric acid, EDTA and sodium tripolyphosphate. The membrane swatches from the cleaning solution were subsequently rinsed with deionised water before placing it into the module.

2.5 Physical Cleaning

Physical cleaning of the membranes were accomplished in situ using forward and backward flushing with water for 1 h at ambient temperature. In forward flushing, water was passed in the same direction of feed flow while in back flushing, the flow direction was reversed. Cleaning of fouled membranes was also carried out ex situ by employing low frequency (25 kHz) ultrasonic irradiation for different intervals. After each cycle of cleaning, flux recovery (F_r) of the cleaned membrane was estimated using Eq.(1)

$$F_r = \frac{J_{w1}}{J_w} \times 100 \qquad (1)$$

Where, F_r = flux recovery, J_{w1} = Pure water flux after cleaning, J_w = Pure water flux of unused membrane

2.6 Determination of permeate flux and membrane rejection coefficient

Permeate flux (J_w) of the membrane was determined using following relation

$$J_w = \frac{Q_p}{A} \qquad (2)$$

where Q_p is the permeate flow per h and 'A' is the active surface area of the membrane (m^2). Membrane rejection coefficient (R) was estimated by

$$R = (1 - \frac{C_p}{C_b}) \times 100 \qquad (3)$$

Where C_p is the concentration of the permeate and C_b is the bulk concentration.

2.7 Scanning electron microscopy

The scanning electron microscopy (SEM) analysis of the pristine (unused) and fouled membranes was done on Leo 1430VP (England). All membrane samples were dried overnight at 40 °C before preparing 3 mm × 3 mm strips for silver sputter coating. The silver-coated strips were used for recording the SEM images.

*2.8 Fourier transform infrared spectros*copy (FTIR)

The surface organic functional groups of the membranes were studied by the Fourier transform infrared spectroscopy (Perkin Elmer Spectrum GX). The spectra were recorded from a wave number of 400 – 4000 cm^{-1} at a resolution of 4.0 cm^{-1} with an acquisition time of 1 min. Infrared absorption spectra are usually obtained by placing the sample in one beam of a double-beam infrared spectrophotometer and measuring the relative intensity of transmitted (and therefore absorbed) light energy versus wavelength (or wave number). A common light source for infrared radiation is the Nernst glower, a molded rod containing a mixture of zirconium oxide, yttrium oxide and erbium oxide that was

heated to around 1500ºC by electrical means. Wet samples were prepared by thoroughly cleaning virgin membrane coupons with deionized water and soaking them in a water bath for 24 h. Samples were then dried in a vacuum drier before analysis. The membrane active layers were pressed tightly against the crystal plate, and carbon dioxide and water vapor were removed during the measurements. At least 2 replicates were obtained for every sample type without applying any baseline corrections.

2.9 Atomic force microscopy

Atomic force microscopy (AFM) was carried out using a NT-MDT NTEGRA Aura Autoprobe CP atomic force microscope. Measurements were performed on dry membrane samples under ambient atmospheric conditions. Silicon cantilevers with integrated pyramidal tips were used to image membrane surface topography. The membrane surfaces were imaged in a non-contact or tapping (intermittent contact) mode. Differences in the membrane surface morphology were expressed in terms of various roughness parameters such as average roughness and root means square (RMS) roughness calculated from the AFM images using an AFM software program. The surface roughness was reported in terms of the root mean square roughness (RMS) and calculated by using Eq. (4)

$$RMS = \sqrt{\frac{\sum (Z_{cu} - Z_{av})^2}{p}} \quad (4)$$

where Z_{av} is the average of the z values within the given area; Z_{cu} is the current z value; and p is the number of points within a given area. The surface roughness parameter was calculated from the AFM images using an AFM software program.

3. Results and discussion

3.1. Chemical cleaning

In chemical cleaning, the choice of the cleaning agent assumes paramount importance. The optimal selection of the cleaning agent depends mainly on membrane material and type of foulants. These agents must be able to dissolved most of the deposited materials on the surface and removed them from the surface without causing any structural damage. In general, acids are often used to remove precipitated salts or scalants, while alkaline cleaning is suitable for organic fouling removal [2, 4]. Since the feed solution in the present study consisted predominantly of ethylene glycol and sodium sulphate, we selected citric acid (CA), EDTA and sodium tripolyphosphate (STPP) to study their suitability in flux recovery. Volumetric flux of pure water and EG wastewater as a function of time is presented in Figure.1.

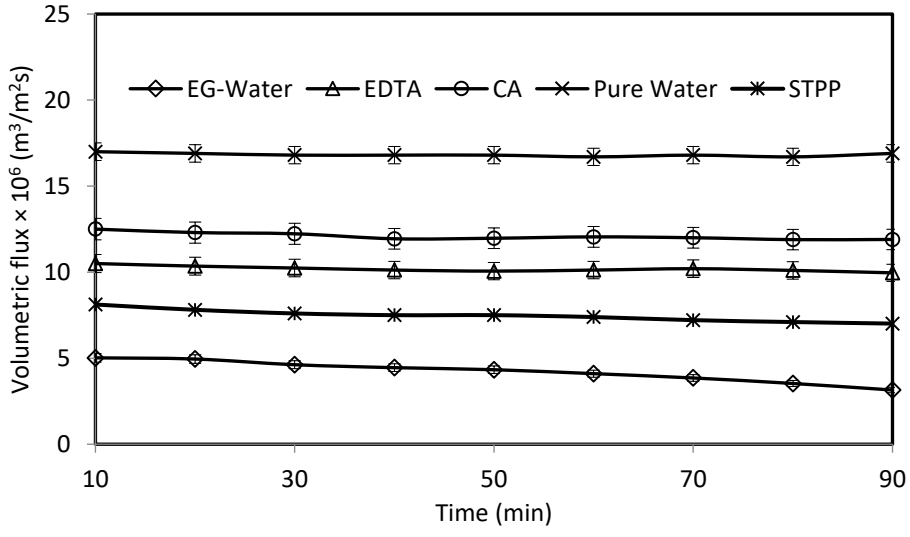

Fig. 1. Volumetric flux of permeate as a function of time for pure water, EG wastewater and pure water after chemical cleaning with different cleaning agents (trans-membarne pressure 490 kPa; Temp: 32±2ºC; Run Time: 90 min. cross flow velocity: 0.45 ms^{-1})

In the same figure the recovered water flux of cleaned membranes with cleaning agents EDTA, CA and STPP are also compared. A perusal of Figure 1 indicates that for pristine membrane the pure water flux was almost steady throughout the runtime. But with diluted wastewater the flux was observed to decline after 30 min of operation. The initial flux was found out to be 5.02×10^{-6} m^3/m^2s which was reduced to 3.15×10^{-6} m^3/m^2s after 90 min of operation. This corresponds to about 62.7% reduction of flux.

Pure water flux recovery after cleaning with citric acid was 69.84%. When the fouled membrane was cleaned with citric acid, it might have dissolved the deposited salts on the membrane surface thereby removing the adsorbed salts from the membrane, This is because of the fact that cleaning is generally a combination of two factors—the dissolution or desorption effect of the cleaning agent, and the hydrodynamic shear stress applied to the foulant layer [19]. Since the salts adsorbed on the membrane surface blocking the pores, are removed, the solvent passage through the membrane was facilitated with subsequent increase in permeate flux.

Flux recovery after cleaning with EDTA and STPP were estimated to be 55.77% and 47.85% respectively. Figure 1 indicates that the flux recovery was more with citric acid as compared to EDTA and STPP. This may be due to the better ability of dissolving or more interactions of the solutes with citric acid solution. EDTA can also form some complexes with the solutes and hence the solutes could be detached from the membrane. However, in the present experiment the EDTA solution with pH 8.0 and STTPP with pH 9.8 were found to be not much effective in dissolution of the deposited salts. The water flux was not completely recovered as the initial flux, due to adsorption and permanent fouling.

3.2. Forward and backward flushing

Physical cleaning of membrane was carried out by using forward and backward flushing of water across the membrane surface in the flat sheet module. In forward flushing water was pumped at high cross-flow velocity (0.45 ms^{-1}) through the feed side in order to remove foulants from the membrane surface. Because of the more rapid flow and the resulting turbulence, particles absorbed on to the membrane were released and discharged. In the reverse flushing method, permeate direction was reversed to flush the membrane backwards from permeate side to feed side. The deposited foulants were expelled by the inversed pressure and were then removed out of the membrane module by the reject stream. Reversible fouling caused by loosely adsorbed solute particles could be removed in this process. In forward flushing flux recovery was found out to be 80.97%, whereas in backward flushing it was 89.1%. Backward flushing was more effective for controlling flux decline than increasing shear stress on membrane; because shear stress reduced concentration polarization but back flushing could reduce both external and internal fouling [20]. In case of backward flushing from the permeate to the feed end of the membrane, it results in expansion of the thickness of the fouling layer. After this, a forward flush is usually used to wash out the detached layer or dilute the fouling layer. However to obtain the best performance optimization of the two flows (forward flow and backflow) are required. However, the frequency, duration and backwashing flux are the crucial parameters for fouling mitigation. Backwashing sometimes might affect the production efficiency of permeate stream. [5]. However, these are not studied in the present work.

3.3. Ultrasonic irradiation

Application of ultrasound for mitigation of flux decline during nanofiltration of dye solution has been extensively studied by our research group [3]. Acoustic irradiation is widely considered as an effective pretreatment to minimize fouling specially due to particulate or organic matter. For ultrasonic membrane cleaning the used membranes were subjected to low frequency (25 kHz) ultrasonic irradiation for a period of 2, 4, 6, and 8 min. With increasing in the duration of exposure to irradiation the flux recovery was increased as shown in Figure 2. Flux recovery, after 2, 4, 6

and 8 min were calculated to be 54, 80 92 and 95% respectively. Irradiation was not continued beyond 8 min as there were chances of cracks on the membrane surface.The basic physical phenomenon behind the effect of ultrasound is cavitation, that starts between this range of frequency, and is promoted by the passage of the ultrasound waves through the liquid medium in a series of alternate compression and expansion cycles. Cavitation mainly promotes formation, growth and implosive collapse of bubbles in the liquid that has significant mechanical and chemical effects. In fact, it is reported that each cavitation bubble generates temperatures of 4000-6000 K and pressures of 100-200 MPa, acting as active "hot spots" (Feng et al., 2006) [21].The acoustic streaming and shear forces imposed by cavitation bubbles reduce the fouling on membrane surface.

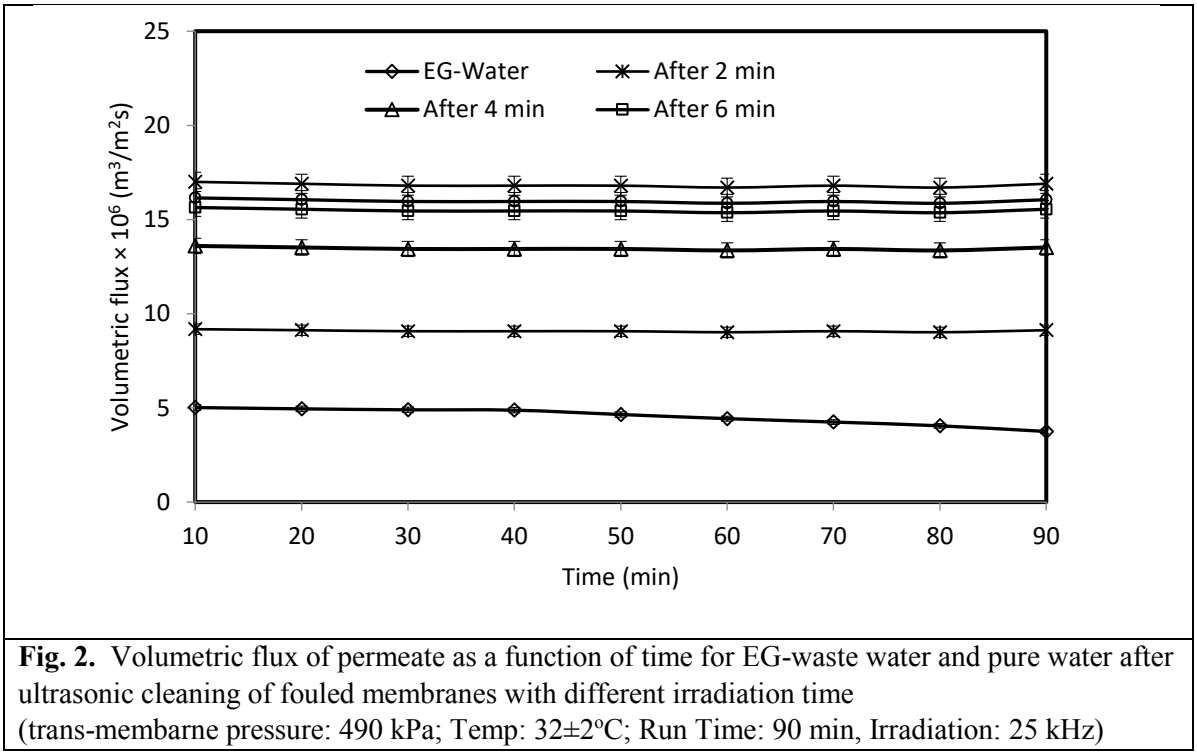

Fig. 2. Volumetric flux of permeate as a function of time for EG-waste water and pure water after ultrasonic cleaning of fouled membranes with different irradiation time
(trans-membarne pressure: 490 kPa; Temp: 32±2°C; Run Time: 90 min, Irradiation: 25 kHz)

3.4. SEM analysis

Figure 3 presents SEM micrographs of the pristine and used membrane samples from the experiments. The surface of the pristine membrane has a denser and tighter network of cellular pores and contained a network of ridges and valleys, which could conceivably trap organic molecules and inorganic salts, such as those believed to cause fouling on the membrane surface. It is obvious that the membrane had an asymmetrical structure consisting of a dense skin layer and a porous sub layer that was occupied by cellular morphologies enclosed in polymer matrix. The skin layer is responsible for the permeation or rejection of solutes, whereas the porous bulk acts only as a mechanical support. The top layer of the pristine membrane, as found from the microgram consisted of a closely packed layer of nodules.SEM images of used membranes were markedly different from those of new membranes. The micrograph of used membranes showed a cake of colloidal particles similar to fine sand or silt. This fouling layer completely occluded the active surface of the membrane. The SEM images also show that the foulant layer was having significant roughness and was textured. Generally speaking, the surface roughness of the different types of membrane is shown to differ based on the number of the peaks and valleys, peaks width and height. This morphological difference is likely caused by differences in the diffusion rate of amine monomers during the interfacial polymerization [22].

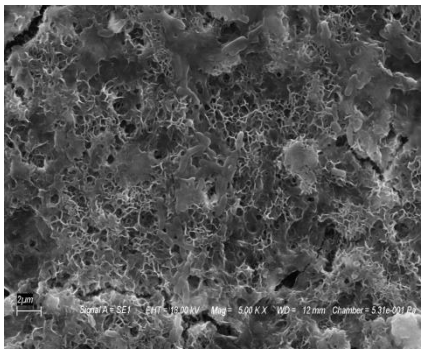

Fig. 3. SEM micrographs

3.5 FTIR Analysis

A closer insight of the surface functional groups was obtained by comparing FTIR spectra of pristine membrane with that of the used one as presented in Figure 4. The principal absorption bands for the virgin membrane consist of frequencies or wave numbers associated with these bond characteristics are N–H stretching vibration at 3438.49, 3440.87 cm^{-1}; C−H stretching in aliphatic structure ($-CH_2-CH_2-CH_3$) at 2925.62, 2926.31 cm^{-1}, N–H bending vibration due to amine at 1632.06, 1633.93 cm^{-1}, and C–C multiple bend stretching due to aromatic at 1410.29 and 1411.23 cm^{-1} [23]. From the FTIR spectra for the fouled membrane it can be seen that the absorption peaks in the used membrane spectra were either eliminated or severely attenuated due to salt deposition. Moreover there were few additional absorption peaks detected at wave numbers of 725, 794, 871, 1664, and 1725 cm^{-1} in the spectra of the fouled membrane. The spectral bands between wave numbers 950 and 1200 cm^{-1} were significantly stronger in intensity for the membrane fouled with EG- water, as compared to the virgin membrane [24]. This peak apparently originated from the di-alcohol O–H bending vibration at 1245.97 cm^{-1}. However, more information about the chemical bonding signatures could not be obtained from the spectral analysis. These differences might be due to the different composition of the proprietary layer structure of the commercial membrane used in the present study. About the more detailed relationship between the materials of the pristine membrane used and fouled membrane need further study. It merits mentioning that a few absorptions detected near 3770 cm^{-1} were probably due to water molecules as a result of inadequate drying of the test sample. These absorptions might have obscured some of the expected bands leading to erroneous assignments of a few bands.

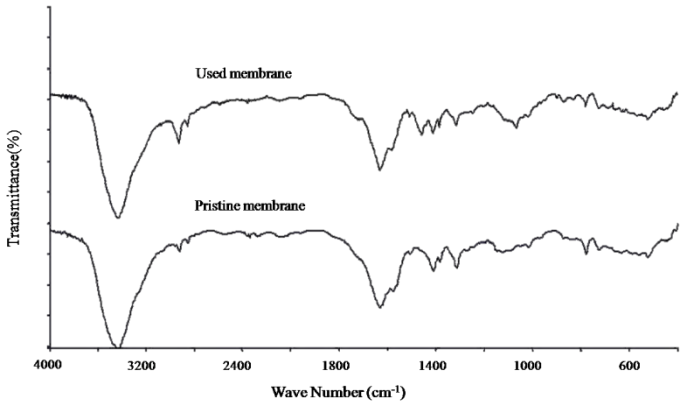

Fig. 4. FTIR Spectra of the pristine and used membrane from the present study

3.6 AFM analysis

The topology and texture of the membrane sample surfaces were investigated using atomic force microscopy (AFM) technique. AFM involves measurement of surface atomic forces to image three-dimensional topographical maps of the surface with high resolution. Representative orthographic plots of tapping mode AFM images of pristine membrane, fouled membrane, and cleaned membranes by chemical and physical cleaning are presented in Figure.5. The surface roughness parameters of the membranes obtained from AFM images using SPM DME software are given in Table 3. The roughness parameters are expressed in terms of the mean roughness (S_1), and the root mean square (RMS) roughness of the Z data (S_2). A close inspection of AFM micrographs from Figure.5 indicates that the surfaces of all the membranes have a "ridge-and-valley" morphology. Occurrence of deep depressions on the membrane surface represents pores whereas the high peaks correspond to nodules. Both these conditions lead to high roughness parameters. However, for a rough membrane, particles are preferentially transported into the valleys. The valleys quickly become clogged with multiple layers of densely packed particles increasing the cumulative resistance to flow in the valleys and leading to a more rapid loss of flux than for a smooth membrane [25]. A perusal of Table 3 indicates that both mean and rms roughness of the fouled membrane were much higher than the pristine membranes. Even though after cleaning the values of roughness decreased, those were still higher than the original roughness values of the unused membranes. The increase in surface roughness was due to the accumulation of solute particles in the concavities of membrane surfaces. Solutes accumulated in such a densely compacted layer that even defouling by chemical or physical cleaning could fail to recover the original roughness values. The pores in the virgin membrane were completely masked by residual foulants and it was evidenced from the consistent flux deterioration during the course of experiments. Moreover there were not much morphological differences between the surface topography of the chemically cleaned membrane with that cleaned by physical method.

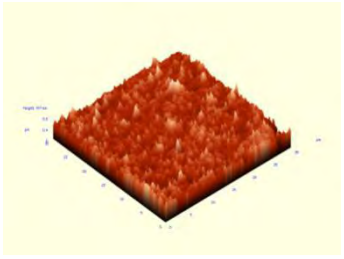

(a) Pristine membrane

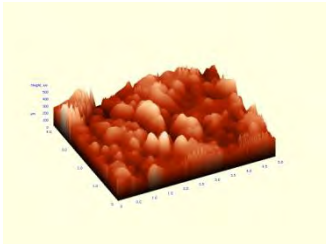

(b) Fouled membrane

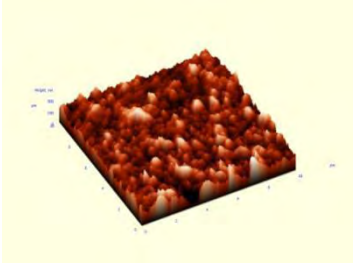

(c) Chemically cleaned membrane

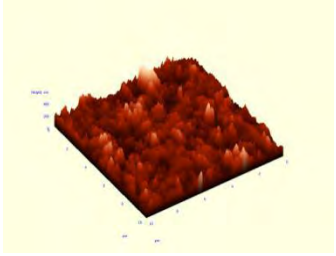

(d) Physically cleaned membrane

Fig.5. AFM micrograph of membranes used in the present study.

4. Conclusion

Membrane cleaning experiments indicate that in chemical cleaning with dilute citric acid (CA) the flux recovery was 69.84% which was higher than the percent recovery obtained with other two chemicals. CA was more effective than the EDTA and STPP solutions for recovering pure water permeability. In forward and backward flushing flux recoveries were found out to be 80.97% and 89.1% respectively. However the maximum flux recovery of 95% was achieved with ultrasonic cleaning for a time span of 8 min. The SEM micrograph of fouled membranes showed a layer of silt like colloidal particles which almost completely occluded the active surface of the membrane. Absorption peaks in the FTIR spectra of the used membrane were appeared to be either eliminated or severely attenuated due to salt deposition. Mass transfer barriers within the fouling layer are likely to be the rate-limiting factor, which are required to be analyzed in depth. Creating favorable hydrodynamic conditions to facilitate mass transfer is likely to enhance the efficiency of cleaning. The chemical cleaning agents tested could not achieve complete flux recovery because residual foulants were strongly embedded in the concavities of membrane surfaces, as reflected by AFM studies.

Acknowledgement

The authors are grateful to Gujarat Council on Science and Technology (GUJCOST), Department of Science & Technology, Government of Gujarat, India for providing grant (File No: GUJCOST/MRP/2015-16/2714) to carry out the work and Sophisticated Instrumentation Centre for Applied Research & Testing (SICART), Vallabh Vidyanagar for carrying out certain analyses.

References

[1] Al-Amoudi.A, and Lovitt. W.L (2007), "Fouling strategies and the cleaning system of NF membranes and factors affecting cleaning efficiency", J. Membr. Sci.,303, 4-28.

[2] Arnal.J.M, Garcia-Fayos.B, Sancho.M, and Verdu.G (2009), "Ultrafiltration membrane cleaning with different chemical solutions after treating surface water", *Desalination and Water Treatment*, **7**, 198-205.

[3] Patel.T.M, and Nath.K (2013), "Alleviation of flux decline in cross flow nanofiltration of two-component dye and salt mixture by low frequency ultrasonic irradiation", *Desalination*, 317, 132-141.

[4] Porcelli.N, and Judd.S (2010), "Chemical cleaning of potable water membranes: A review", *Sep Purif Technol*, 71, 137-143.

[5] Chen.J.P, Kim.S.L and Ting.Y.P (2003), "Optimization of membrane physical and chemical cleaning by a statistically designed approach", *J. Membr. Sci.,* 219 27–45.

[6] Liu.C, Caothien.S, Hayes.J, Caothuy.T, Otoyo.T and Ogawa.T (2001), "Membrane chemical cleaning: from art to science", *Proceedings of 2001 Membrane Technology Conference*, AWWA.

[7] Liikanen.R, Yli-Kuivila.J and Laukkanen.R (2002), "Efficiency of various chemical for nanofiltration membrane fouled by conventionally-treated surface water", *J. Membr.Sci.,* **195**, 265-276.

[8] Smith.P.J, Vigneswaran.S, Ngo.H.H, Ami,R.B and Nguyen.H (2006), "A new approach to backwash initiation in membrane systems", *J. Membr. Sci.,* **278**, 381–389.

[9] Psoch.C and Schiewer.S (2006), "Resistance analysis for enhanced wastewater membrane filtration", *J. Membr. Sci.,* **280**, 284–297.

[10] Cornelissen.E.R, Vrouwenvelder.J.S, Heijman.S.G.J, Viallefont.X.D, van Der Kooij.L and Wessels.L.P (2007), "Periodic air-water cleaning for control of biofouling in spiral wound membrane elements", *J. Membr. Sci.,* **287**, 94–101.

[11] Ducom.G and Cabassud.C (2003), "Possible effects of air sparging for nanofiltration of salted solutions", *Desalination*, **156**, 267-274.

[12] Cui.Z and Taha.T (2003), Enhancement of

ultrafiltration using gas sparging: a comparison of different membrane modules", *J. Chem Tech.Biotech,* **78**, 249-253.

[13] Muthukumaran.S, Yang.K, Seuren.A, Kentish.S, Ashokkumar.M, Stevens.G.W and Grieser.F (2004), "The use of ultrasonic cleaning for ultrafiltration membranes in the dairy industry", *Sep. Purif. Technol.* 39, 99–107.

[14] Juang.R.S and Lin.R.H (2004), "Flux recovery in the ultrafiltration of suspended solutions with ultrasound", *J. Membr. Sci.,* 243, 115-124.

[15] Lee.H.J, Amy.G, Cho.J, Yoon.Y, Moon.S.H and Kim.I.S (2001), "Cleaning strategies for flux recovery of an ultrafiltration membrane fouled by natural organic water", *Water Res*., **35**, 301–3308.

[16] Madaeni.S.S, Mohamamdi.T and Moghadam.M.K (2001), "Chemical cleaning of reverse osmosis membranes", *Desalination,* **134**, 77-82.

[17] Lin.J.C.T, Lee .D.J and Huang.C (2010), "Membrane fouling mitigation: Membrane cleaning" *Sep. Sci. Technol.,* **45**, 858-872.

[18] Patel T.M, Chheda.H, Baheti.A, Patel.P and Nath.K (2012), "Comparative performance of flat sheet and spiral wound modules in the nanofiltration of reactive dye solution", *Environ Sci Pollut Res*., **19**, 2994–3004.

[19] Song.W, Ravindran.V, Koel.B.E and Pirbazari.M (2004), "Nanofiltration of natural organic matter with H_2O_2/UV pretreatment: fouling mitigation and membrane surface characterization", *J. Membr. Sci.*, **241**, 143–160.

[20] Sagiv.A and Semiat.R (2010), "Parameters affecting backwash variables of RO membranes", *Desalination,* **261**, 347-353.

[21] Feng.D, Van Deventer. J.S.J and Aldrich.C (2006), "Ultrasonic defouling of reverse osmosis membranes used to treat wastewater effluents", *Sep. Purif. Technol.*, **50**, 318–323.

[22] Liu.Y, Zhang.S, Zhou.Z, Ren.J, Geng.Z, Luan.J and Wang.G (2012), "Novel sulfonated thin-film composite nanofiltration membranes with improved water flux for treatment of dye solutions", *J Membr. Sci.*, **394– 395**, 218– 229.

[23] Tang.C.Y, Kwon.Y.N and Leckie.J.O (2009), "Effect of membrane chemistry and coating layer on physiochemical properties of thin film composite polyamide RO and NF membranes .FTIR and XPS characterization of polyamide and coating layer chemistry", *Desalination*, **242**, 149–167.

[24] Dyer.J.R (2012), "Applications of Absorption Spectroscopy of Organic Compounds", *PHI Learning Pvt. Ltd., New Delhi,* 23–41.

[25] Hoek.E.M.V, Bhattacharjee.S and Elimelech.M (2003), "Effect of membrane surface roughness on colloid-membrane DLVO interactions", *Langmuir*, **19**, 4836–4847.

PRAJÑĀ - Journal of Pure and Applied Sciences Vol. 26 : 96 – 103 (2018)
ISSN 0975 - 2595

HIGH PERFORMANCE THIN LAYER CHROMATOGRAPHIC METHOD FOR SIMULTANEOUS ESTIMATION OF PIPERINE AND 6-GINGEROL IN TRIKATU CHURNA

SAUMIL PATEL AND VIJAYKUMAR PARMAR
Department of Pharmaceutical Sciences, Sardar Patel University, Vallabh Vidyanagar – 388 120

ABSTRACT

A sensitive high-performance thin layer chromatographic (HPTLC) method was developed for simultaneous determination of piperine and 6-gingerol from ayurvedic formulation. Chromatographic separation was achieved on aluminium plates pre-coated with silica gel G60 F254 as the stationary phase and hexane:ethyl acetate:toluene:diethyl ether (4.5:5.5:1.0:0.5) as the mobile phase. The densitometric evaluation was carried out at 282 nm. The developed method was validated as per the ICH guidelines. The Rf value of piperine and 6-gingerol was found to be 0.45±0.02 and 0.60±0.02, correspondingly. The response in terms of peak area was linear over the concentration range of 100-500 ng/spot for piperine and 6-gingerol, individually, with the regression coefficient values greater than 0.99 for both the drugs. The limits of detection were found to be 7.65 ng/spot and 8.83 ng/spot for piperine and 6-gingerol, respectively. The method can be applied for the simultaneous estimation of piperine and 6-gingerol in ayurvedic formulation.

Keywords: piperine, 6-gingerol, HPTLC, ayurvedic formulation.

INTRODUCTION

Trikatu churna is an Ayurvedic formulation composed of equal parts of Pipali (Black pepper, Piper longum), Maricha (Long pepper, Piper longum) and Sunthi (Ginger, Zingiber officinalis) [1]. Piperine is an active marker constituent of Pipali and Maricha whereas 6- Gingerol is of Sunthi. Piperine is an alkaloid and chemically it is (2E,4E)-5-(1,3-benzodioxol-5-yl)-1-piperidin-1-ylpenta-2,4-dien-1-one (Figure 1A). Gingerol is an pungent principle present in ginger. Chemically, it is (5S)-5-hydroxy-1-(4-hydroxy-3-methoxyphenyl)decan-3-one (Figure 1B). Several studies have shown that Trikatu and its constituents possessed bioavailability enhancing activity [1-3].

Spectrophotometric [4, 5], HPLC [6, 7] and HPTLC [8-10] methods are reported in the literature for determination of piperine in sample material and formulations. Several methods are also reported for simultaneous determination of piperine and other phytocompounds [11, 12]. The HPLC method with UV [13], MS [14] and electrochemical [15] detection and HPTLC method [16, 17] are reported for determination of 6-gingerol in the literature. Literature survey revealed that there is no HPTLC method reported for simultaneous estimation of piperine and 6-gingerol in ayurvedic formulation. Therefore, the aim of this present work was to develop rapid and sensitive HPTLC method for simultaneous estimation of piperine and 6-gingerol. The developed HPTLC method was validated and found to be simple, rapid, sensitive and robust and can be successfully applied for estimation of piperine and 6-gingerol in ayurvedic formulation.

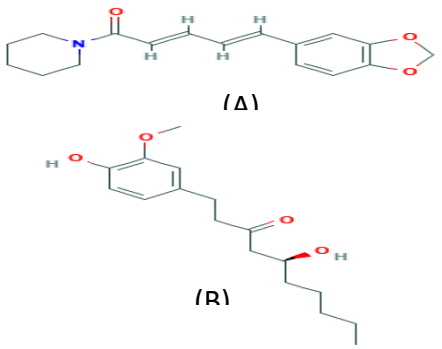

Figure 1. Chemical Structure of (A) Piperine and (B) 6-gingerol

METHODOLOGY

Instrumentation

The HPTLC system (Camag Sonnenmattstr, Mutenz, Switzerland) consisting of a Linomat V semi-automatic spotting device connected to a nitrogen cylinder, a glass twin-trough TLC chamber (20×10 cm), a TLC scanner-III, a data station with winCATS (V 1.4.7) software and an HPTLC syringe (100 µL capacity; Hamilton Company, NV, USA) was used for thin layer chromatographic studies.

Chemicals

Piperine (>95%) was procured from Sigma Aldrich, Mumbai, India. 6- gingerol (>95%) was purchased from Naturl Remedies, Bangalore, India. Methanol, ethyl acetate, toluene, diethyl ether, and n-hexane were purchased from Sisco Chem Pvt. Ltd., Mumbai, India. Analytical reagent grade solvents were used for HPTLC analysis. Marketed formulation containing piperine and 6-gingerol was purchased from local pharmacy.

Chromatographic conditions

Separation was performed on pre-coated silica gel G60 F254 aluminum plates (20×10 cm) with 0.2 mm thickness (E. Merck, Darmstadt, Germany). Samples were spotted on the TLC plate in the form of band leaving 10 mm from the bottom edge using Linomat V semi-automatic spotter and analyzed using following parameters; bandwidth, 4 mm; track distance, 10 mm; migration distance, 40 mm; spraying rate, 150 nL/s; volume of mobile phase, 7.15 mL; temperature, 27±2 ◦C; chamber saturation time, 15 min; migration distance, 40 mm; slit dimension, 3.00×0.30 mm; scanning speed, 20 mm/s; detection wavelength, 232 nm. Mobile phase consisted of methanol: ethyl acetate: toluene: ammonia (3: 1: 3: 0.15 v/v/v/v).

Preparation of Standard Solutions

Accurately weighed 10 mg of Piperine drug powder was transferred to 10 ml volumetric flask, and was dissolved in 3 ml of Methanol. The volume was made up with Methanol to get a stock solution containing 1mg/ml of Piperine (1000 µg/ml of Piperine). Accurately weighed 10 mg of 6-Gingerol drug powder was transferred to 10 ml volumetric flask, and was dissolved in 3 ml of Methanol. The volume was made up with methanol to get a stock solution containing 6-gingerol (1000 µg/ml of 6-Gingerol). Stock solutions of standard piperine (0.5 ml) and standard 6-gingerol (0.5 ml) were transferred into the 10 ml volumetric flask and diluted using methanol up to the mark to get the concentration of 50 µg/ml of Piperine and 50 µg/ml of 6-Gingerol.

Preparation of Sample Solution

Ayurvedic lab formulation (3 g) or marketed ayurvedic formulation (2 g) was accurately weighed and transferred to 25 ml volumetric flask and methanol (10 ml) was added. The volume was made up to the mark with Methanol. The solution was sonicated for 45 min and filtered. This solution was used for HPTLC analysis.

Calibration curve of Piperine and 6-Gingerol

Combined working standard solution (2 µl, 4 µl, 6 µl , 8 µl, 10 µl), was spotted on the TLC plates which cover the range of 100-500 ng/spot for piperine and 100-500ng/spot for 6-gingerol to determine the linearity. Each concentration was spotted three times on TLC plate and mobile phase

was run up to 70 mm and scanned by scanner. Calibration curve was constructed by plotting mean peak areas of piperine and 6-gingerol against respective concentration.

Validation of developed HPTLC method

The specificity of the method was ascertained by analyzing standard drug and sample solutions. The spot for piperine and 6-gingerol in sample solution prepared from marketed formulation was confirmed by comparing absorbance/reflectance spectrum with that of standard piperine and 6-gingerol. The peak purity of piperine and 6-gingerol was assessed by correlating the spectra at three different levels, i.e., peak start (S), peak apex (M) and peak end (E) position of the spot. The linearity of piperine and 6-gingerol were determined in the range of 100-500 ng/spot. Five sets of such solutions were prepared and analyzed by plotting a calibration curve of mean peak area versus concentration. Standard deviation (SD), slope, intercept and correlation coefficient (r) of the calibration curves were calculated to ascertain linearity of the method.

The precision is measured by the degree of reproducibility and repeatability of analytical method. The precision of analytical method is expressed as a %RSD. Repeatability of measurement of peak area was carried out by repeated scan of the same spot (100 ng/spot of piperine and 6-gingerol) seven times without changing the plate position. The % RSD for peak area was calculated. Repeatability of sample application is based on seven-time application of combined standard solution. The % RSD for peak area was computed. Variations of results within same day (intra-day precision) and among days (inter-day precision) are called as reproducibility. The intra-day precision (% RSD) was determined by analyzing standard solution of piperine and 6-gingerol for three times on the same day. The inter-day precision (% RSD) was determined by analyzing standard solution of piperine and 6-gingerol for 3 days. The intra- and inter-day variation for determination of piperine and 6-gingerol was carried out at three different concentration levels 100, 300, 500 ng/spot of piperine and 6-gingerol.

Recovery study was performed by addition of known amounts of standard drugs to pre-analyzed formulation extract (standard addition method). To a fixed amount of sample, an increasing amount of standard drugs, piperine and 6-gingerol, was added at 3 levels and the amount of drugs recovered was calculated at each level. The average recoveries after the analysis were calculated. Robustness of the method was evaluated by altering parameters such as volume of mobile phase, saturation time and solvent front position. The measurement of signal to noise ratio approach was used for determination of LOD and LOQ. Signal to noise ratio of 3:1 and 10:1 were considered acceptable for estimating the detection limit and quantification limit respectively.

Analysis of marketed formulations

Sample solution (10 µL) was spotted on the TLC plate and analyzed. The experiment was repeated 3 times. The peak areas of the spots were measured. The % content was calculated using straight line equation derived from calibration curves for piperine and 6-gingerol.

RESULTS AND DISCUSSION

Method development and optimization

To optimize the chromatographic conditions for the separation of piperine and 6-gingerol, mobile phase composition, effect of saturation time, and detection wavelength were investigated. Initially, trials for mobile phase optimization were carried out using experimental conditions: stationary phase, pre-coated silica gel G60 F254 aluminum sheets; standard solution, piperine 200 ng/spot and 6-gingerol 200 ng/spot; detection wavelength, 254 nm; saturation time, 30 min. Solvent system consisting of hexane:ethyl acetate:toluene:diethyl ether (4.5:5.5:1.0:0.5) resulted in separation of piperine and 6-gingerol spots at Rf values of 0.45±0.02 and 0.60±0.02, respectively (Figure 2A). Chromatographic plate was developed up to 70 mm migration distance. Pre-saturation of TLC chamber with mobile phase for 15 min produced good reproducibility and peak shape. Photometric evaluation was performed at 282 nm. Quantitative determinations of piperine and 6-gingerol were made by considering the peak areas from chromatograms and regression line equation using optimized conditions.

Method validation

Comparison of chromatograms of standard solution and sample solution from formulation showed identical Rf values i.e. 0.45±0.02 for piperine and 0.60±0.02 for 6-gingerol (Figure 2). Comparison of the spectra scanned at peak start (S), middle (M) and end (E) showed high degree of correlation (above 0.990). This confirmed the purity of the corresponding spots. Also, the spectrum of individual drug was compared with the spectrum of standard piperine and 6-gingerol. The correlation obtained was 0.9991 for piperine and 0.9997 for 6-gingerol; this confirmed the identity of spots. The excipients and other components present in the churna did not interfere in the resolution of piperine and 6-gingerol.

The calibration curves for piperine and 6-gingerol were found to be linear in the concentration range of 100-500 ng/spot for both the analytes with correlation coefficients greater than 0.99. The linear regression equations were found to be $y = 21.75x+1087$ for piperine and $y = 4.76x-159$ for 6-gingerol, where, y – peak area and x – concentration in ng/spot.

The repeatability (% RSD) of sample application was found to be 1.16 and 1.71 for piperine and 6-gingerol, respectively. The scanner precision (% RSD) for measurement of peak area was found to be 0.29 and 0.98 for piperine and 6-gingerol, respectively. The repeatability studies ensured precision of scanner and spotting devices. The % RSD for intra-day precision was found to be 0.03-0.38 and 0.22-1.29 for piperine and 6-gingerol, respectively (Table 1). The % RSD for inter-day precision was found to be 1.00-1.61 and 1.43-1.76 for piperine and 6-gingerol, respectively (Table 2).

Accuracy of the developed method was calculated by performing recovery studies. Results of recovery studies are shown in Table 3. The % recoveries were found out to be 97.32–103.80 % for piperine and 97.91–102.20 % for 6-gingerol. The LODs and LOQs were found to be 7.65 ng/spot and 23.18 ng/spot for piperine and 8.83 ng/spot, 26.76 ng/spot for 6-gingerol, respectively. Results of robustness studies indicated that the selected chromatographic factors (Rf Value and peak purity) remained unaffected by small variation of

these parameters, which demonstrates that the developed method is robust.

Analysis of ayurvedic formulations

The spots at Rf value 0.45 (for piperine) and 0.60 (for 6-gingerol) was observed in the densitogram of the drug samples extracted from ayurvedic formulations. Amounts of piperine and 6-gingerol were calculated using linear regression equation derived. The % contents of piperine and 6-gingerol are presented in Table 4.

CONCLUSION

The proposed HPTLC method provides precise, accurate and reproducible quantitative analysis for the simultaneous estimation of piperine and 6-gingerol in ayurvedic formulations. The method was validated as per the ICH guidelines. It can be concluded that the developed method is simple, accurate, sensitive and precise. The method is suitable for routine analysis of piperine and 6-gingerol in marketed ayurvedic formulations.

REFERENCES

[1] Johri, R. K., & Zutshi, U. (1992). An Ayurvedic formulation 'Trikatu' and its constituents. Journal of Ethnopharmacology, 37(2), 85-91.

[2] Karan, R. S., Bhargava, V. K., & Garg, S. K. (1999). Effect of trikatu, an Ayurvedic prescription, on the pharmacokinetic profile of rifampicin in rabbits. Journal of ethnopharmacology, 64(3), 259-264.

[3] Kang, M. J., Cho, J. Y., Shim, B. H., Kim, D. K., & Lee, J. (2009). Bioavailability enhancing activities of natural compounds from medicinal plants. Journal of Medicinal Plants Research, 3(13), 1204-1211.

[4] Singh, N. K., Kumar, P., Gupta, D. K., Singh, S., & Singh, V. K. (2011). UV-spectrophotometric method development for estimation of piperine in Chitrakadi Vati. Der Pharmacia Lettre, 3(3), 178-182.

[5] Vishvnath, G., & Jain, U. K. (2011). Quantitative analysis of piperine in ayurvedic formulation by UV Spectrophotometry. Int J Pharm Sci Res (IJPSR), 2, 58-61.

[6] Sunita, S., Menon, S. N., & Singh, A. (2010). Quantitative analysis of piperine from Ayurvedic Polyherbal formulations using reverse phase high performance liquid chromatography. International Journal of Pharma and Bio Sciences, 1(1), 1-10.

[7] Gupta, V., & Jain, U. K. (2011). Quantitative estimation of piperine in Pancasama churna by RP-HPLC. Der Pharmacia Lettre, 3, 400-406.

[8] Shanmugasundaram, P., Maheswari, R., & Vijayaanandhi, M. (2008). Quantitative estimation of piperine in herbal cough syrup by HPTLC method. Rasayan J Chem, 1(02), 212-7.

[9] Sarkar, B., Tiwari, S., Patel, R., & Dubey, G. (2011). High performance thin layer chromatographic method for quantification of piperine in an ayurvedic formulation. Asian J. Pharmacy Life Sci, 1(2), 128-132.

[10] Tapadiya, G., Metku, M., Deokate, U., Khadabadi, S., Saboo, S., & Sahu, K. (2009). Quantitative estimation of piperine from pharmaceutical dosage form by HPTLC. Asian J Pharm Cli Res, 2, 47-50.

[11] Vyas, N., Gamit, K., Khan, M. Y., Panchal, S., & Pundarikakshudu, K. (2011). Simultaneous estimation of curcumin and piperine in their crude powder mixture and ayurvedic formulation using high performance thin layer chromatography. Int J Res Pharm Biomed Sci, 2(01), 231-6.

[12] Patel, R. K., Kanani, R. J., Patel, V. R., & Patel, M. G. (2010). Development and validation of HPTLC method for simultaneous quantification of vasicine

and piperine in Vasavaleha. Int J Pharm Res, 2(3), 14-17.

[13] Schwertner, H. A., & Rios, D. C. (2007). High-performance liquid chromatographic analysis of 6-gingerol, 8-gingerol, 10-gingerol, and 6-shogaol in ginger-containing dietary supplements, spices, teas, and beverages. Journal of Chromatography B, 856(1-2), 41-47.

[14] Wang, W., Li, C. Y., Wen, X. D., Li, P., & Qi, L. W. (2009). Simultaneous determination

[15] Zick, S. M., Ruffin, M. T., Djuric, Z., Normolle, D., & Brenner, D. E. (2010). Quantitation of 6-, 8-and 10-gingerols and 6-shogaol in human plasma by high-performance liquid chromatography with electrochemical detection. International journal of biomedical science: IJBS, 6(3), 233.

[16] Rai, S., Mukherjee, K., Mal, M., Wahile, A., Saha, B. P., & Mukherjee, P. K. (2006). Determination of 6-gingerol in ginger (Zingiber officinale) using high-performance thin-layer chromatography. Journal of separation science, 29(15), 2292-2295.

[17] Krüger, S., Bergin, A., & Morlock, G. E. (2018). Effect-directed analysis of ginger (Zingiber officinale) and its food products, and quantification of bioactive compounds via high-performance thin-layer chromatography and mass spectrometry. Food chemistry, 243, 258-268.

PRAJÑĀ - Journal of Pure and Applied Sciences Vol. 26 : 96 – 103 (2018)
ISSN 0975 - 2595

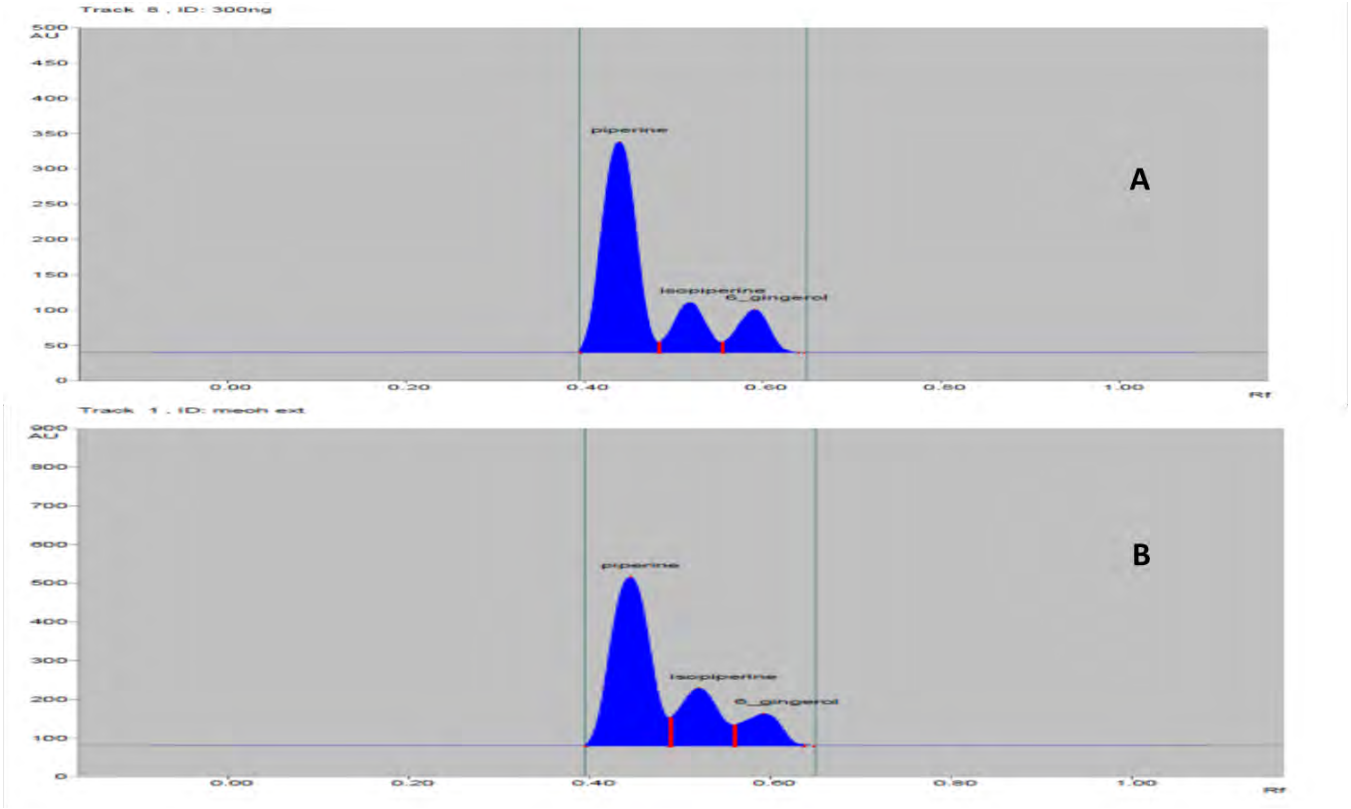

Figure 2 HPTLC chromatogram showing separation of piperine and 6-gingerol in (A) standard mixture solution and (B) ayurvedic formulation

Table-1 : Intra-day Precisions of piperine and 6-gingerol (*n*=3)

Name of Drug	Amount (ng/spot)	Intra-day Precision		
		Peak area (Mean±SD)	RSD	SE
Piperine	100	3135.18 ± 11.82	0.38	6.83
	300	7656.09 ± 11.79	0.15	6.81
	500	11251.94 ± 3.31	0.03	1.91
6-Gingerol	100	644.41 ± 8.31	1.29	4.79
	300	2157.90 ± 4.64	0.22	2.68
	500	2931.71 ± 14.43	0.49	8.33

Table-2 : Inter-day Precisions of piperine and 6-gingerol (*n*=3)

Name of Drug	Amount (ng/spot)	Inter-day Precision		
		Peak area (Mean±SD)	RSD	SE
Piperine	100	2858.93 ± 46.12	1.61	26.63
	300	7769.4 ± 77.89	1.00	44.97
	500	11517.27 ± 168.49	1.46	97.28
6-Gingerol	100	345.83 ± 6.07	1.76	3.50
	300	1180.5 ± 16.87	1.43	9.74
	500	1950.2 ± 33.34	1.71	19.25

Table-3 : Recovery studies for piperine and 6-gingerol

Name of the drug	Amount of standard spiked (ng)	Average of amount Recovered (ng)	Recovery (%) ± S.D	%RSD
Piperine	200	207.66	103.8 ± 1.55	1.50
	300	291.97	97.32 ± 1.67	1.71
	400	396.75	99.19 ± 1.81	1.83
6-Gingerol	200	195.83	97.91 ± 1.68	1.71
	300	306.58	102.2 ± 1.81	1.77
	400	401.17	100.3 ± 1.81	1.81

Table-4 : Analysis of ayurvedic formulation

Name of the drug		Ayurvedic lab formulation	Marketed formulation
Average content (%w/w)	Piperine	0.05	0.087
	6-Gingerol	0.06	0.07

PRAJÑĀ - Journal of Pure and Applied Sciences Vol. 26 : 104 - 111 (2018)
ISSN 0975 - 2595

EFFECT OF SUPPLEMENTATION OF PRICKLY PEAR JUICE ON THE ANTIOXIDANT STATUS OF YOUNG ADULT FEMALES

VIRAJ ROGHELIA
Laboratory of Foods and Nutrition, P. G. Department of Home Science, Sardar Patel University,
Vallabh Vidyanagar-388120, Gujarat, India. Email: virajshalin@gmail.com

ABSTRACT

Prickly pear (Opuntia spp.) belongs to Cactaceae family and commonly known as cactus fruit. The fruit contains various phenolic compounds, antioxidant vitamins and hence possess good antioxidant activity. In the present study, the effect of prickly pear juice supplementation on the antioxidant status of young adult female was assessed. For this, 20 female subjects with the age group 20-25 years were enrolled in each control and experimental group. 100 ml of prickly pear juice was fed to the females in experimental group and 100 ml water was fed to the subjects in the control group for one month. Prickly pear juice contained 13.87mg% ascorbic acid, 237.75 mg% total phenols and 36.03 mg% flavonoids. The total antioxidant capacity of juice was 97.41 mg% while DPPH and ABTS radical scavenging activity of juice was 71.88% and 48.61% respectively. Thirty days supplementation of prickly pear juice significantly elevated blood glutathione level by 17.75 %, blood vitamin C by 54.44% and plasma total antioxidant activity by 33.30%. The present study concludes that consumption of prickly pear juice positively affect the antioxidant status of an individual.

Keywords: prickly pear, antioxidants capacity, vitamin-C, glutathione

INTRODUCTION

Antioxidants are crucial for animal and plant life as they are involved in complex metabolic and signalling mechanisms [1, 2]. In animals, free radicals are steadily produced by oxidation reactions that can start multiple chain reactions and finally, it causes damage or death to the cell [3]. Antioxidants are the substances that delay, prevent or remove oxidative damage to a target molecule by their free radical scavenging activity and thus preventing the harmful chain reactions [3, 4, 5]. Antioxidants are capable of stabilizing, or deactivating, free radicals before they attack cells. Antioxidants are absolutely critical for maintaining optimal cellular and systemic health and well-being [6]. Antioxidants like vitamin-C, vitamin-E and β-carotene play a vital role in inactivating reactive oxygen species that are responsible for initiation as well as progression of various chronic diseases. Antioxidants are reported to decrease oxidative stress induced carcinogenesis [7, 8].

Prickly pears (*Opuntia s*pp.) are underutilized and widely growing fruits belong to the family *Cactaceae* [9]. The other common names for prickly pears are cactus fruit, cactus pear, Indian fig, and Barbary fig. In India, it is known as *Nagphani* and in Gujarat especially in Saurashtra region, it is popular as *findla* or *hathla* [10]. Prickly pears are fleshy berry, elongated, edible, and varying in colour and size as per their species. The taste of fruit is sweet due to presence appreciable amount of sugar [11]. These fruits contain vitamin-C, vitamin-E, β-carotene, minerals, free amino acids such as proline, phenylalanine, lysine, histindie as well as good amounts of total phenols, flavonoids, betalains and carotenoids [12] and hence, prickly pears are reported to possess good antioxidant activity . These nutritional compounds and nutraceuticals are associated mainly with better health of an individual [13]. A diet rich in prickly pear cactus is positively correlated with reduced risk of chronic diseases associated with oxidative stress, such as diabetes, cancer, cardiovascular and neurodegenerative diseases [14]. Hence, in this context, the present study was aimed to check the effect of supplementation of prickly pear juice on the antioxidant status of young adult females.

METHODOLOGY

Development and analysis of prickly pear juice: Prickly pear fruits were procured from Jasdan taluka of Rajkot district of Gujarat. The fruits were cleaned, washed and peeled. The seeds were separated and the pulp was used for

juice preparation. The pulp was mixed with water and sugar. The fruit pulp, water and sugar mixed in varying proportion to obtain different samples of prickly pear juices. All the juice samples were subjected to sensory evaluation for finalizing the composition of prickly pear juice for the feeding trial. Also as per the suggestions of the panellist, to increase the acceptability of juice, natural flavours like lemon juice and ginger juice were also added. The final composition and appearance of optimized prickly pear juice is presented in figure 1 and plate 1 respectively. The juice was analysed for ascorbic acid, total phenolic content, flavonoid content and total antioxidant capacity.

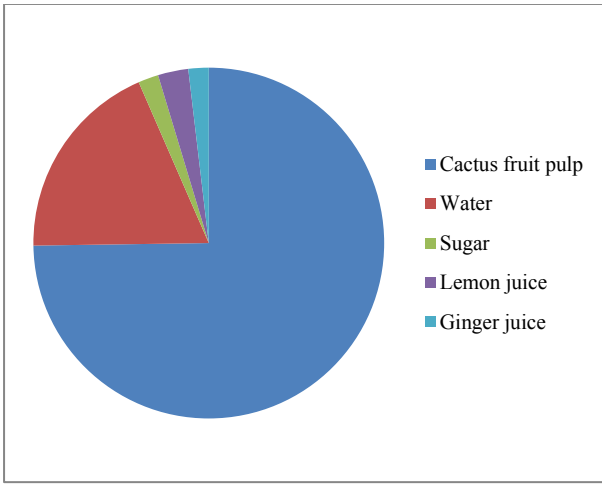

Figure 1: composition of prickly pear juice

Plate 1: Appearance of prickly pear juice

Ascorbic acid estimation: It was done by titration method with dye (2,6 dichlorophenol indophenols) [15]. For this, 5 ml of juice was mixed with 3% meta phosphoric acid and titrated against dye . The results are expressed in mg/100ml of juice.

Sample extraction: For this, 5 ml of prickly pear juice was extracted with 80% methanol and samples were stored at -20°C and used for total phenol flavonoids and antioxidant activity analysis.

Determination of total phenol and flavonoids: Total phenol estimation was done by folin cio-caltue method [16].The value of total phenol was expressed as % gallic acid equivalent per 100ml of juice. Flavonoid estimation was done by colorimetric method [17]. The result was expressed as % rutin equivalent per 100ml of juice.

Determination of total antioxidant activity: Ferric Reducing Antioxidant Power Assay (FRAP) was determined by method given by Benzie and strain [18] and the results were depicted as % trolox equivalent per 100 ml of juice. DPPH (1, 1- diphenyl, 2-picrylhydrazyl) scavenging activity was measured by the spectrophotometric method [19] and 2, 2, Azinobis, 3 ethyl benzo-thiazolin 6-sulphonic acid (ABTS) radical scavenging activity of juice was determined using the modified ABTS radical depolarization assay [20]. The results of DPPH and ABTS radical scavenging activity are expressed in % inhibition.

Clinical trial: Total 40 young adult females in the age group 20-25 years were enrolled on the basis of their willingness to participate in the study. The subjects were divided into control (N=20) and experimental group (N=20). All the subjects were explained the objectives of the study and written consent was taken. 100 ml of freshly prepared prickly pear juice was fed to the subjects in the experimental group and water was fed to each of the subject in the control group for 30 days. Antioxidant profile of the selected subject from both the groups was studied prior to and at the end of the study period. For this, 5 ml fasting venous blood sample was collected from each subject. Whole

blood was checked for glutathione and ascorbic acid levels while from serum was analysed for total antioxidant activity. All the samples were analysed on the same day of the collection.

Glutathione estimation: Blood glutathione was evaluated by the method given by Ellman [21]. For this, 0.5 ml. of blood sample was mixed with 1 ml of 5% tricholoro acetic acid (TCA). The mixture was mixed and centrifuged. From the supernatant, 0.1 ml aliquote was taken. Sample was treated with 3.9 ml of phosphate buffer and 0.2 ml of DTNB solution.The samples were incubated at room temperature for 10 minutes. The absorbance was read at 412 nm.

Vitamin-C estimation: Blood vitamin C was analyzed by the method given by Roe and Kuether [22] and Bessy et al. [23]. For this, 0.5 ml of blood sample was mixed with 1 ml of chilled 5% TCA. The samples were centrifuged for ten minutes. The samples were prepared with 0.4 ml of supernatant and 0.6 ml of 5% TCA to make the volume 1.0 ml. The samples were treated with 0.2 ml of 2,4-Dinitrophenylhydrazine / Thiourea / Copper sulphate solution and were incubated for 3 hours at 37°C .After incubation, 1.5 ml of 65% sulphuric acid was added and the samples were further incubated for 30 minutes at room temperature. The colour developed in the samples were read at 520 nm.

Total Antioxidant Capacity using FRAP method: Serum total antioxidant activity was evaluated by the method of Benzie and Strain [18]. About 0.02 ml of serum was mixed with distilled water to make the volume upto 300 µl. To this, 1.8 ml of FRAP reagent was added and incubated at 37°C for 10 minutes. The samples were read at 593 nm.

Statistical analysis: The data were analysed by SPSS (version 15.00). Results are expressed in mean ± S.D. For studying the effect of supplementation, paired t test was done. A p value less than 0.05 was considered as spastically significant.

RESULTS AND DISCUSSION

Prickly pear juice was developed using its fruit pulp, sugar and water. Lemon juice and ginger juice were added to increase the flavour of juice. Overall acceptability of freshly prepared prickly pear juice was 88% as scored by the panellist.

Table 1 depicts the average value of ascorbic acid, total phenol, flavonoid content and antioxidant activity of prickly pear juice. Mean ascorbic acid content of prickly pear juice was 13.87 mg/100 ml. Kuti et al. [24] reported ascorbic acid content of different cactus fruit ranged from 12.1 mg% to 81.5 mg% . Diaz Medina et al. [25] and Fernández-López [26] have reported little higher ascorbic acid content of *opuntia ficus indica*. In the present study, the pulp was mixed with water, hence ascorbic acid content was found to be lower.

Table 1: Ascorbic acid, total phenol, flavonoid content and antioxidant activity of prickly pear juice.

Ascorbic acid (mg/100ml)	13.87 ± 0.80
Total phenol (mgGAE/100ml)	237.75 ± 19.09
Flavonoids (mgRE/100ml)	36.03 ± 3.75
Antioxidant capacity (FRAP) (mgTE/100ml)	97.41 ± 4.95
DPPH radical scavenging activity (% inhibition)	71.88 ± 0.76
ABTS radical scavenging activity (% inhibition)	48.61 ± 1.32

Values are Mean ±S.D.

Polyphenols are an important group of natural compounds, recently considered to be of high scientific and therapeutic interest [27]. Polyphenols are also considered as a class of

free radical terminator. The products of the metal oxide reduction have a blue colour that exhibits a broad light absorption with a maximum at 765 nm. The intensity of light absorption at that wavelength is proportional to the concentration of phenols [**9].** Total phenol content of prickly pear juice was 237.75 mg GAE/100 ml of juice. The phenol content was found to be in the line with that reported by Fernández-López [26] and Yeddes et al. [27]. Albano et al. [13] reported lower value of total phenol of hydrophilic extract of purple cactus fruit. The mean value of flavonoid content of prickly pear juice was 36.03 mgRE/100 ml which was higher than the flavonoid content of prickly pears reported by Kuti et al.[24] and Fernández-López [26].

FRAP assay is a method to determine the total antioxidant power interpreted as the reducing capacity of the sample. In the present study, antioxidant capacity by FRAP was 97.41 mg TE/ 100 ml of juice. As noted by Albano et al. [13], pulp of purple cactus pear fruit showed significant higher trolox equivalent antioxidant capcacity as compared to pulp of orange cactus pear fruits. Zenteno-Ramirez et al. [28] noted a positive correlation between betalain content and antioxidant capacity by FRAP method.

DPPH and ABTS radicals are commonly used to test the free radical scavenging ability of the sample. ABTS measure the activity of compounds of both lipophilic and hydrophilic nature, while DPPH can only be dissolved in organic media [29]. Higher reduction in colour indicates higher ability to scavenge these radical. In the present study, DPPH radical scavenging activity of prickly pear juice was 71.88 % that is higher than DPPH radical scavenging activity of pomegranate juice, orange juice, apple juice and cranberry juice as reported by Sreeram et al.[30]. While, ABTS radical scavenging activity was 48.61%. Hassan and Hassan [31] have reported 19.34% to 92.59% for 50 µl/ml to 600 µl/ml of cactus pear juice respectively. Madrigal-Santillán et al. [29] reported the best inhibition corresponded to the red-purple juice variety, reaching an inhibition of 65%

Butera et al. [32] have reported that antioxidant activity of cactus fruits is mainly attributed to its chief pigment betalian. The other contributory factors are ascorbic acid, tocopherols, phenolic compounds as well as various flavonoids [24, 33, 34]. Chavez et al. [33] reported higher antioxidant capacity of cactus fruit as compared to apples, pears, tomatoes, bananas and white grapes. Various factors affect phenolic content of cactus fruits such as cultivar, colour, geographical location [24, 35, 36,]. Also, the type of solvent used for extraction and processing of food also affect the antioxidant potential of the food [37].

Effect of supplementation of prickly pear juice on the antioxidant status of young adult females: Prickly pear juice was prepared freshly and supplemented to young adult females. Table 2 shows the mean values of blood glutathione and ascorbic acid level of the subjects prior to and at the end of the experimental period.

Glutathione is a powerful and major tissue antioxidant that prevents damage to cellular component by reactive oxygen species. Increased glutathione level decreases muscle damage, reduce recovery time as well as increases strength and endurance [38]. In the present study, initial level blood glutathione of control subjects was 8.07 mg/dl which increased to 8.59 mg/dl after 30 days, however no significant increase was noticed. In the experimental group, the initial level of blood glutathione was 8.73 mg/dl. Supplementation of prickly pear juice for 30 days significantly ($p<0.01$) increased it by 17.75%. Tesoriere et al., (2004)[38] reported that GSH :GSSG level in red blood cells was elevated by the supplementation of cactus pear which indicates reduction in oxidative stress. Glutathione is a tripeptide comprising of cystine, glycine and glutamic acid. Ali et al. [39] reported that red prickly pear fruits contains good amount of these three amino acids. In present study, increase in glutathione level in experimental

subjects due to prickly pear supplementation may be attributed to presence of reduced glutathione and cysteine in prickly pear fruits [40] which are important constituents of reduced glutathione.

The mean level of whole blood vitamin-C of control subjects at initial level was 1.80 mg/dl. After 30 days, no significant change was noticed in average vitamin-C level. While, in experimental group, the initial level of whole blood vitamin C (1.80 mg/dl) significantly ($p<0.01$) increased up to 2.78 mg/dl. Supplementation of prickly pear juices for thirty days raised the level of vitamin C by 54.44%. This is due to presence of appreciable amount of vitamin C in prickly pear juice (13.87 mg%) analysed in the present study. According to Tesoriere et al [38], vitamin C is well characterized antioxidant in cactus pear fruit and hence, significant increase in vitamin C was noted after two weeks of cactus pear fruit supplementation to healthy human subjects.

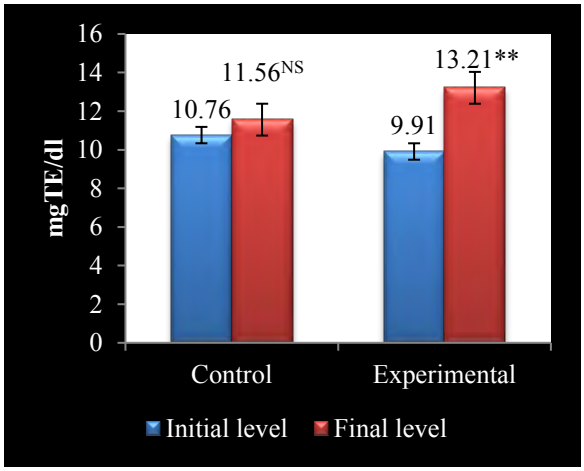

Figure 2: Plasma antioxidant capacity of control and experimental subjects

The difference in mean value of plasma antioxidant capacity of the subjects is presented in figure 2. The average value of plasma antioxidant capacity was 10.75 mg TE/dl at the initial level in control group. No significant change was observed in control group after 30 days pertaining to plasma antioxidant capacity. Prickly pear juice supplementation for one month to the experimental subjects showed a significant ($p<0.01$) elevation in plasma antioxidant capacity by 33.30%. Trolox equivalent antioxidant activity (TEAC) indicates body's overall antioxidant status. Betanin and indicaxanthin, two important pigments as well as other phenolic compounds, biothiols, water and lipid soluble antioxidant vitamins present in prickly pear are potent free radical scavengers [32, 40]. The rise in plasma antioxidant activity may be associated with the presence of phenolic compounds in the prickly pear fruits. Moreover, the increase in blood vitamin-C and glutathione levels might have contributed to rise in total antioxidant capacity among the experimental subjects in the present study.

CONCLUSION

Supplementation of 100 ml of prickly pear fruit juice significantly increased blood vitamin-C and glutathione levels as well as plasma antioxidant capacity among young adult females. This reveals that prickly pear juice improves antioxidant status of an individual and may help to prevent many chronic diseases.

ACKNOWLEDGEMNT

The author acknowledges University Grant Commission (UGC), New Delhi for financial support under Minor Research Project (B-16/VNR/14-15/42).

REFERENCES

[1] Yadav, A., Kumari, R., Yadav, A., Mishra, J. P., Srivatva, S., & Prabha, S. (2016): Antioxidants and its functions in human body-A Review. *Res. Environ. Life Sci*., **9(11)** 1328-1331.

[2] Wilson, D., Nash, P., Buttar, H., Griffiths, K., Singh, R., De Meester, F., Horiuchi, R. & Takahashi, T. (2017): The role of food antioxidants, benefits of functional foods, and influence of feeding habits on the health of the older person: an overview. *Antioxidants*, **6(4):** 81.

[3] Shebis, Y., Iluz, D., Kinel-Tahan, Y., Dubinsky, Z., & Yehoshua, Y. (2013): Natural antioxidants: function and

sources. *Food and Nutrition Sciences*, **4(06):** 643.

[4] Halliwell, B., & Gutteridge, J. M. (1995): The definition and measurement of antioxidants in biological systems. *Free radical biology & medicine*, **18(1):** 125-126.

[5] Halliwell, B. (2007): Biochemistry of oxidative stress. *Biochemical Society Transactions*, **35(5):** 1147-1150.

[6] Percival, M. (1996): Antioxidants. *Clinical Nutrition Insights*, **1***:* 1-4.

[7] Duthie, S. J., Jenkinson, A. M., Crozier, A., Mullen, W., Pirie, L., Kyle, J., Yap, L.S., Christen, P. & Duthie, G. G. (2006): The effects of cranberry juice consumption on antioxidant status and biomarkers relating to heart disease and cancer in healthy human volunteers. *European journal of nutrition*, ***45*(2):** 113-122.

[8] Lobo, V., Patil, A., Phatak, A., & Chandra, N. (2010): Free radicals, antioxidants and functional foods: Impact on human health. *Pharmacognosy reviews*, **4(8):** 118-126.

[9] Roghelia,V. and Panchal,J. (2016): Antioxidant capacity of cactus pear fruit. World journal of pharmaceutical research, **5(5):** 1298-1307.

[10]Chauhan, S., Sheth, N., Jivani, N., Rathod, I., & Shah, P. (2010): Biological actions of Opuntia species. *Systematic Reviews in Pharmacy*, **1(2):** 146-151.

[11]Piga, A. (2004): Cactus pear: a fruit of nutraceutical and functional importance. *Journal of the Professional Association for Cactus Development*, **6**: 9-22.

[12]Ghazi, Z., Ramdani, M., Tahri, M., Rmili, R., Elmsellem, H., El Mahi, B., & Fauconnier, M. L. (2015): Chemical Composition and Antioxidant Activity of seeds oils and fruit juice of Opuntia Ficus Indica and Opuntia Dillenii from Morocco. *Journal of Materials and Environmental Science*, **6(8):** 2338-2345.

[13]Albano, C., Negro, C., Tommasi, N., Gerardi, C., Mita, G., Miceli, A., Bellis, L.D. & Blando, F. (2015): Betalains, phenols and antioxidant capacity in Cactus Pear [Opuntia ficus-indica (L.) Mill.] fruits from Apulia (South Italy) Genotypes. *Antioxidants*, **4(2):** 269-280.

[14]Osuna-Martínez, U., Reyes-Esparza, J., & Rodríguez-Fragoso, L. (2014): Cactus (Opuntia ficus-indica): a review on its antioxidants properties and potential pharmacological use in chronic diseases. *Natural Products Chemistry & Research*. **2(6):** 1000153.

[15]Sadasivam, S. (1996): Volumetric method for ascorbic acid. *Biochemical Methods,* New age international, 184.

[16]Singleton, V. L., & Rossi, J. A. (1965): Colorimetry of total phenolics with phosphomolybdic-phosphotungstic acid reagents. *American journal of Enology and Viticulture*, **16(3):** 144-158.

[17]Singleton, V. L., Orthofer, R., & Lamuela-Raventós, R. M. (1999): Analysis of total phenols and other oxidation substrates and antioxidants by means of folin-ciocalteu reagent. In *Methods in enzymology* . 299: 152-178.

[18]Benzie, I. F. F, Strain, J J. (1996): The ferric reducing ability of plasma (FRAP) as a measure of antioxidant power: the FRAP assay, *Analytical Biochemistry*, **239:** 70-6

[19]Brand-Williams, W., Cuvelier, M. E., & Berset, C. L. W. T. (1995): Use of a free radical method to evaluate antioxidant activity. *LWT-Food science and Technology*, **28(1):** 25-30.

[20]Re, R., Pellegrini, N., Proteggente, A., Pannala, A., Yang, M., & Rice-Evans, C. (1999): Antioxidant activity applying an improved ABTS radical cation decolorization assay. *Free radical biology and medicine*, **26(9-10):** 1231-1237.

[21]Ellman, G. L. (1959): Tissue sulfhydryl groups. *Archives of biochemistry and biophysics*, **82(1):** 70-77.

[22]Roe, J. H., & Kuether, C. A. (1943): The determination of ascorbic acid in whole

blood and urine through the 2, 4-dinitrophenylhydrazine derivavative of dehydroascorbic acid. *Journal of Biological chemistry*, **147**: 399-407.

[23]Bessey, O. A., Lowry, O. H., & Brock, M. J. (1947): The quantitative determination of ascorbic acid in small amounts of white blood cells and platelets. *Journal of Biological Chemistry*, **168**: 197-205.

[24]Kuti, J. O. (2004): Antioxidant compounds from four Opuntia cactus pear fruit varieties. *Food chemistry*, **85(4):** 527-533.

[25]Medina, E. D., Rodríguez, E. R., & Romero, C. D. (2007): Chemical characterization of Opuntia dillenii and Opuntia ficus indica fruits. *Food chemistry*, **103(1):** 38-45.

[26]Fernández-López, J. A., Almela, L., Obón, J. M., & Castellar, R. (2010): Determination of antioxidant constituents in cactus pear fruits. *Plant Foods for Human Nutrition*, **65(3):** 253- 259.

[27]Yeddes, N., Chérif, J. K., Guyot, S., Sotin, H., & Ayadi, M. T. (2013): Comparative study of antioxidant power, polyphenols, flavonoids and betacyanins of the peel and pulp of three Tunisian Opuntia forms. *Antioxidants*, *2*(2), 37-51.

[28]Zenteno-Ramirez, G., JUÁREZ-FLORES, B. I., Aguirre-Rivera, J. R., Monreal-Montes, M., García, J. M., Serratosa, M. P., VaroSantos, M.A., Ortiz Perez, M.D. & Rendon-Huerta, J. A. (2018): Juices of prickly pear fruits (opuntia spp.) As functional foods. *Italian Journal of Food Science*, **30(3):**614-627.

[29]Madrigal-Santillán, E., García-Melo, F., Morales-González, J. A., Vázquez-Alvarado, P., Muñoz-Juárez, S., Zuñiga-Pérez, C., Sumaya-Martínez, M.T., Madrigal-Bujaida, A. & Hernández-Ceruelos, A. (2013): Antioxidant and anticlastogenic capacity of prickly pear juice. *Nutrients*, **5(10):** 4145-4158.

[30]Seeram, N. P., Aviram, M., Zhang, Y., Henning, S. M., Feng, L., Dreher, M., & Heber, D. (2008): Comparison of antioxidant potency of commonly consumed polyphenol-rich beverages in the United States. *Journal of agricultural and food chemistry*, **56(4):**1415-1422.

[31]Hassan, F., El-Razek, A., & Hassan, A. A. (2011): Nutritional value and hypoglycemic effect of prickly cactus pear (Opuntia ficus-indica) fruit juice in Alloxan-induced diabetic rats. *Australian Journal of basic and applied sciences*, **5(10):** 356-377.

[32]Butera, D., Tesoriere, L., Di Gaudio, F., Bongiorno, A., Allegra, M., Pintaudi, A. M., Kohen, R. & Livrea, M. A. (2002): Antioxidant activities of Sicilian prickly pear (Opuntia ficus indica) fruit extracts and reducing properties of its betalains: betanin and indicaxanthin. *Journal of agricultural and food chemistry*, **50(23):** 6895-6901.

[33]Chavez-Santoscoy, R. A., Gutierrez-Uribe, J. A., & Serna-Saldívar, S. O. (2009): Phenolic composition, antioxidant capacity and in vitro cancer cell cytotoxicity of nine prickly pear (Opuntia spp.) juices. *Plant Foods for Human Nutrition*, **64(2):** 146-152.

[34]Wu, X., Beecher, G. R., Holden, J. M., Haytowitz, D. B., Gebhardt, S. E., & Prior, R. L. (2004): Lipophilic and hydrophilic antioxidant capacities of common foods in the United States. *Journal of agricultural and food chemistry*, **52(12):** 4026-4037.

[35]Miean, K. H., & Mohamed, S. (2001): Flavonoid (myricetin, quercetin, kaempferol, luteolin, and apigenin) content of edible tropical plants. *Journal of agricultural and food chemistry*, **49(6):** 3106-3112.

[36]Stintzing, F. C., Schieber, A., & Carle, R. (2001): Phytochemical and nutritional significance of cactus pear. *European Food Research and Technology*, **212(4):** 396-407.

[37]Bhatt, A., & Patel, V. (2013): Antioxidant activity of garlic using conventional extraction and in vitro gastrointestinal digestion. *Free Radicals and Antioxidants*, **3(1):** 30-34.

[38] Tesoriere, L., Butera, D., Pintaudi, A. M., Allegra, M., & Livrea, M. A. (2004): Supplementation with cactus pear (Opuntia ficus-indica) fruit decreases oxidative stress in healthy humans: a comparative study with vitamin C. *The American journal of clinical nutrition*, **80(2):** 391-395.

[39] Ali, H. S. M., Al-Khalifa, A. S., & Brückner, H. (2014): Taurine is absent from amino components in fruits of Opuntia ficus-indica. *SpringerPlus*, **3(1):** 663.

[40] Tesoriere, L., Fazzari, M., Allegra, M., & Livrea, M. A. (2005): Biothiols, taurine, and lipid- soluble antioxidants in the edible pulp of Sicilian cactus pear (Opuntia ficus-indica) fruits and changes of bioactive juice components upon industrial processing. *Journal of agricultural and food chemistry*, **53(20):** 7851-7855.

Table 2: Blood glutathione and vitamin-C level of control and experimental subjects prior to and at the end of experimental period

Parameter	Control			Experimental		
	Initial level	Final level	% change	Initial level	Final level	% change
Glutathione (mg/dl)	8.07 ± 2.12	8.59^{NS} ± 1.64	6.44	8.73 ± 3.54	10.28** ± 2.83	17.75
Vitamin-C (mg/dl)	2.10 ± 0.58	2.24 ^{NS} ± 0.59	6.67	1.80 ± 0.65	2.78** ±0.73	54.44

Values are Mean ± S.D., ** indicates significant difference at P<0.01 level and NS indicates no significant difference between initial and final level of a parameter

PRAJÑĀ - Journal of Pure and Applied Sciences Vol. 26: 112 - 119 (2018)
ISSN 0975 – 2595

EXACT SOLUTION FOR SZEKERES INHOMOGENEOUS COSMOLOGICAL MODELS IN STT OF GRAVITY [1]

A. H. Hasmani[2], Ahmed M. Al-Haysah[3]
Department of Mathematics, Sardar Patel University, Vallabh
Vidyanagar-388120, Gujarat India.
E-mail: [2] ah_hasmani@spuvvn.edu,[3]alhaysah2017@spuvvn.edu

ABSTRACT

The Szekeres metric represents an exact inhomogeneous and anisotropic solution of the Einstein Equations and it has no Killing vector fields [Georg and Hellaby, Physical Review D 95, (2017)]. This means that this solutions presents a more general class of solutions. It is known to possess axial symmetry.

The inhomogeneous Szekeres cosmological models (ISCM) within the framework of scalar-tensor theory (STT) of gravity are obtained.

Inhomogeneous generalizations of the Friedmann-Lemaitre-Robertson-Walker (FLRW) cosmological models have gained interest in the astrophysical community and are more often employed to study cosmologicalphenomena.

In this paper, we first give the solutions of the STT field Equations. Andthen it's physical and geometrical properties of this metric and the reviews of recent developments in the field and shows the importance of an inhomogeneous framework in the analysis of cosmological observations.

Keywords: **ISCM, STT of gravity.**

1. INTRODUCTION

Einstein's general theory of relativity (GR) is a geometrical theory of space-time. The fundamental building block is a metric tensor field g_{ij}which is a tensor of rank two. Alternatives to GR are physical theories that attempt to describe the phenomenon of gravitation in competition to Einstein's theory of GR. In an alternative theory based on a metric tensor field along with another dynamical scalar field coupled to it is proposed by Brans and Dicke [4] accordingly called STT of gravity.

The theory formulated in [4] which is an STT of gravitation in which the tensor field alone is geometrized and the scalar field is aligned to the geometry. Sen and Dunn [12] have proposed a new STT of gravitation in which both the scalar and tensor fields have intrinsic geometrical significance.

The fields Equations in STT are given by,

$$G_{ij} + \frac{\omega(\phi)}{\phi^2}\left[\nabla_i\phi\nabla_j\phi - \frac{1}{2}g_{ij}\nabla_k\phi\nabla^k\phi\right] + \frac{1}{\phi}\left[\nabla_i\nabla_j\phi - g_{ij}\Box\phi\right] = \frac{8\pi}{\phi}T_{ij}, \qquad (1.1)$$

where G_{ij} is the Einstein tensor, $\omega(\phi)$ is some function of ϕ, ϕ is scalar field, ∇_i is the covariant derivative operator, $\Box = \nabla^k\nabla_k = g^{kl}\nabla_l\nabla_k$ is the d'Alembert operator for a scalar field. One can take the trace of Equation (1.1) overall space to g^{ij}, by using $g^{ij}G_{ij} = -R$, we obtain

$$(2\omega(\phi) + 3)\Box\phi = 8\pi T - \frac{d\omega}{d\phi}\nabla_k\phi\nabla^k\phi, \qquad (1.2)$$

where $T = g^{ij}T_{ij}$ is the trace of the stress-energy. Also, the matter satisfies the following conservation Equation

$$\nabla_i T^{ij} = 0. \qquad (1.3)$$

The conservation Equation gives above implies that the test-particles describes geodesics as in the case of GR.

2. THE METRIC AND THE FIELD EQUATIONS

The Szekeres metric is given by [9]

$$ds^2 = dt^2 - e^{2A}(dx^2 + dy^2) - e^{2B}dz^2, \qquad (2.1)$$

[1]**This paper was awarded, "Sardar Patel Research Award" in December 2018**.

where the metric coefficients A and B are functions of all space-time co-ordinates i.e.,

$$\mathrm{A} = \mathrm{A}(\mathrm{x},\mathrm{y},\mathrm{z},\mathrm{t}), \mathrm{B} = \mathrm{B}(\mathrm{x},\mathrm{y},\mathrm{z},\mathrm{t}).$$

The computations of relevant tensors ; for metric (2.1) gives,

$$\begin{aligned}\mathrm{R} = 2\mathrm{e}^{-2\mathrm{A}}\left(\mathrm{B}_{\mathrm{y}}^2 + \mathrm{A}_{\mathrm{yy}} + \mathrm{B}_{\mathrm{yy}} + \mathrm{B}_{\mathrm{x}}^2 + \mathrm{A}_{\mathrm{xx}} + \mathrm{B}_{\mathrm{xx}}\right) \\ - 2\mathrm{e}^{-2\mathrm{B}}(3\mathrm{A}_{\mathrm{z}}^2 - 2\mathrm{A}_{\mathrm{z}}\mathrm{B}_{\mathrm{z}} + 2\mathrm{A}_{\mathrm{zz}}) \\ +2\left[3\dot{A}^2 + 2\dot{A}\dot{B} + \dot{B}^2 + 2\ddot{A} + \ddot{B}\right], \quad (2.2)\end{aligned}$$

where an overhead dot denotes derivative with respect to time t and partial derivatives with respect to space variable are denoted by relevant subscripts e.g., $B_{xy} = \frac{\partial^2 B}{\partial x \partial y}$, etc.

The energy-momentum tensor for a perfect fluid is given by,

$$T_{ij} = (\rho + p)u_i u_j - p g_{ij}, \quad (2.3)$$

where ρ is the proper energy density, p is the isotropic pressure and choosing a comoving observer we take, $u^i = (0,0,0,1)$ as 4-velocity of the fluid particles which satisfy the condition $u^i u_i = 1$. The average scale-factor $a(t)$, and spatial volume V are given by,

$$V = \sqrt{-g} = a^3 = \mathrm{e}^{2A+B}. \quad (2.4)$$

In a cosmological setting, we define Hubble, deceleration, jerk, and snap parameters by,

$$H(t) = \frac{\dot{a}}{a} = \frac{1}{3}\frac{\dot{V}}{V} = \frac{1}{3}\sum_{i=1}^{3} H_i = \frac{1}{3}\left(2\dot{A} + \dot{B}\right), \quad (2.5)$$

$$\begin{aligned}q(t) = -\frac{\ddot{a}}{a}H^{-2} = -\left(1 + \frac{\dot{H}}{H^2}\right) \\ = -\left(1 + \frac{2\ddot{A}+\ddot{B}}{3H^2}\right), \quad (2.6)\end{aligned}$$

$$j(t) = \frac{\dddot{a}}{a}H^{-3} = q + 2q^2 - \frac{\dot{q}}{H} = 1 + 3\frac{\dot{H}}{H^2} + \frac{\ddot{H}}{H^2}, \quad (2.7)$$

$$s(t) = \frac{\ddddot{a}}{a}H^{-4} = \frac{\ddddot{a}a^3}{\dot{a}^4}. \quad (2.8)$$

In terms of the these parameters, we consider the following definitions

$$\dot{H} = -H^2(1+q), \quad (2.9)$$

$$\ddot{H} = H^3(j + 3q + 2), \quad (2.10)$$

$$\dddot{H} = H^4(s - 2j - 5q - 3). \quad (2.11)$$

To realize how this term arises, consider the Taylor expansion of the scale factor, about the present time, t_0

$$\begin{aligned}a(t) = a_0 + \dot{a}_0(t - t_0) \\ + \frac{1}{2}\ddot{a}_0(t - t_0)^2 + \cdots, \quad (2.12)\end{aligned}$$

where the sub-zeros indicate the terms are evaluated at the present. Using Equations of deceleration, jerk, and snap parameters are dimensionless, and we can write

$$\begin{aligned}a(t) = a_0\left[1 + H_0(t - t_0) - \frac{1}{2}q_0H_0^2(t - \right. \\ t_0)^2 + \frac{1}{3!}j_0H_0^3(t - t_0)^3 + \frac{1}{4!}s_0H_0^4(t - \\ \left. t_0)^4 + O([t - t_0]^5)\right], \quad (2.13)\end{aligned}$$

where H_0, q_0, j_0 and s_0, are the present time at $t = t_0$. In terms, the red-shift of Taylor expansion reads

$$\begin{aligned}\frac{1}{z+1} = H_0(t - t_0) - \frac{1}{2}q_0H_0^2(t - t_0)^2 + \\ \frac{1}{3!}j_0H_0^3(t - t_0)^3 + \\ \frac{1}{4!}s_0H_0^4(t - t_0)^4 + O([t - t_0]^5). \quad (2.14)\end{aligned}$$

For small $H_0(t - t_0)$ this can be inverted to yield

$$t - t_0 = H_0^{-1}\left[z - (1 + \tfrac{q_0}{2})z^2 + \ldots\right]. \quad (2.15)$$

If coordinates are chosen so cosmic time $t = 0$ denotes the time of the big bang (phase), then $t = 0$ is the age of the universe. The Hubble parameters (HPs) in the directions of x, y and z-axes are given by

$$H_1 = H_2 = \dot{A}, \qquad H_3 = \dot{B}. \quad (2.16)$$

The cosmological parameters such as the scalar expansion (θ), shear scalar (σ^2), shear parameter (Σ^2), and anisotropy parameter A_m are given by,

$$\theta = 3H = 2H_1 + H_3, \quad (2.17)$$

$$\begin{aligned}\sigma^2 = \frac{1}{2}\sigma_{ij}\sigma^{ij} = \frac{1}{2}\left(\sum_{i=1}^{3} H_i^2 - 3H^2\right) = \\ \frac{1}{3}(H_1 - H_3)^2, \quad (2.18)\end{aligned}$$

$$\Sigma^2 = \frac{\sigma^2}{3H^2} = \frac{1}{3}\left(\frac{H_1 - H_3}{H}\right)^2, \quad (2.19)$$

$$A_m = \frac{1}{3}\sum_{i=1}^{3}\left[\frac{H_i-H}{H}\right]^2 = \frac{1}{3}\left(2\left[\frac{H_1-H}{H}\right]^2 + \left[\frac{H_3-H}{H}\right]^2\right), \quad (2.20)$$

where H_1, H_2, and $H_3$are given as in Equation (2.16).

3. EXACT SOLUTION FOR SZEKERES MODEL

Here we first develop some important cosmological parameters and EFEs for SMs and then find the exact solutions of EFEs. In fact, the differential Equation obtained in terms of the metric coefficient for$\phi = \phi(t)$is apparently not solvable.By using Equations (1.1), (2.1), and (2.3), we obtain a set of differential Equations for SMs,

$$\dot{H}_1 + \dot{H}_3 + H_1^2 + H_3^2 + H_1H_3 - \mathrm{e}^{-2A}\left[B_y^2 + B_{yy} - A_yB_y + A_xB_x\right] + \mathrm{e}^{-2B}[A_zB_z - A_z^2 - A_{zz}] + \frac{\omega}{2}\left(\frac{\dot{\phi}}{\phi}\right)^2 + \frac{\ddot{\phi}}{\phi} + (H_1 + H_3)\frac{\dot{\phi}}{\phi} = -\frac{8\pi p}{\phi}, \quad (3.1)$$

$$\dot{H}_1 + \dot{H}_3 + H_1^2 + H_3^2 + H_1H_3 - \mathrm{e}^{-2A}\left[B_x^2 + B_{xx} - A_xB_{yx} + A_yB_y\right] + \mathrm{e}^{-2B}[A_zB_z - A_z^2 - A_{zz}] + \frac{\omega}{2}\left(\frac{\dot{\phi}}{\phi}\right)^2 + \frac{\ddot{\phi}}{\phi} + (H_1 + H_3)\frac{\dot{\phi}}{\phi} = -\frac{8\pi p}{\phi}, \quad (3.2)$$

$$2\dot{H}_1 + 3H_1^2 - \mathrm{e}^{-2A}\left[A_{yy} + A_{xx}\right] - \mathrm{e}^{-2B}A_z^2 + \frac{\omega}{2}\left(\frac{\dot{\phi}}{\phi}\right)^2 + \frac{\ddot{\phi}}{\phi} + (2H_1)\frac{\dot{\phi}}{\phi} = -\frac{8\pi p}{\phi}, \quad (3.3)$$

$$H_1^2 + 2H_1H_3 - \mathrm{e}^{-2A}\left[A_{xx} + B_{xx} + B_y^2 + A_{yy} + B_{yy} + B_x^2\right] + \mathrm{e}^{-2B}[2A_zB_z - 3A_z^2 - 2A_{zz}] - \frac{\omega}{2}\left(\frac{\dot{\phi}}{\phi}\right)^2 + (2H_1 + H_3)\frac{\dot{\phi}}{\phi} = \frac{8\pi\rho}{\phi}, \quad (3.4)$$

$$B_x\left[A_y - B_y\right] + A_xB_y - B_{xy} = 0, \quad (3.5)$$

$$B_xA_z - A_{xz} = 0, \quad (3.6)$$

$$B_yA_z - A_{yz} = 0, = \quad (3.7)$$

$$B_x[H_1 - H_3] - (H_1)_x - (H_3)_x = 0, \quad (3.8)$$

$$B_y[H_1 - H_3] - (H_1)_y - (H_3)_y = 0, \quad (3.9)$$

$$A_z[H_1 - H_3] - (H_1)_z = 0. \quad (3.10)$$

From Equations (3.6), (3.7), and (3.10) after differentiating with respect to x, y, and t respectively we say,

$$(\mathrm{e}^{-B}A_z)_x = (\mathrm{e}^{-B}A_z)_y = 0, \text{and}$$

$$(\mathrm{e}^{A-B}A_z)_t = 0 \quad (3.11)$$

Using the integrability condition, the first two Equations of (3.11) imply that,

$$\mathrm{e}^{-B}A_z = u(z,t)\,. \quad (3.12)$$

The cases $u = 0$ and $u \neq 0$ have to be considered separately because the integration proceeds in a different way in each case, and the limit $A_z \to 0$ of the solution for $A_z \neq 0$ is singular. Thus, if $A_z \neq 0$ we must have $(H_1)_{xy} = 0$, we shall consider the following possibilities

(1) $A_z = 0$,

(2) $A_z \neq 0$, $(H_1)_{xy} = 0$,

to get solutions of the field Equations.

3. 1 THE SUBFAMILY $A_z = 0$

The Equations (3.6), (3.7), and (3.10) are equal zero and fulfilled identically. In solving the other Equations, we can assume that $(H_1)_x = (H_1)_y = 0$ because otherwise, the Equations have no solutions; [11]. Then

$$\mathrm{e}^A = \Phi(t)\mathrm{e}^{\nu(x,y)}\,, \quad (3.13)$$

where Φ and ν are unknown functions, while Equations (3.8), and (3.9) are equal zero imply that

$$\mathrm{e}^{B-A}B_x = \tilde{\eta}_1(x,y,z), \mathrm{e}^{B-A}B_y = \tilde{\eta}_2(x,y,z), \quad (3.14)$$

where $\tilde{\eta}_1$ and $\tilde{\eta}_2$ are other unknown functions. Using Equation (3.13) for e^A, and denoting

$$\tilde{\eta}_1(x,y,z) = \eta_1\mathrm{e}^{-\nu}, \tilde{\eta}_2(x,y,z) = \eta_2\mathrm{e}^{-\nu}, \quad (3.15)$$

we obtain

$$\mathrm{e}^BB_x\ \Phi(t)\eta_1(x,y,z), \quad \mathrm{e}^BB_y\Phi(t)\eta_2(x,y,z). \quad (3.16)$$

The integrability condition $(\mathrm{e}^BB_x)_y = \left(\mathrm{e}^BB_y\right)_x$ implies $(\eta_1)_y = (\eta_2)_x$. This means that a function $\eta(x,y,z)$ exists such that $\eta_1 = \eta_x$, $\eta_2 = \eta_y$.Knowing this, (3.14) can be integrated to give

$$\mathrm{e}^B = \Phi(t)\eta(x,y,z) + \mu(z,t). \quad (3.17)$$

where μ is an unknown function. Now if we replace A , and B from Equations (3.13), and

(3.17) in the field Equation (3.3), we have similar differential Equations in Φ as

$$2\Phi\ddot{\Phi} + \dot{\Phi}^2 + 2\Phi\dot{\Phi}\left(\frac{\dot{\phi}}{\phi}\right) + \Phi^2\left[\frac{8\pi p}{\phi} + \frac{\omega}{2}\left(\frac{\dot{\phi}}{\phi}\right)^2 + \frac{\ddot{\phi}}{\phi}\right] = -K, \quad (3.18)$$

where Φ, and p depend only on t, and K an arbitrary constant [6],

$$K = -\mathrm{e}^{-2\nu}\left[\nu_{xx} + \nu_{yy}\right], \quad (3.19)$$

because ν depends only on x, and y. Here we take the solution for ν in the form

$$\mathrm{e}^{-\nu} = \alpha(z)(x^2 + y^2) + \beta_1(z)x + \beta_2(z)y + \gamma(z), \quad (3.20)$$

with the restriction

$$\beta_1^2 + \beta_2^2 - 4\alpha\gamma = -K, \quad (3.21)$$

where $\alpha(z), \beta_1(z), \beta_2(z)$, and $\gamma(z)$ are arbitrary functions (α, and γ being real) Now to determine the function η, we have from the field Equations (3.1), and (3.2), the solution

$$(\mathrm{e}^{-\nu}\eta)_{xx} = (\mathrm{e}^{-\nu}\eta)_{yy} = 0. \quad (3.22)$$

From the field Equation (3.5), we have the solution

$$\mathrm{e}^{-\nu}\eta = P(z)[x^2 + y^2] + Q_1(z)x + Q_2(z)y + S(z), \quad (3.23)$$

where $P(z), Q_1(z), Q_2(z)$, and $S(z)$ are arbitrary functions. Also the metric (2.1) can be written as

$$ds^2 = dt^2 - \Phi(t)^2\mathrm{e}^{2\nu(x,y)}(dx^2 + dy^2) - (\Phi(t)\eta(x,y,z) + \mu(z,t))^2dz^2. \quad (3.24)$$

The average scale-factor $a(t)$, spatial volume V, Mean HP, and deceleration parameter are

$$V = a^3 = \sqrt{-g} = \mathrm{e}^{2\nu}\eta\mu\Phi^3, H = \frac{\dot{\Phi}}{\Phi} + \frac{\dot{\mu}}{3\mu}, \quad (3.25)$$

$$q = \frac{-\mu\left[6\mu\dot{\Phi}^2 + 3\mu\Phi\ddot{\Phi} + 6\Phi\dot{\Phi}\dot{\mu} + \Phi^2\ddot{\mu}\right]}{\left(3\mu\dot{\Phi} + \Phi\dot{\mu}\right)^2}, \quad (3.26)$$

in which HPs in the directions of x, y, and z axes are,

$$H_1 = H_2 = \frac{\dot{\Phi}}{\Phi}, H_3 = \frac{\dot{\Phi}}{\Phi} + \frac{\dot{\mu}}{\mu}. \quad (3.27)$$

The cosmological parameters such as the scalar expansion θ, and shear scalar σ are given by,

$$\theta = \frac{3\dot{\Phi}}{\Phi} + \frac{\dot{\mu}}{\mu}, \sigma = \frac{1}{\sqrt{3}}\frac{\dot{\mu}}{\mu}. \quad (3.28)$$

Using Equations (3.1) to (3.4), we have the expression for density as

$$\rho = \frac{-\phi}{8\pi}\left[6\frac{\ddot{\Phi}}{\Phi} - \left(\frac{\dot{\mu}}{\mu}\right)^2 + 2\frac{\ddot{\mu}}{\mu} + \frac{4\dot{\Phi}\dot{\mu}}{\Phi\mu} - 3p + 2\omega\left(\frac{\dot{\phi}}{\phi}\right)^2 + \frac{3\ddot{\phi}}{\phi} + \frac{\dot{\phi}}{\phi}\left(\frac{3\dot{\Phi}}{\Phi} + \frac{\dot{\mu}}{\mu}\right)\right]. \quad (3.29)$$

An addition singularity of infinite density occurs where (and if) $\mathrm{e}^B = 0$. Krolak et al [5], showed that the Big-Bang (BB) singularity at $\Phi = 0$ in the $K = 0$ subcase of IS solution is a naked strong curvature singularity. Therefore, the SSs are another counter example to the oldest and simplest formulation of the cosmic censorship hypothesis. In fact, Krolak et al [5] result shows that the SSs are not sufficiently generic from the point of view of the cosmic censorship paradigm. The shell-crossing singularity (the one at, $\Phi_z = 0$), although naked as well, is not strong. Several other papers have been published in which the spherically symmetric limit of the $A_z \neq 0$ SSs (i.e. the Lemaitre-Tolman model) has been discussed as a testing ground for cosmic censorship [9].

The computations of relevant tensors; for metric (3.24) gives,

$$R = 4\left(\frac{\dot{\Phi}}{\Phi}\right)^2 + 4\left(\frac{\ddot{\Phi}}{\Phi}\right) + 8\frac{\dot{\Phi}\dot{\mu}}{\Phi\mu} + 2\frac{\ddot{\mu}}{\mu} + 2\frac{\mathrm{e}^{-2\nu}}{\eta\Phi^2}\left[\eta(\nu_{xx} + \nu_{yy}) + \eta_{xx} + \eta_{yy}\right]. \quad (3.30)$$

We consider the hyperbolic counterparts of these space-times even though they are of Bianchi type-III, ifwe take $\beta_1 = \beta_2 = 0, \alpha = \frac{K}{4}$, and $\gamma = 1$, the Equation (3.20) becomes

$$\mathrm{e}^{-\nu} = 1 + \frac{K}{4}(x^2 + y^2). \quad (3.31)$$

Further simplifications may be introduced by coordinate transformations one of these if $\alpha = \beta_2 = \gamma = 0$, and $\beta_1 = 1$, then the Equation (3.23) becomes $\eta = \mathrm{e}^{\nu}x$, so the metric (3.24) becomes,

$$ds^2 = dt^2 - \left[\frac{\Phi(t)}{1+\frac{K}{4}(x^2+y^2)}\right]^2 (dx^2 + dy^2 + x^2dz^2). \quad (3.32)$$

Using the spatial transformation

$$x = rsin\theta, y = rcos\theta, z = \phi.$$

The metric (3.32) reduces to,

$$ds^2 = dt^2 - \left[\frac{\Phi(t)}{1+\frac{K}{4}r^2}\right]^2 \left(dr^2 + r^2(d\theta^2 + sin^2\theta d\phi^2)\right), \quad (3.33)$$

where $r^2 = x^2 + y^2$, and the metric is group of G_3. This form metric is similar to FLRW metric.

(1) when $K = 0$, (flat) the metric is Bianchi type-I, and Bianchi type- VII_0,
(2) when $K = +1$, (closed) the metric is Bianchi type-IX,
(3) when $K = -1$, (open) the metric is Bianchi type-V, and Bianchi type-VII_h,

Introducing complex variables for convenience

$$\xi = x + iy, \bar{\xi} = x - iy,$$

in which the Equation (3.19) becomes

$$4\mathrm{e}^{-2\nu}\nu_{\xi\bar{\xi}} = -K. \quad (3.34)$$

Differentiating this by ξ we obtain,

$$\left(\nu_{\xi\xi} - \nu_{\xi}^2\right)_{\bar{\xi}} = 0,$$

and hence without loss of generality, we take

$$\nu_{\xi\xi} - \nu_{\xi}^2 = 0. \quad (3.35)$$

This implies

$$(\mathrm{e}^{-\nu})_{\xi\xi} = (\mathrm{e}^{-\nu})_{\bar{\xi}\bar{\xi}} = 0, \quad (3.36)$$

since ν, is real,

$$\mathrm{e}^{-\nu} = \alpha\xi\bar{\xi} + \beta_1\xi + \bar{\beta}_2\bar{\xi} + \gamma, \quad (3.37)$$

so by substitution in Equation (3.34) implies

$$\alpha\gamma - \beta_1\bar{\beta}_2 = \frac{K}{4}, \quad (3.38)$$

if we take $\beta_1 = \beta_2 = 0, \alpha = \frac{K}{2}$, and $\gamma = \frac{1}{2}$, the Equation (3.37) becomes

$$\mathrm{e}^{-\nu} = \frac{1}{2}\left(1 + K\xi\bar{\xi}\right). \quad (3.39)$$

Now to determine the function η, from the field Equation (3.5) we have,

$$(\mathrm{e}^{-\nu}\eta)_{\xi\xi} = (\mathrm{e}^{-\nu}\eta)_{\bar{\xi}\xi} = 0. \quad (3.40)$$

Now from the field Equations (3.1), and (3.2), we have the solution

$$\mathrm{e}^{-\nu}\eta = \alpha(z)\xi\bar{\xi} + \beta_1(z)\frac{\xi+\bar{\xi}}{2} + \beta_2(z)\frac{\xi-\bar{\xi}}{2i} + \gamma(z), \quad (3.41)$$

with the restriction as gives in Equation (3.21). Further simplifications may be introduced by coordinate transformations one of these if $\alpha = \beta_2 = \gamma = 0$, and $\beta_1 = 1$, then the Equation (3.41) becomes, $\eta = \frac{\xi+\bar{\xi}}{2}\mathrm{e}^{\nu}$. Also the metric (2.1) can be written as

$$ds^2 = dt^2 - \left[\frac{\Phi(t)}{1+\frac{K}{4}\xi\bar{\xi}}\right]^2 \left(d\xi d\bar{\xi} + \left(\frac{\xi+\bar{\xi}}{2}\right)^2 dz^2\right). \quad (3.42)$$

This metric is a general axially symmetric space-time.

3. 2 THE SUBFAMILY $A_z \neq 0, (H_1)_{xy} = 0$

This case gives useful information in astrophysics, and cosmology. From Equation (3.12), it is clear that $u(z,t) \neq 0$, hence we write,

$$\mathrm{e}^{B} = \frac{A_z}{u(z,t)}. \quad (3.43)$$

Using Equation (3.43) in Equation (3.11), we get

$$(e^{A-B}A_z)_t = (e^A u)_t = 0. \quad (3.44)$$

The solution of which can be given as,

$$e^A = \Phi(z,t)e^{\nu(x,y,z)}, \quad (3.45)$$

where $\Phi(z,t) = \frac{1}{u}$, it follows that $(H_1)_x = (H_1)_y = 0$, so Equation (3.43) implies that

$$e^B = \Phi(z,t)A_z. \quad (3.46)$$

The arbitrary factor dependent on z can be introduced in e^B by a transformation of the form $z = f(z')$. This will simplify the limiting transition to the RW models. Thus,

$$e^B = h(z)\Phi(z,t)A_z = h(z)(\Phi_z + \Phi\nu_z). \quad (3.47)$$

The evolution Equation for Φ gives

$$2\Phi\ddot{\Phi} + \dot{\Phi}^2 + 2\Phi\dot{\Phi}\left(\frac{\dot{\phi}}{\phi}\right) + \Phi^2\left[\frac{8\pi p}{\phi} + \frac{\omega}{2}\left(\frac{\dot{\phi}}{\phi}\right)^2 + \frac{\ddot{\phi}}{\phi}\right] = -K(z), \quad (3.48)$$

The function ν satisfies

$$e^{-2\nu}[\nu_{xx} + \nu_{yy}] - D^2 = K(z), \quad (3.49)$$

where $D = \frac{1}{h}$. Following the procedure adopted by Szafron [14] discussed in [9]. we may write the solutions in the form

$$e^{-\nu} = \alpha(z)[x^2 + y^2] + \beta_1(z)x + \beta_2(z)y\,\gamma(z), \quad (3.50)$$

with the restriction

$$\beta_1^2 + \beta_2^2 - \alpha\gamma = \frac{-1}{4}\left(D^2 + K(z)\right). \quad (3.51)$$

The first integral of the Equation (3.48), may be given by

$$\dot{\Phi}^2 = \frac{M}{\Phi} + K(z) - \frac{1}{\Phi}\int \dot{\Phi}\frac{\partial}{\partial t}(\Phi^2)\left(\frac{\dot{\phi}}{\phi}\right)dt - \frac{1}{3\Phi}\int \frac{\partial}{\partial t}(\Phi^3)\left[\frac{8\pi p}{\phi} + \frac{\omega}{2}\left(\frac{\dot{\phi}}{\phi}\right)^2 + \frac{\ddot{\phi}}{\phi}\right]dt. \quad (3.52)$$

Now using conservation Equation (1.3) we get

$$\dot{\rho} + (H_3 + 2H_1)(\rho + 2p) = 0. \quad (3.53)$$

If we further assume that the perfect fluid obeys the barotropic Equation of state of the form

$$p = \omega\rho, \qquad 0 \le \omega \le 1,$$

with the equation of state parameter ω as time-independent. In this case, Equation (3.53) can be integrated for the energy density to yield

$$\rho = \left(\frac{1}{a}\right)^{3(1+2\omega)}. \quad (3.54)$$

In this model, the BB is not simultaneous in the comoving, and synchronous time t. With this t, the BB is a process extended in time rather than a single event in space-time.

The ISCM that could model our universe began with a BB a moment in time at which the scale factor $a(t)$ vanishes, and the geometry of the universe is singular. The singular nature of the BB is apparent from Equation (3.54). The densities of matter, and radiation are infinite when $a = 0$ [9].

The BB occurred at every place in space at one moment in time. The notion of a geometry of spaceï-time breaks down at a singularity, along with the predictive power of the law of geometry, such as Einstein's Equation As far as making predictions in physic, concerned, the universe began at the BB. For this reason, the BB is conventionally assigned the time $t = 0$. Also the metric (2.1) can be written as

$$ds^2 = dt^2 - \Phi^2 e^{2\nu}(dx^2 + dy^2) - (h\Phi A_z)^2 dz^2. \quad (3.55)$$

The average scale-factor $a(t)$, spatial volume V, and Mean HP are

$$V = a^3 = \sqrt{-g} = e^{2\nu}\, h^2\, \Phi^2\, (\Phi_z + \Phi\, \nu_z), \quad (3.56)$$

$$H = \frac{\Phi\,\dot{\Phi}_z + \dot{\Phi}\,(2\,\Phi_z + 3\,\Phi\,\nu_z)}{3\,\Phi\,(\Phi_z + 3\,\Phi\,\nu_z)}, \quad (3.57)$$

in which HPs in the directions of x, y, and z axes are,

$$H_1 = H_2 = \frac{\dot{\Phi}}{\Phi},\ H_3 = \frac{\dot{\Phi}_z + \dot{\Phi}\,\nu_z}{\Phi_z + \Phi\,\nu_z}. \quad (3.58)$$

The cosmological parameters such as the scalar expansion (θ), and shear scalar (σ) are given by,

$$\theta = \frac{\Phi\,\dot{\Phi}_z + \dot{\Phi}\,(2\,\Phi_z + 3\,\Phi\,\nu_z)}{\Phi\,(\Phi_z + 3\,\Phi\,\nu_z)}, \qquad (3.59)$$

$$\sigma = \frac{\dot{\Phi}\,\Phi_z - \Phi\,\dot{\Phi}_z}{\sqrt{3}\,\Phi\left(\dot{\Phi} + \Phi\,\nu_z\right)}, \qquad (3.60)$$

From Equations (3.59) and (3.60), we obtain

$$\frac{\sigma^2}{\theta^2} = \frac{\left(\dot{\Phi}\,\Phi_z - \Phi\,\dot{\Phi}_z\right)^2}{3\,\left(\Phi\,\dot{\Phi}_z + \dot{\Phi}\,(2\,\Phi_z + 3\,\Phi\,\nu_z)\right)} = constant. \qquad (3.61)$$

Since, $\frac{\sigma}{\theta}$ is a non-zero constant the model does not approach to isotropy.

For the model (3.55), and by using Equation (3.54), the energy density ρ becomes

$$\rho = \left(\frac{e^{-2\nu}}{h^2\,\Phi^2\,(\Phi_z + 3\,\Phi\,\nu_z)}\right)^{1+2\omega}, 0\ \omega \leq 1 \qquad (3.62)$$

The sign of one of them fixes the geometry of the $t = constant$ 3-surfaces, and the type of evolutions are elliptic, parabolic, and hyperbolic. The sign of another function determines the geometry of the $t = constant$, and $z = constant$, 2-surfaces they quasi-spherical, quasi-plane, and quasi-hyperbolic models. Only the quasi-spherical model has been found useful in astrophysical cosmology, thus our results match with [10].

In the exact IS can be employed not only for studying the dynamics, and the geometry of the universe, but also to investigate the formation, and evolution of structures.

4. CONCLUSION

In this paper, we have considered that the ISC solutions with perfect fluid as the matter distribution. We can classify the solutions into two categories namely, (1) $A_z = 0$, and (2) $A_z \neq 0$. The first set of solutions are known as a quasi-spherical solution while the second class of solution is termed as a cylindrical type of solutions.

Two properties have already been mentioned, the lack of any symmetry in general, and the existence of the surfaces of constant curvature $t = z = constant$. In fact, the lack of symmetry was proved by Bonnor, Sulaiman, and Tomimura(1977) [3] for the Szekeres solutions, but since they assume $p = 0$ of the Szafron space-times, it follows immediately that the latter has, in general, no symmetry either. Other properties in common are as follows, thus properties were discussed in [9].

The Weyl tensor of the Szafron space-times has its magnetic part with respect to the velocity field of the source equal to zero (Szafron, and Collins 1979 [7], Barnes and Rowlingson 1989 [1]), and is in general of Petrov type D (Szafron 1977). It degenerates to zero in the FLRW limit only.

The slices $t = constant$ of these space-times are conformally flat (Berger, Eardley, and Olson 1977 [2]). This indicates that the space-times are non-radiative in the sense of York (1972) [16].

Note that the curvature of the xy-surfaces is a global constant only in the $A_z = 0$ subfamily, and there it is equal to the curvature index of the $t = constant$ slices in the resulting FLRW limit. In the $A_z \neq 0$ subfamily, the curvature of the xy-surfaces is determined by $\Delta = \beta_1^2 + \beta_2^2 - \alpha\gamma$ and is independent of the curvature index of the FLRW limit, which is determined by $K(z)$. Both $K(z)$, and Δ are only constant within each xy-surface and can vary within $t = constant$ slice. The variation of K over $t = constant$ slice has an interesting consequence: Ifobservers in different spatial locations of the Szafron $A_z \neq 0$ Universe are trying to approximate it by FLRW models, then each of them may choose a different FLRW model. Even the sign of K is not a global property of a general Universe. Its global constancy is a peculiarity of the FLRW class.

The Szafron space-times trivialize: those with $A_z \neq 0$ become FLRW, and those with $A_z = 0$ acquire either FLRW or K-S geometry or the plane and hyperbolic counterparts of the latter (Spero and Szafron 1978 [13]).

ACKNOWLEDGMENTS

AMA is thankful to the Al-Bayda' University, and Government of the Republic of Yemen for providing financial support. The authors are thankful to the University Grant Commission,

India for providing financial support under UGC-SAP-DRS(III) provided to the Department of Mathematics, Sardar Patel University, Vallabh Vidyanagar, where the work was carried out.

5. REFERENCES

[1] Barnes, A. and Rowlingson, R. R. (1989): Irrotational perfect uids with a purely electric weyl tensor. Classical and quantum gravity, 6(7): 949-960.

[2] Berger, B. K., Eardley, D. M., and Olson, D. W. (1977): Note on the spacetimes of Szekeres. Physical Review D, 16(10): 3086-3089.

[3] Bonnor, W., Sulaiman, A., and Tomimura, N. (1977): Szekeres's space-times have no killing vectors. general relativity and gravitation, 8(8): 549-559.

[4] Brans, C. and Dicke, R. H. (1961): Mach's principle and a relativistic theory of gravitation. Physical Review, 124(3): 925-935.

[5] Brown, J. D. (1994) Proceedings of the cornelius Lanczos international centenary conference, SIAM.

[6] Chakraborty, S. and Debnath, U. (2004): A study of higher dimensional inhomogeneous cosmological model. International Journal of Modern Physics D, 13(06): 1085-1093.

[7] Collins, C. and Szafron, D. (1979): A new approach to inhomogeneous cosmologies: intrinsic symmetries. I. Journal of Mathematical Physics, 20(11): 2347-2353.

[8] Georg, I. and Hellaby, C. (2017): Symmetry and equivalence in Szekeres models. Physical Review D, 95(12):124016-1 to 124016-16.

[9] Krasinski, A. (2006) Inhomogeneous cosmological models, Cambridge University Press.

[10] Krasinski, A. and Bolejko, K. (2011): Redshift propagation equations in the $\beta' \neq 0$ Szekeres models. Physical Review D, 83(8): 083503-1 to 083503-23.

[11] Plebanski, J. and Krasinski, A. (2006) An introduction to general relativity and cosmology. Cambridge University Press.

[12] Sen, D. and Dunn, K. (1971): A scalar-tensor theory of gravitation in a modified riemannian manifold. Journal of Mathematical Physics, 12(4): 578-586.

[13] Spero, A. and Szafron, D. A. (1978): Spatial conformal atness in homogeneous and inhomogeneous cosmologies. Journal of Mathematical Physics, 19(7): 1536-1541.

[14] Szafron, D. (1977): Inhomogeneous cosmologies: New exact solutions and their evolution. Journal of Mathematical Physics, 18(8): 1673-1677.

[15] Szekeres, P. (1975): A class of inhomogeneous cosmological models. Communications in mathematical physics, 41(1): 55-64.

[16] York Jr, J. W. (1972): Role of conformal three-geometry in the dynamics of gravitation. Physical review letters, 28(16): 1082-1085.

Instructions for preparation of manuscripts:

1. The paper should be submit into template format of the PRAJÑĀ.
2. The paper should be written in English and typed with double spacing.
3. The title of the paper and the name(s) of the author(s) be in the capital letters. The name of the institution be given in small letters below the name(s) of the author(s).
4. The 'Abstract of the paper, in not more than 150 words, should be provided on a separate page along with 4-6 keywords.
5. The heading, e.g. INTRODUCTION, should be written in capital letters and sub heading e.g. Chemical reagents and materials, should be written in sentence case.
6. Displayed formulae, mathematical equations and expressions should be numbered serially. Table should be with a title in addition to a serial number for it.
7. Photographs/Figures should be original with good contrast so as to be in a form suitable for direct reproduction scanning.
8. Footnotes are not normally allowed, except to identify the author for correspondence.
9. All figures must be numbered serially as they appear in the text, and their legends/captions should necessarily be provided.
10. References should be numbered in brackets [ ] in the order of appearance in the text. All the references in the bibliographic list must correspond to in-text references and vice versa. Abbreviated periodical titles should follow standard subject Abstracts. Names which are not listed by any standard subject indexing organizations should be spelled out in full.
11. All references should be clear and follow the examples below:

Periodical articles

[2] Sadqui, M., Fushman, D. and Munoz, V. (2006) Atom-by-atom analysis of global downhill protein folding. *Nature*, **442: 317-321.**

Books

[16] Stebbins, G. L. (1974) *Flowering plants: Evolution above the species level,* Amold Press, London, pp. 1-399.

Chapters from a book

[19] Schafer, H. and Muyzer, G. (2001) Denaturing gradient gel electrophoresis in marine microbial ecology, In *Methods in Microbiology* (Ed. Paul, J. H.), Academic Press, London, Vol. 30, pp. 425-468.

Thesis or other diplomas

[21] Nayak, S. (2004) *The visionary studies on the lichen genus Lecanora sensu lato in India.* Ph. D. Thesis, Dr. R. M. L.
Ayadh University, Faizabad, India.

Conference proceedings

[4] Mohapatra, G. C. (1981) Environment and culture of early man in the valley of river Chenab and Ravi, western sub-
Himalayas. In *Proceeding X Congress of IUPPS,* Mexico, pp. 90-123.

Online documentation

[9] Koning, R. E. (1994) Home Page for Ross Koning. Retrieved 26-6-2009 from *Plant Physiology Information Website:*
http://plantphys.info/index.html

Note: - Manuscripts prepared faithfully in accordance with the instructions will accelerate their processing towards publication; otherwise it would be delayed in view of their expected re-submission.

For and on behalf of Editorial
Dr. M. N. Patel
Department of Chemistry
Sardar Patel University
Vallabh Vidyanagar, Gujarat-388 120
spu.prajna@gmail.com
jeenen@gmail.com
Website: www.spuvvn.edu

NOTE: This information may kindly be circulated among your colleagues.